FLEXURAL FATIGUE STUDIES ON UNIDIRECTIONALLY REINFORCED GLASS FIBRE EPOXY COMPOSITES

by

SURENDRA KUMAR JONEJA

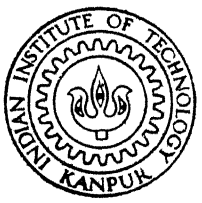

DEPARTMENT OF MECHANICAL ENGINEERING

INDIAN INSTITUTE OF TECHNOLOGY KANPUR

APRIL, 1979

FLEXURAL FATIGUE STUDIES ON UNIDIRECTIONALLY REINFORCED GLASS FIBRE EPOXY COMPOSITES

A Thesis Submitted
In Partial Fulfilment of the Requirements
for the Degree of

DOCTOR OF PHILOSOPHY

by

SURENDRA KUMAR JONEJA

to the

DEPARTMENT OF MECHANICAL ENGINEERING
INDIAN INSTITUTE OF TECHNOLOGY KANPUR

APRIL, 1979

To My Reverent

Grand-parents, and Parents

CERTIFICATE

This is to certify that this thesis entitled, 'Flexural Fatigue Studies on Unidirectionally Reinforced Glass Fibre Epoxy Composites', by Mr. S.K. Joneja is a record of work carried out under my supervision and has not been submitted elsewhere for a degree.

(B.D. Agarwal)
Assistant Professor
Department of Mechanical Engineering
Indian Institute of Technology
Kanpur

April 1979

ACKNOWLEDGEMENTS

I wish to express my deep sense of gratitude and appreciation to my advisor Prof. B.D. Agarwal for his valuable guidance and constructive criticism throughout the present work. His generous attitude towards academic liberty has been a constant source of inspiration for me.

I am grateful to Prof. B.L. Dhoopar for his encouragement during the work.

I deeply appreciate the discussion and helpful comments of my friends Messrs S.K. Chaturvedi and G.S. Giare.

I am thankful for the cooperation and help of the technical staff of Mechanical Engineering Department, in particular that of Messrs D.K. Sarkar, S.L. Srivastava, S.N. Yadav, B.L. Sharma, B.P. Vishwakarma, Joginder Singh, R.M. Jha, B.P. Bhartiya and M.M. Singh. I also acknowledge the help of Mr. K.P. Mukherjee of Metallurgical Engineering Department and Messrs T.A. Ansari and H.N. Sharma of Central Workshop.

I am grateful to Mr. B.L. Arora for his sincere efforts in preparing illustrations without any delay. I am also thankful to Mr. S.S. Kushwaha for his help in some of the illustrations. I highly appreciate the careful

typing of the thesis by Mr. J.D. Varma.

I am thankful to Dr. S.D. Shukla, Director and Prof. N.L. Kachhara, Head, Department of Mechanical Engineering of Harcourt Butler Technological Institute, Kanpur for their encouragement and help to carry out this research work.

Last, but not the least, I must thank my wife Parmodh and children Saurabh and Bhavana for keeping a very cheerful environment around me which made it possible to carry out present research work in short time.

S.K. Joneja

TABLE OF CONTENTS

LIST OF TABLES

LIST OF FIGURES

NOMENCLATURE

A	Stress Ratio
b	Constant defined in Eq. (4.9)
c	Constant defined in Eq. (4.11)
E	Modulus of Elasticity
G	Shear modulus
h	Thickness of the specimen
I	Moment of inertia of cross-section
k	Constant defined in Eq. (4.11)
l	Length of the specimen
M	Bending moment
m	Constant defined in Eq. (4.9)
N	Number of cycles
n	Frequency of cycling
R	Constant defined in Eq. (2.5)
$\bar{S}_{12}$, $\bar{S}_{16}$	Elements of compliance matrix

Greek Symbols

δ	Deflection
ε	Strain amplitude
θ	Fibre orientation
ν	Poisson's ratio
σ	Normal stress
τ	Shear stress

Subscripts

d	Dynamic stiffness
d_o	Dynamic stiffness in first load cycle
f	failure/fracture
L	Modulus of elasticity in longitudinal direction
LU	Ultimate strength in longitudinal direction
LT	Properties referred to L-T coordinate axes
LTU	Ultimate shear strength referred L-T axes
o	Initial stiffness / Bending moment
R	Residual stiffness
T	Modulus of elasticity in transverse direction
TU	Ultimate strength in transverse direction
U	Ultimate mechanical properties
UR	Residual strength
X	Off-axis properties of a composite lamina
XA	Apparent off-axis modulus of a composite lamina
XU	Off-axis strength

SYNOPSIS

FLEXURAL FATIGUE STUDIES ON UNIDIRECTIONALLY REINFORCED GLASS FIBRE EPOXY COMPOSITES

A Thesis Submitted
In Partial Fulfilment of the Requirements
for the Degree of

DOCTOR OF PHILOSOPHY

by

SURENDRA KUMAR JONEJA

to the

Department of Mechanical Engineering
Indian Institute of Technology, Kanpur

April, 1979

Real structures of fibrous composites generally consist of laminates having layers of unidirectional composites with different fibre orientations. Design of such laminates will require the knowledge of the static and fatigue strengths in the longitudinal and transverse directions as well as in-plane shear strength of unidirectional laminae. With this in mind fatigue behaviour of unidirectionally reinforced glass fibre epoxy composites has been studied.

Unidirectional composite plates were fabricated by hand lay out technique in the laboratory. Two fatigue testing machines were designed and fabricated. The flexural fatigue tests were performed on flat specimens by keeping

their one end fixed and cycling the other end between fixed displacement limits with zero mean displacement. Bending moment at the fixed end of the specimen was measured by means of a dynamometer employing electrical resistance strain gauges and was recorded at desired intervals without interrupting the fatigue tests.

Fatigue tests were performed on specimens in which fibres were oriented at 0, 10, 45 and 90 degree to the longitudinal edge. For each fiber orientation four different displacement limits were selected so that fatigue life of specimens varied from less than 1000 to more than a million cycles. At least twenty specimens were tested at each displacement limits. For each fibre orientation, the records of bending moment at the fixed end have been used to obtain several S - N curves, each of which represents a fixed stage of fatigue damage. The ratio of the instantaneous bending moment to the bending moment in first loading cycle, which represents fraction of the stiffness retained by the specimens, has been taken as a measure of fatigue damage.

It is observed that the fatigue behaviour of composites with different fibre orientations are quite different. In case of 0 and 10 degree specimens the stiffness gradually reduces before failure whereas for 45 and 90 degree specimens significant stiffness drop occurs suddenly during fatigue loading. Before this

sudden drop, the loss of specimen stiffness is only marginal whereas after the drop further loss in stiffness is gradual. The 10 degree specimens show a peculiar behaviour in that the stiffness of the specimens appears to stabilise at a value lower than the initial stiffness. When these specimens are further cycled, no further drop in stiffness occurs and no separation is observed even if the additional cycles are twice the number of cycles in which the stabilised stiffness was first observed. This behaviour has been explained through observed crack propagation and strain field in the specimen.

Progressive fatigue damage of specimens has been further investigated by cycling additional specimens to different fractions of fatigue life for all displacements in each orientation. On all these precycled specimens static flexural tests to failure were conducted. The records of bending moment versus displacement were used to obtain residual stiffness and residual strength. A good correlation is obtained among residual dynamic stiffness, static stiffness and strength. Different fatigue laws have been proposed from which one can obtain the fatigue strength (in terms of strain amplitude) for a given cyclic life from static fracture strain only.

CHAPTER 1

INTRODUCTION

1.1 INTRODUCTION TO FATIGUE OF COMPOSITES

Fibre reinforced composites are certainly one of the oldest and most widely used form of composite materials. Their study and development have been largely carried out due to their vast structural applications. The two outstanding features of oriented fibrous composites are their specific strength and stiffness and controlled anisotropy. High specific strength and stiffness make them attractive structural materials where weight saving is at a premium. Controlled anisotropy means that the desired ratio of its properties values in different directions can be easily obtained. Other advantages of fibrous composites include ease of processing and structural forms otherwise inconvenient or impossible to manufacture. Their utilization, therefore, in aerospace and transportation industries is continuously increasing.

Most of the structural elements made of fibrous composites consist of several distinct layers of unidirectional laminae. The unit thus formed from two or more laminae bonded together to act as an integral structural element is called a laminate. Orientations of individual laminae are selected such that the laminate has desired

properties in all directions and meets design strength and stiffness requirements. Analysis and design of a laminate would require a complete knowledge of the behaviour of constituent laminae. A lamina, therefore, represents a basic building block for laminate construction. Thus, it is desirable that all the properties be established for a single ply or lamina. Then, one can use laminate theory to calculate the properties of laminates. However, practical considerations often prevent the construction of single layer test specimen and it becomes necessary to conduct tests on multilayered specimens and use appropriate laminate theory to reduce the results in terms of lamina properties. If the laminates are unidirectional, of course, their behaviour simulates the lamina behaviour. With this in mind, present investigations have been carried out on unidirectional composites.

The superior strength and stiffness of composite materials can be used to full advantages in structural applications only when their behaviour under different loading conditions is properly understood. Any uncertainty in this regard results in the underutilization of material properties by use of unusually large margins of safety in actual design. Keeping this in mind, fatigue behaviour of a unidirectional glass fibre reinforced composite has been studied.

It is well known that when materials are subjected to repeated fluctuating or alternating loads, they fail even though the maximum stress may never exceed the ultimate static strength of the material. In other words, the load cycling reduces the strength of a material, or the fatigue strength of a material is lower than its static strength. This is true of almost all existing materials including metals, plastic and composite materials. In service, the fatigue loads are usually unavoidable, for this reason recent design do not specify static strength alone as a primary design criterion but also include fatigue analysis. The demand for improved performance of structural materials in transportation industries, particularly in aircraft, makes fatigue analysis an important consideration. With this view fatigue of composite materials has been studied by a large number of investigators. Clear design criteria similar to the ones which exist for fatigue of metals have not yet been established. The present investigations are only a step in that direction.

An important feature of the fatigue of composite materials is that composites exhibit evidence of physical damage to the material much before the final fracture. The damage may be in one or more forms such as failure of fibre matrix interface, matrix cracking, fibre breaking and void growth etc. In metals, the appearance of detectable

damage such as a crack, is generally considered unsafe because it rapidly grows to final fracture. In composites, however, it is not necessarily so because although initial damage appears very early in fatigue life, its propogation is not rapid for the major part of the fatigue life. The damage in individual plies generally causes lowering of mechanical properties of the laminate and could eventually lead to its structural failure, e.g., excessive deformation. However, this may happen long before the laminate is in any danger of fracturing. Thus, the definition of failure in composite materials may change from one application to another. In an application, where deformation has to be limited, loss of stiffness by a fixed percentage of the original stiffness is the failure criterion and failure is expected to occur much earlier than in another application in which the separation is the criterion. With metals, the two criteria practically coincide because they exhibit little change in stiffness unless cracking is extensive.

1.2 LITERATURE SURVEY

Investigations of Boller [1, 2] and Davis, McCarthy and Schurb [3] are among the earliest studies on fatigue of fibre reinforced composites. Their studies were performed on glass fibre reinforced plastics

in which several parameters were varied such as fiber content, orientation of fibres, type of weave, type of resin (thermosetting and thermo-plastic), mean stress, temperatures, etc. Although their results are nearly twenty years old, they are still quoted for relative ranking of matrix materials and many other parameters. Broutman and Sahu [4] working with a glass epoxy-cross ply composite were probably the first to recognise that the process of fatigue damage in fibre reinforced composites is progressive. Mechanical properties of these materials progressively deteriorate during fatigue cycling due to internal cracking. Dally and Agarwal [5, 6] confirmed this behaviour and also obtained a quantitative relationship between modulus change and crack density for an E - glass epoxy cross-ply laminate. Glass cloth reinforced polyester resins have also been observed to exhibit similar behaviour [7, 8]. It has been reported that the residual interlaminar shear strength follows the same trend as residual tensile strength. Hahn and Kim [9], while studying fatigue of glass-epoxy angle ply laminates observed that the secant modulus of material decreases due to exposure to fatigue loading and indicated that the decrease in secant modulus is related to internal damage. Phillips and Scott [10, 11] have observed that damage during shear fatigue of unidirectional carbon fibre reinforced epoxy is progressive. More

recently Agarwal and Joneja [12, 13]have reported that damage to unidirectional glass epoxy composite during constant deflection flexural fatigue is also progressive when the specimens loaded in the transverse direction or at 45° to the fibre directions.

There have been several studies [4, 5, 6, 14, 15, 16, 17] to investigate mechanism of damage initiation and propagation during fatigue of composite laminates. It has been established that the damage first initiates by debonding of fibre in the fibre rich region of the plies in which the fibres lie perpendicular to the loading direction. The cracks are known to appear during the first cycle of loading itself even when maximum cyclic stress is only 20% of the ultimate stress [4]. The initial damage in randomly oriented fibrous composites also commences in a similar manner [15]. The initial damage is associated in this case also, with the strands lying perpendicular to the line of load. In cross-ply materials, the cracks in the longitudinal ply and delamination cracks appear much latter in the fatigue life. However, these cracks are responsible for final fracture of the composites [4, 5]. Internal damage to the material during fatigue loading is manifested through changes in structural properties, such as static and dynamic modulus, strength and temperature rise. Attempts have been made to correlate the changes in structural properties with internal damages. Non-destructive

inspection techniques, such as ultrasonics, holographic interferometry, X-ray radiography, etc., are being developed for detection of fatigue damage [18].

Fatigue behaviour of composite materials is influenced by various material and testing variables such as type of matrix, ply orientation, volume fraction of reinforcement, interface condition, type of loading, mean stress, frequency and environment etc. Influence of type of matrix has been studied by Boller [2] and Davis et al[3]. Of the various thermosetting resins commonly used in glass fibre laminates, the best fatigue properties are obtained with epoxy resins. Superiority of epoxy resin is attributed due to their inherent toughness and durability. Fatigue strength of composites increases with increasing glass content both in axial fatigue and rotating bending fatigue [7, 8]. Hofer et al studied the effect of interfacial bond strength on the fatigue of composites [19]. The influence of mean stress on fatigue strength has been studied by many investigators[1, 7, 15, 16, 20]. For a fixed cyclic life fatigue strength of composite decreases as the mean stress increases, as in metals. The fatigue life of fibre reinforced epoxy and polyester is only modestly influenced by the frequency effects [21]. This insensitivity of the fatigue life to the frequency and resulting temperature rise is probably due to the fact that the properties of

glass fibres, which are the primary load bearing members in the composites, remain unaffected at these temperatures. Phillips, Scott and Buckley [22] studied the effect of moisture on the shear fatigue of carbon fibre, glass fibre and Kevlar - 49 fibre reinforced epoxy resins and observed that absorbed water causes significant decrease in their strengths.

An almost infinite variety of laminates can be used for structural applications. Once it has been decided to use a specific laminate one may obtain its fatigue characteristics through experiments. However, the experimental methods can be used to obtain guidelines for choice of some simple equations which can be used in design analysis. Broutman and Sahu [23] have proposed a theory to predict loss of strength due to fatigue. Agarwal and Dally [6] and Hahn and Kim [9] have proposed linear relationships between cyclic stress and fatigue life. However, these theories [6, 9, 23] cannot be used in design analysis because they predict fatigue strength of a laminate only in a specific direction and do not predict the angular dependence of fatigue strength.

To the best of the author's knowledge only a few studies have been performed to develop failure theory for fatigue strength of laminates. Hashin and Rotem [24] have proposed that ratio of fatigue strength to static strength is

a function of stress ratio in fatigue cycling, fatigue life, frequency of load cycling and the fibre orientation. The function can be determined through limited experiments and, then, can be used to predict the fatigue strength. Their limited experiments show good agreement with their prediction. Sims and Brogdon [25] have extended the Tsai - Hill [26] failure theory for static strength to fatigue strength. Their work has shown that the Tsai - Hill failure theory may be adopted to predict the angular dependence of fatigue strength. Different possibilities in this regard have been explored in the present work.

Different reviews[27, 28, 29, 30] on fatigue of composite materials have been very helpful in selecting the present problem for investigation.

1.3 PRESENT WORK

In the present work unidirectional composite plates were fabricated by hand layout technique in the laboratory. It was decided to perform the fatigue tests in alternating bending because real structures are more often subjected to bending stresses and also because very little work appears to have been done on flexural fatigue of composites. Two testing machines were designed and fabricated. The experimental details along with static material characterization have been discussed in Chapter 2.

Fatigue tests were performed on specimens in which fibres were oriented at 0, 10, 45 and 90 degree to the longitudinal edge. For each fibre orientation different displacement limits were selected so that fatigue life of specimen varied from less than 1000 to more than a million cycles. Measurements have been made to study and analyse progressive fatigue damage of specimens. The fatigue results are discussed in Chapter 3. Different failure theories have been examined in Chapter 4. Conclusions drawn from the investigations and some suggestions for future work have been given in Chapter 5.

CHAPTER 2

TESTING SYSTEMS AND MATERIALS: DESIGN, FABRICATION AND CHARACTERIZATION

2.1 TESTING SYSTEMS

In many applications, fibre reinforced composites are subjected to primarily bending loads. For a more realistic understanding of material behaviour, it is desirable that they are characterised through flexural tests. It was therefore decided to conduct fatigue tests on composite materials in flexural mode. Out of the fatigue testing machines available in this country none could be used for the purpose. Therefore, two fatigue testing machines were designed, fabricated, instrumented and used in the present studies. It is known that the ratio of static strengths in the longitudinal and transverse directions of a unidirectional composite material depends upon the type and the volume fraction of fibres and it is large for composites of practical importance. Since the fatigue tests were to be performed in the longitudinal as well as transverse directions, it was deemed appropriate to design separate machines. Moreover, availability of two machines greatly reduced overall testing time. Basic design of both the machines was same. Design and dimensions of some components and linkages were changed to suit different specimens in cyclic

bending. The specimens were fixed at one end while the other end was cycled between known transverse displacement limits (displacements perpendicular to the plane of the specimen) with zero mean displacement. This cycling produces alternating tensile and compressive bending stresses in the specimen. Schematic diagram of testing machines is shown in Fig. 2.1. One end of the specimen is fixed in grips which in turn are mounted on a dynamometer. The grips can be removed and replaced by another set to suit any specimen dimensions. Grips were designed to ensure proper gripping and alignment of the specimens. Schematic diagram of the grips is shown in Fig. 2.2.

The dynamometers, on which the grips are mounted, have been designed and fabricated so that they are used to measure the bending moment at the fixed end of specimens. In the low capacity machine in which small bending moments are expected to be encountered, a simple octagonal ring type dynamometer is provided. In the high capacity machine a sturdier extended ring type dynamometer is provided. Each dynamometer employs four electrical resistance strain gauges K-5-118 (a product of Rohits and Company, India) protected from environment. Schematic diagrams of the two dynamometers along with the positions of strain gauges are shown in Fig. 2.3. The strain gauges have been connected to form Wheatstone bridge (also shown in Fig. 2.3) such

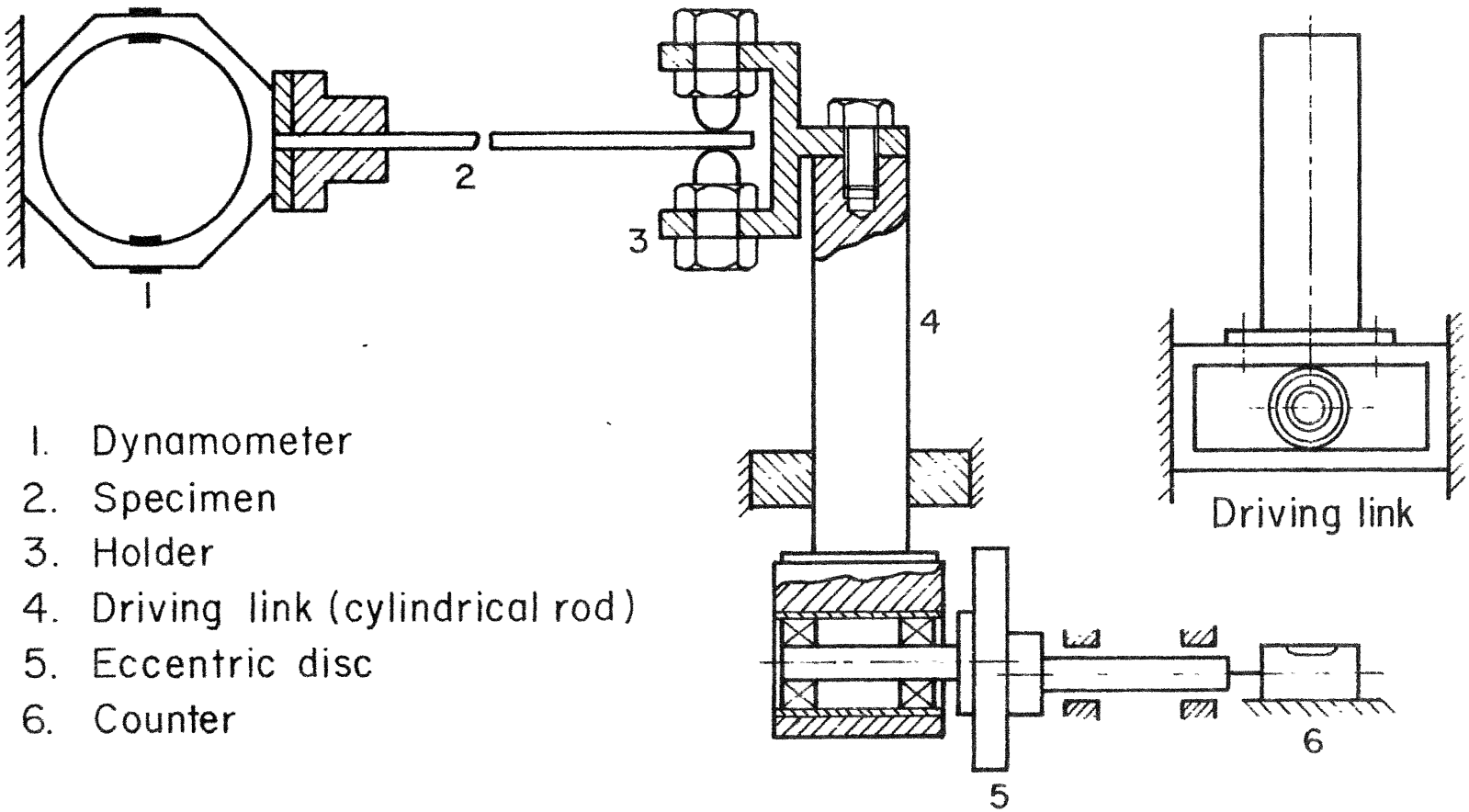

Fig. 2.1 Schematic diagram of flexural fatigue testing machine

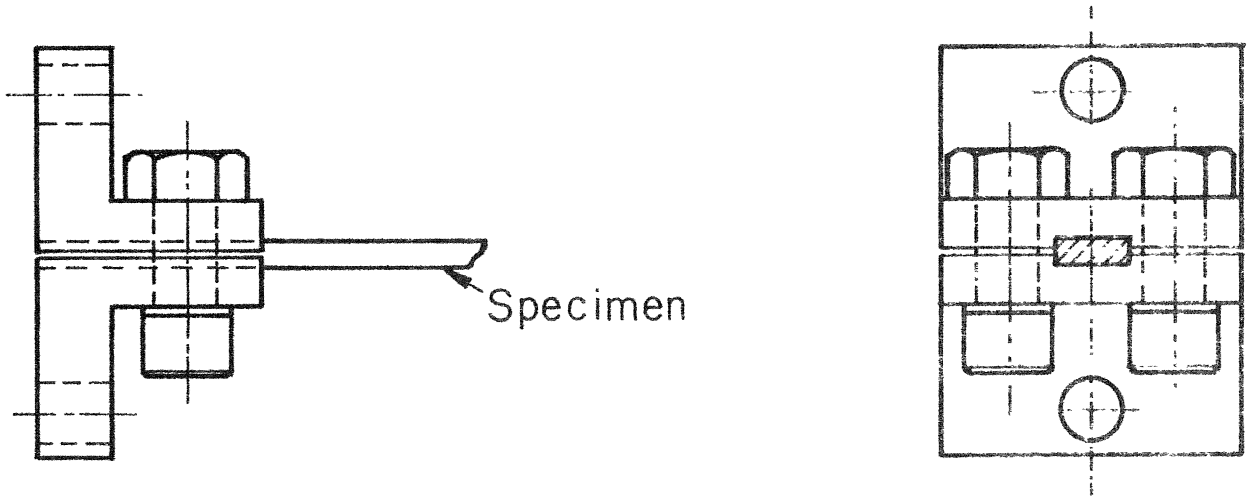

Fig. 2.2 Schematic diagram of the grips at the fixed end

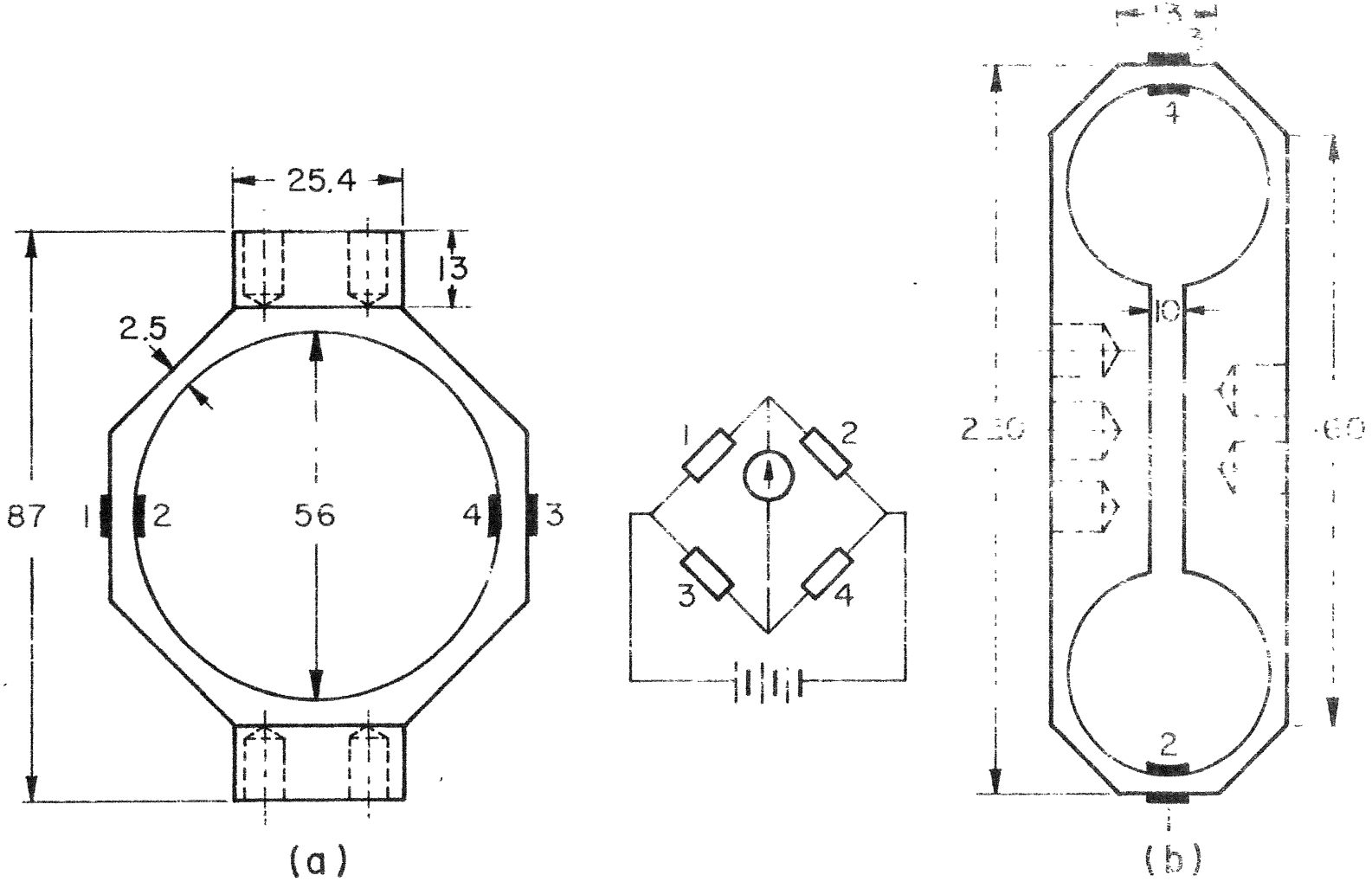

Fig. 2.3 Schematic diagram of (a) ring and (b) extended ring type dynamometers

that the output of the bridge is proportional to bending moment at the fixed end. Since arms of the bridges have active identical gauges, the bridges are automatically temperature compensated. The output of the bridge is measured by means of Budd strain indicator. The output can be read directly in the strain indicator or it can be displayed in an oscilloscope or recorded in a visicorder or any other recording instrument. The dynamometers were calibrated using a thick mild steel specimen. Increasing loads through standard weights were applied at a known distance from fixed end. Bending moment at the fixed end was calculated from the geometry. Plots of the dynamometer outputs are shown as a function of calculated bending moment in Figs. 2.4 (a) and 2.4 (b). It can be seen that the calibration curves are linear upto the applied bending moments which are much more than the bending moments expected during the fatigue tests. Further, through approximate calculations based on endurance limit of dynamometer material, it was established that the maximum allowable bending moment for the low capacity ring type dynamometer is 5 N-m and that for the extended ring type dynamometer is 100 N-m. It was also established that the natural frequencies of two dynamometers are much smaller than the expected frequencies of fatigue cycling.

Each dynamometer is mounted on a rigid column with its base fixed in the foundation. The dynamometers

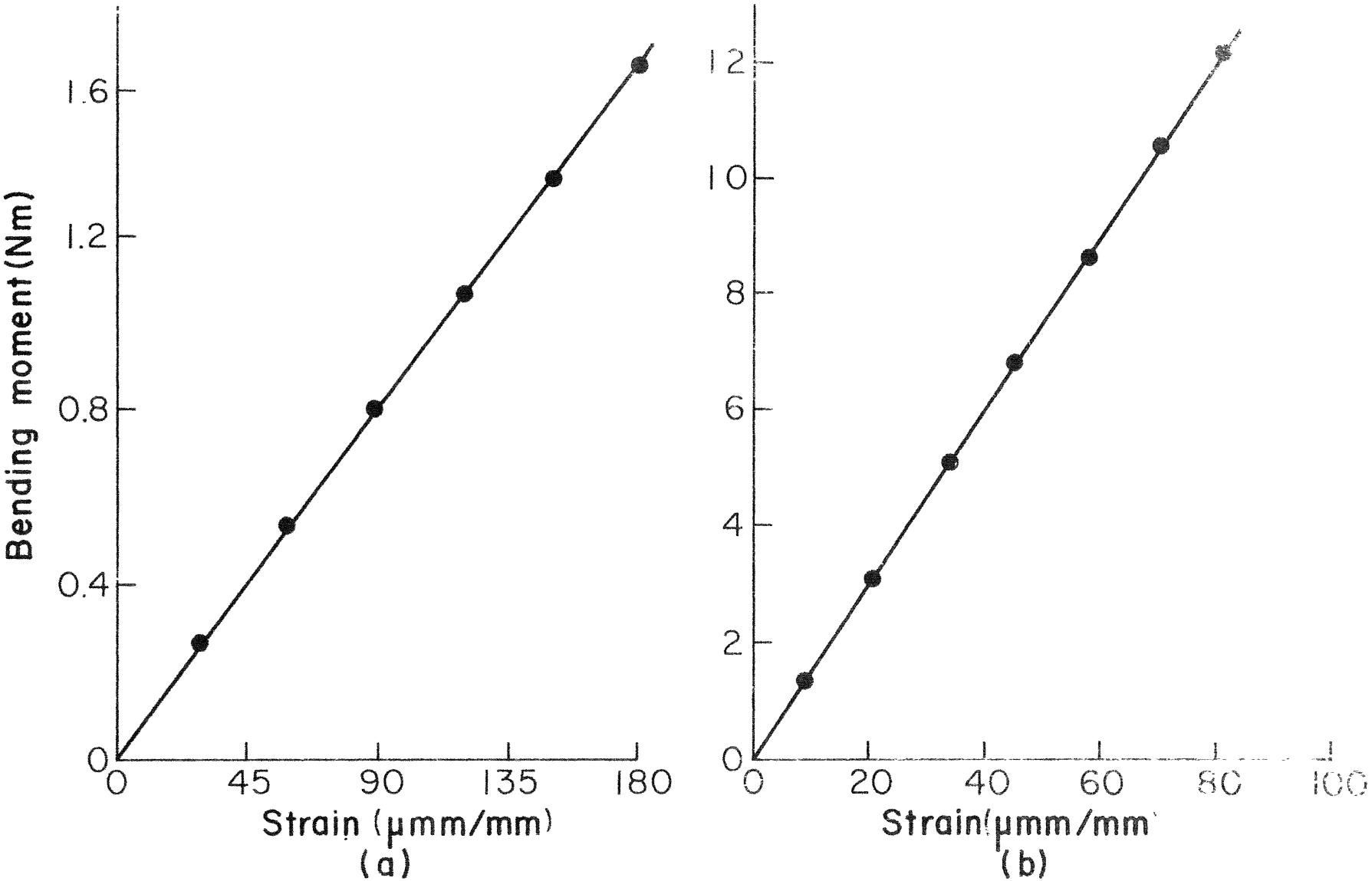

Fig. 2.4 Calibration curves for (a) ring and (b) extended ring dynamometers

are mounted by means of screws and can be removed if necessary.

The second end of the specimen is placed in a specimen holder through which transverse displacement is provided to this end. For the low capacity machine in which only small displacements are given to the specimens, the specimen holder has a simple design as shown in Fig. 2.5 (a). It consists of a rigid fork type frame with two screws having rounded ends. The screws are made to touch the top and the bottom surfaces of the specimen in its natural position and locked in the position through locknuts so that the position does not get disturbed during fatigue cycling. Care is taken to see that the screws do not press hard against the specimens and permit relative slip during bending so that no axial strain is introduced in the specimens. In the high capacity machine larger displacements are given to the specimens for producing high stresses in the specimens. These large displacements cause free end of the specimen to deform to a finite curvature. In order to avoid axial strain in such cases it is necessary that the point of loading is permitted to shift slightly along the length of the specimen. This has been achieved by placing the specimen$ between two cylindrical rollers which are free to rotate in the bearings whereas the bearing themselves are free to move back and forth in the T - slots provided in

the specimen holder. The schematic diagram of this type of specimen holder is shown in Fig. 2.5 (b). Positions of the rollers in the undeformed and deformed states of specimen are schematically shown in Fig. 2.5 (c, d). It is clear that if the rollers were fixed in positions they could cause axial strain as well as compressive stress normal to the plane of the plate which can cause transverse splitting due to Poisson's effect.

The specimen holder is mounted on a cylindrical rod which is moved up and down through a guide. Vertical motion to the rod is provided through a circular pin eccentrically mounted on a rotating disc. Motion of the pin is transferred to the rod through bearings mounted on the pins. The bearings are free to rotate on the pin and they move a rectangular guide rigidly connected to the vertical rod. Since bearing can freely move in smooth horizontal surfaces of the guide, the horizontal movement of the pin is not transferred to the rod and only its vertical moment is transferred to the rod. The amplitude of displacement of the rod (and also of the specimen) from neutral position is equal to the eccentricity of the pin. Thus, amplitude of displacement can be changed by changing the eccentricity of the pin. Rotations of the guide about horizontal axes are suppressed by providing adequate constraints. Details of the driving link (rectangular guide and pin) are illustrated through a separate

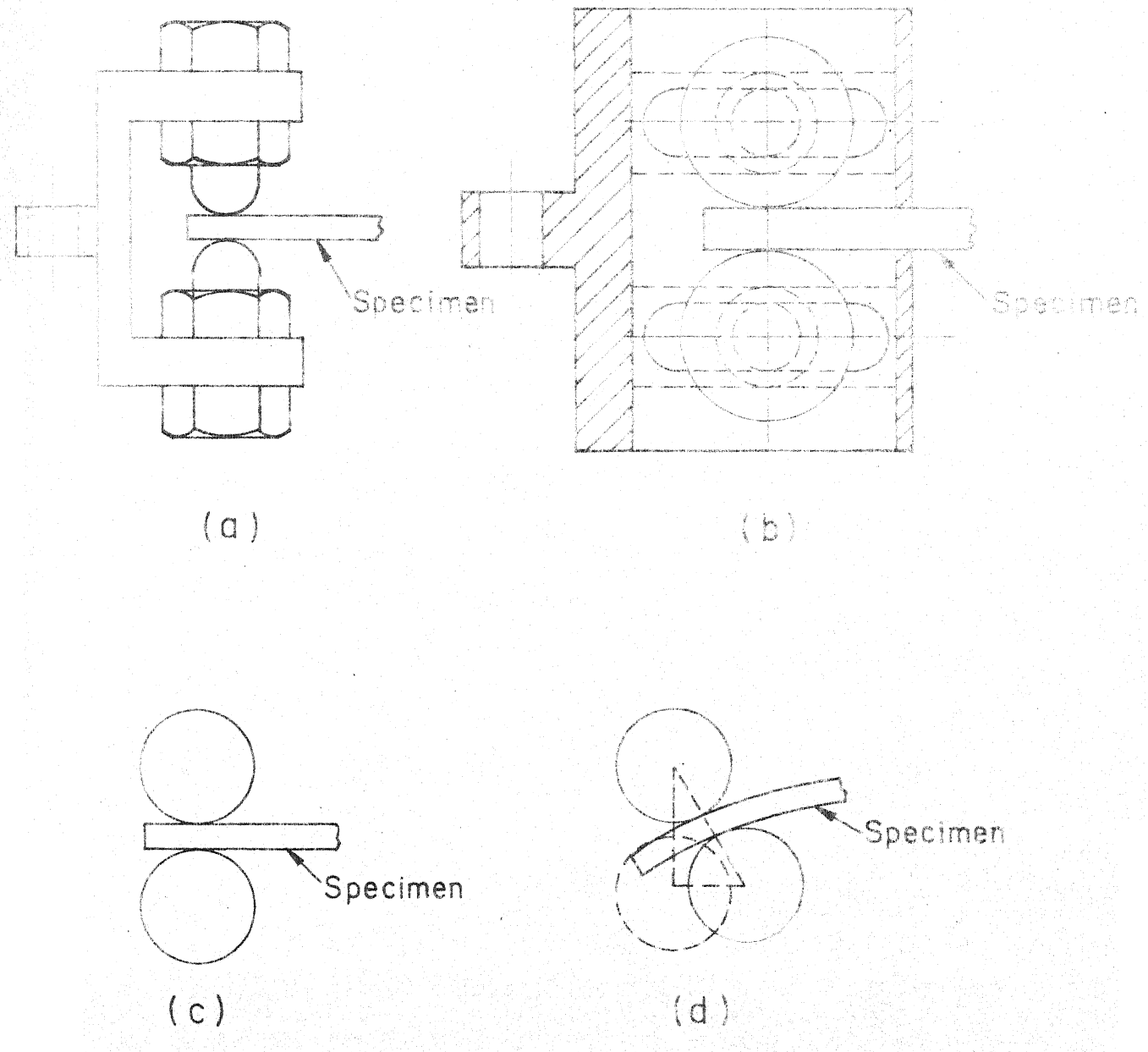

Fig. 2.5 Schematic diagrams of specimen holders (a) low capacity machine and (b) high capacity machine; position of the rollers with specimens (c) undeformed and (d) deformed (dotted circle shows the position if the roller axes were fixed

diagram in Fig. 2.1. It may be noted that the vertical motion of the specimen end thus obtained is simple harmonic so that the changes in velocity and acceleration are smooth.

Drive to the disc is provided by an electrical motor. In case of low capacity machine the disc is directly mounted on a 1/8 H.P. A.C./D.C. motor. In case of high capacity machine the drive is provided through a belt and pulley arrangement. In this case the disc is quite thick and acts also as a flywheel to smoothen the motion. Speed of the motor in low capacity machine can be varied continuously from a very low speed to 4000 rpm with the help of auto-transformer. In case of high capacity machine it can be changed by changing the size of the pulley on the motor shaft. Fatigue tests in all cases were carried out at low speeds which cause no significant heating of the specimens. Digital counters were employed to register the number of cycles.

Photographs showing overall views of the two machines are shown in Figs. 2.6 and 2.7. Some important components of the machines are shown in Fig. 2.8.

2.2 MATERIAL FABRICATION

Present studies were performed on a continuous E - glass fibre (a product of Fibre Glass Pilkington of India Ltd.) reinforced epoxy resin Araldite LY 553 cured

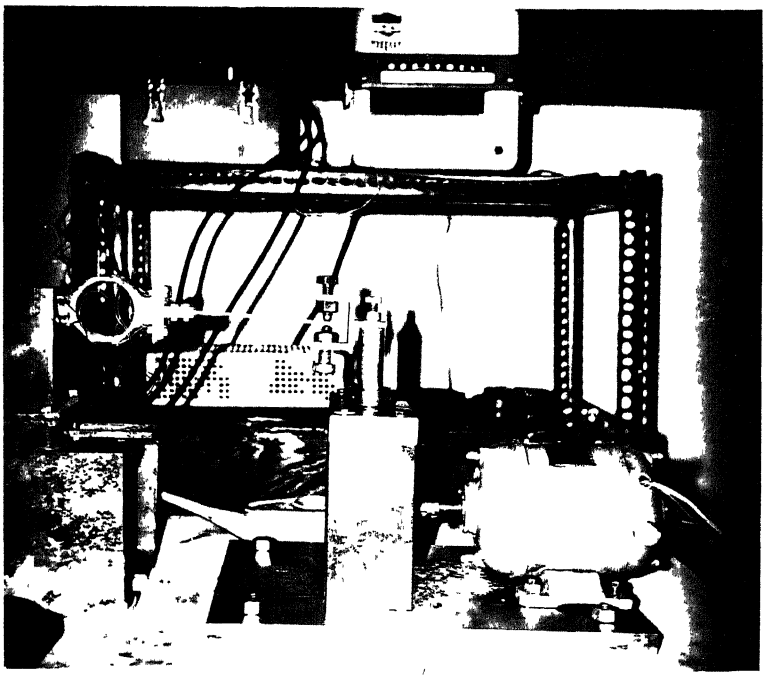

Fig.2.6 Overall view of the low capacity flexural fatigue testing machine

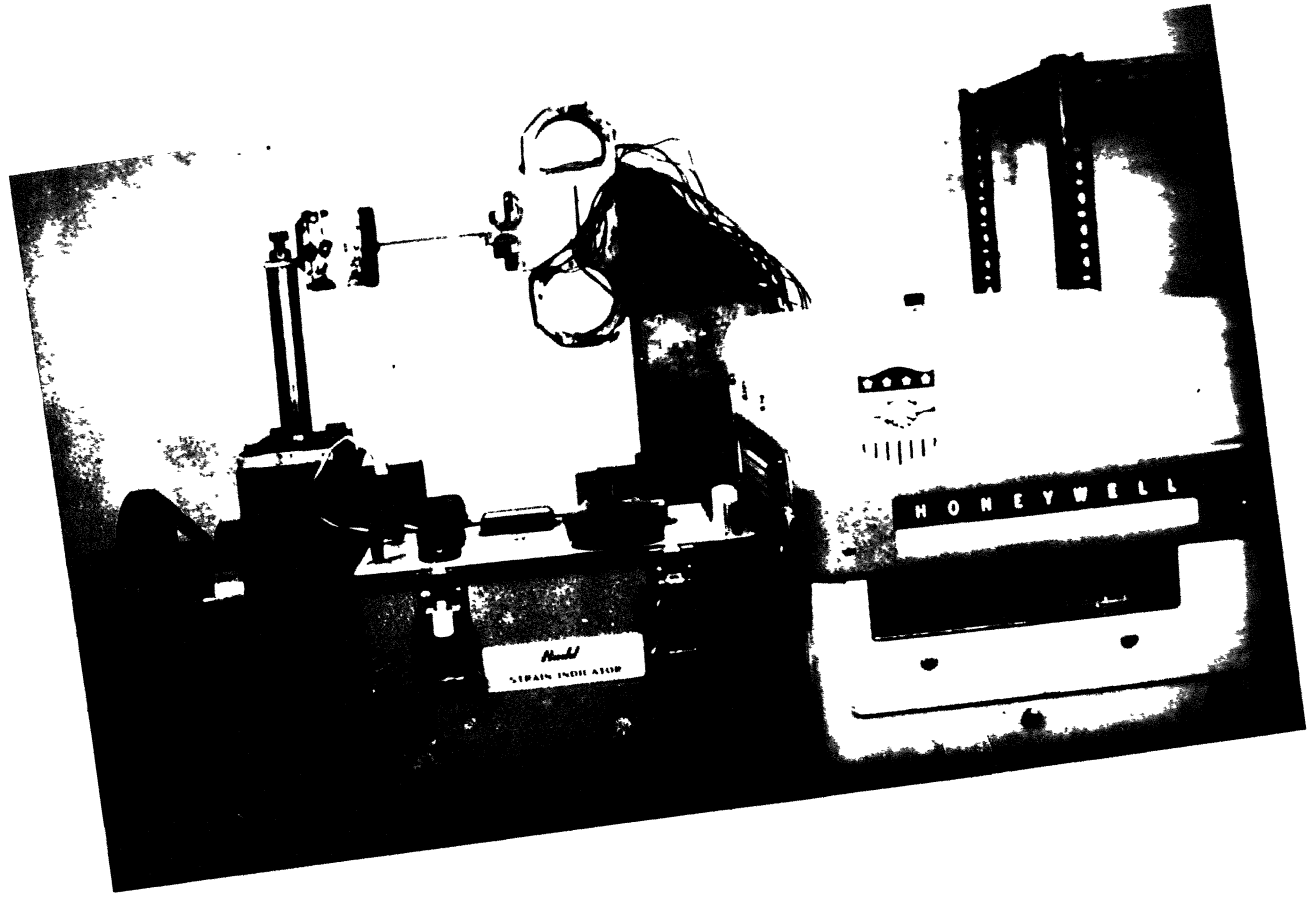

Fig.2.7 Overall view of the high capacity flexural fatigue testing machine

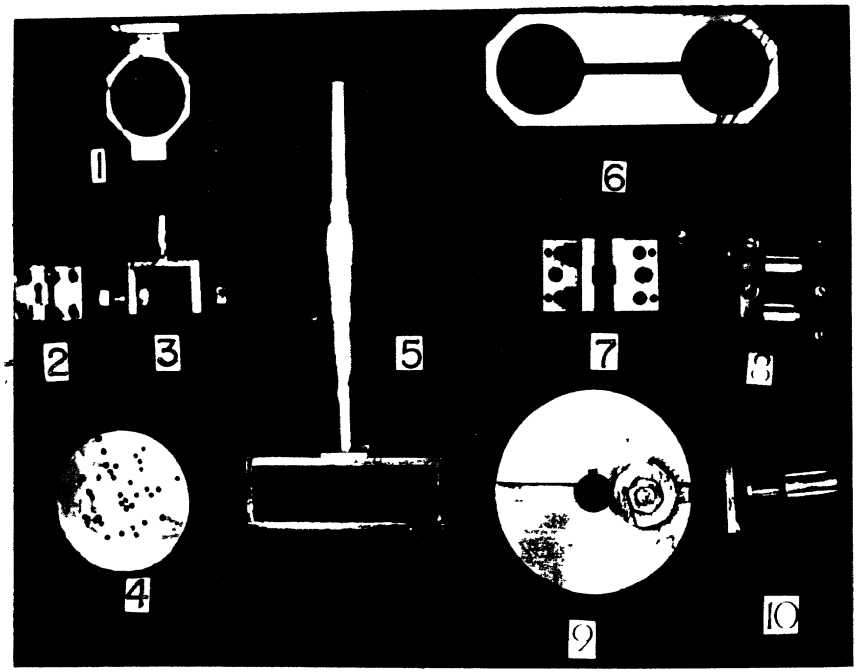

Low capacity machine

1. Dynamometer
2. Grips
3. Specimen holder
4. Rotating disc

High capacity machine

5. Rectangular guide with vertical rod
6. Extended ring dynamometer
7. Grips
8. Specimen holder with rollers
9. Rotating disc with balancing weight
10. Crank pin

Fig. 2.8 Components of the fatigue testing machines

by a hardener designated as HY 551 (Products of CIBA Greigry India Ltd.). Glass epoxy system is probably the most widely used fibre reinforced material. Unidirectional prepregs of glass epoxy are not commercially available in India. It was, therefore, decided to fabricate the material in the laboratory to maintain a good quality control of the material.

Plates of unidirectional composite were cast between two 30 mm thick mild steel mould plates separated by washers of 3.3 mm thickness. A rectangular frame whose inner dimensions are larger than the mould plates, was fabricated from a 12 mm thick aluminium flat. Two rows of equispaced screws have been provided on the opposite sides of the frame. This frame has been used for laying the fibres unidirectionally as shown schematically in Fig. 2.9. Screws act as pegs for fibres during winding and can withstand tension in fibres. Untwisted fibres from the roving were laid down uniformly over the required area of the frame. The fibres were laid down three times over the area to achieve required thickness of the plate. After laying the fibres, the frame is placed around the lower mould plate so that the fibres are on top surface of the plate. Nearly one-third of the total resin mixed with curing agent was spread on top surface of mould plate before placing the fibres and the remaining is poured on the fibres and spread

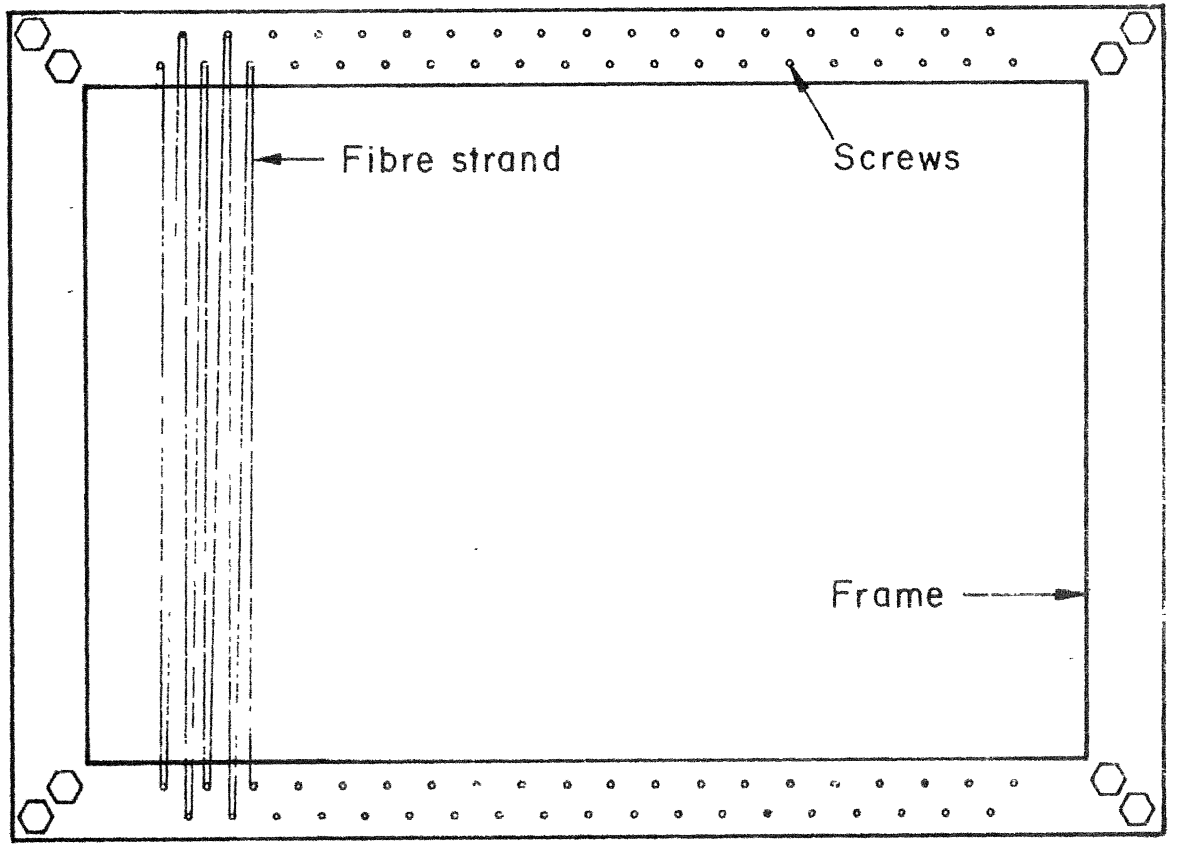

Fig. 2.9 Frame for fibre winding

by brushing it gently. To enhance wetting, the matrix was tapped and dabbed with spatula. The material was gently rolled with a rubber roller after placing a mylar sheet on the top. This removes the entrapped air. The second mould plate is then placed on the top. The top mould plate rests on the separating washers so that the thickness of the plate being cast is the same as the thickness of the washers. The mould plate applies a uniform pressure due to its own weight and due to tightening of nuts on the bolts going through both the mould plates. Excess resin gets squeezed out to the sides. With the help of a dial gauge, it is ensured at different stages that the surfaces of the mould plates are horizontal and do not deform at any position. A good surface finished of composite plates is obtained by placing mylar sheets on the faces of both mould plates. Figure 2.10 (a) shows lower mould plate and frame around it before placing the top mould plate. Figure 2.10 (b) shows a cured plate before being removed from the frame.

The plates were cured at room temperature for two days and post cured in an oven at 80 ^{o}C for 4 hours. The cured plates exhibit 42% glass fibres by weight (approximate volume fraction equal to 25%). Variation in the thickness of the cured plate was found to be small except near the edges which were discarded. The plates obtained have a uniform distribution of fibres. Photomicrograph

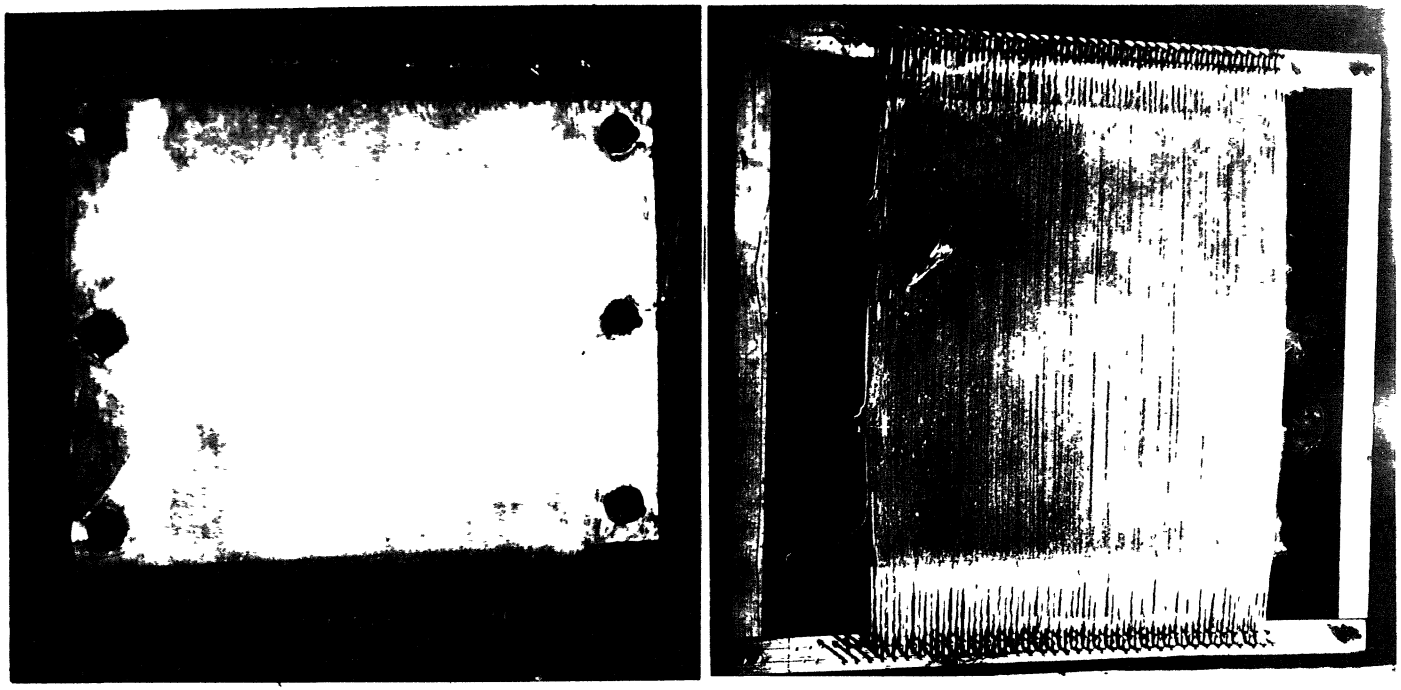

(a) (b)

Fig. 2.10 (a) Fibre wound on the frame placed around the lower mould plate and

(b) cured plate before being removed from the frame

of a typical cross-section of a specimen is shown in Fig. 2.11.

Rectangular specimens were cut from the plates by keeping fibres at 0, 10, 45 and 90 degree to the longitudinal edge of the specimens. Edges of the specimens were finished in a routing machine. Size of the specimens with different fibre orientation have been discussed in a later section.

2.3 MATERIAL CHARACTERIZATION

Elastic constants and static strength of the material were obtained in tension as well as in bending. Static tension tests were performed on straight sided specimens with end tabs in an Instron machine. Load cell recorded the applied load whereas strains were measured by means of electrical resistance strain gauges fixed on the specimens. Elastic moduli in the longitudinal and transverse directions, Poisson's ratio (ν_{LT}) and longitudinal and transverse tensile strengths were obtained through tension tests on specimens with fibers parallel and perpendicular to the applied load. Shear modulus (G_{LT}) and shear strength (τ_{LTU}) were obtained indirectly by conducting tension tests on off-axis specimens in which off-axis modulus and strength were evaluated. From the knowledge of an off-axis modulus, E_x, shear modulus, G_{LT}, can be calculated using the following transformation equation:

Fig. 2.11 Photo-micrograph of a typical cross-section of a specimen

$$\frac{1}{E_X} = \frac{1}{E_L}\,\mathrm{Cos}^4\,\theta + \frac{1}{E_T}\,\mathrm{Sin}^4\,\theta + \frac{1}{4}\left(\frac{1}{G_{LT}} - \frac{2\,\nu_{LT}}{E_L}\right)\mathrm{Sin}^2\,2\,\theta \qquad (2.1)$$

where E_L and E_T are elastic moduli in longitudinal and transverse directions and θ is the angle between the fibres and the load axis. For calculating shear strength, it was observed that the off-axis specimens loaded in tension fail due to matrix failure alone in tension and or in shear. Thus, from the knowledge of an off-axis tensile strength, shear strength can be calculated using the following failure criterion:

$$\frac{\mathrm{Sin}^4\,\theta}{\sigma^2_{TU}} + \frac{\mathrm{Sin}^2\,\theta}{\tau^2_{LTU}} = \frac{1}{\sigma^2_{XU}} \qquad (2.2)$$

where σ_{TU} and σ_{XU} are transverse and off-axis tensile strengths. This criterion can be obtained from the maximum work failure criterion for composite materials by neglecting terms arising due to fibre failure. Hashin and Rotem [24] have found that this criterion accurately predicts off-axis strength. In the present work, off-axis tension tests were conducted on specimens with fibre orientations of 10 and 45 degree. Values of shear strength calculated from off-axis tensile strengths with different fibre orientations were found to be within 3 percent of each other. Average properties of material are shown in table 2.1. Properties are an average of values obtained from at least three

Table 2.1: Average Properties of the Material in Tension and Flexure

Properties	Tensile	Flexural
Longitudinal modulus, E_L (GN/m^2)	32.17	19.86
Transverse modulus, E_T (GN/m^2)	8.28	5.36
Shear modulus, G_{LT} (GN/m^2)	4.75	2.49
Poisson's ratio, ν_{LT}	0.366	-
Longitudinal strength, σ_{LU} (MN/m^2)	381.80	400.00
Transverse strength, σ_{TU} (MN/m^2)	25.10	36.00
Shear strength, τ_{LTU} (MN/m^2)	35.45	33.18

different specimens in each case. It was observed that the variation in properties for different specimens is within the expected accuracy of experimental measurements. This indicated uniform quality of material fabricated. It was also observed that the tensile stress-strain curves for all fibre orientations are nearly linear upto failure.

Flexural tests were performed on the machine designed and fabricated for fatigue testing. Flat specimens were fixed at one end and the load was applied to the other end. Bending moment at fixed end was measured by means of dynamometer and the deflection at the free end was measured with the help of a unislide which has a least-count of .05 mm. Elastic modulus in bending was calculated from the following expression

$$E = \frac{M}{\delta} \frac{l^2}{3I} \qquad (2.3)$$

where $\frac{M}{\delta}$ is initial slope of bending moment versus displacement curve, l is the free length of the specimen and I moment of inertia of the cross-section of the beam with respect to neutral axis. When the tests are conducted on the off-axis specimens the off-axis modulus calculated from Eq. (2.3) has a small error as will be discussed in a later section. However, length to width ratio was kept to make the error negligible. Shear modulus in bending also was calculated from the knowledge of off-axis modulus using transformation Eq. (2.1).

Flexural strength is calculated from the knowledge of bending moment at failure. The following equation was used to calculate the flexural strength

$$\sigma_U = \frac{M_U}{I} \cdot \frac{h}{2} \qquad (2.4)$$

where M_U is the maximum bending moment, and h is the thickness of the specimen. Again, the error in off-axis strength are negligible because the length to width ratio was large. Shear strength in bending was obtained from knowledge of off-axis strength using Eq. (2.2). Flexural properties of material are also given in Table 2.1.

2.4 ANALYSIS OF OFF-AXIS SPECIMEN DIMENSIONS

It is known that the off-axis specimens in flexure as well as in tension show shear coupling effects and hence present difficulties in achieving desired boundary conditions. Halpin et al [31] and Whitney and Dauksys [32] have shown that when it is desired to perform tests on off-axis specimens the results may be significantly affected by the shear coupling effects. The effects of shear coupling, however, can be reduced by selecting proper dimensions of the specimen. In the present case the specimen dimensions have been selected such that the error in the measurement of bending modulus is less than five percent.

Whitney and Dauksys' analysis [32] of a three point bending off-axis specimen has been modified to obtain

appropriate dimensions for a cantilever specimen. Whitney's analysis is based on comparing the deflection calculated from exact laminated plate theory and from Euler - Bernoulli theory. In case of cantilever, the following relation between the apparent modulus as calculated from the free end deflection using Euler-Bernoulli theory and the actual bending modulus can be obtained by equating measured deflections to the deflection predicted by laminated plate theory:

$$E_{XA} = \frac{E_X}{[1 - R\,(|\bar{S}_{16}| - R\,\bar{S}_{12})\,E_X]} \qquad (2.5)$$

where $R = \frac{b}{2l}$ with b being width and l being length of the cantilever beam. $\bar{S}_{16}$ and $\bar{S}_{12}$ are elements of compliance matrix referred to the beam axis and are given in terms of elastic constants in principal directions, by the following equations:

$$\bar{S}_{12} = \frac{\mathrm{Cos}^2\theta}{E_L} + \left(\frac{1}{G_{LT}} - \frac{2\nu_{TL}}{E_T}\right)\mathrm{Sin}^2\theta\,\mathrm{Cos}^2\theta + \frac{\mathrm{Sin}^4\theta}{E_T} \qquad (2.6)$$

$$\bar{S}_{16} = \left(\frac{2}{E_L} + 2\frac{\nu_{TL}}{E_T} - \frac{1}{G_{LT}}\right)\mathrm{Sin}\,\theta\,\mathrm{Cos}^3\theta - \left(\frac{2}{E_T} + \frac{2\nu_{TL}}{E_T} - \frac{1}{G_{LT}}\right)\mathrm{Sin}^3\theta\,\mathrm{Cos}\,\theta \qquad (2.7)$$

where θ is the angle between the specimen axis and the fibre direction.

Off-axis tests were conducted with fibre orientation of 10 and 45 degree. Value of R was kept 0.048 for

45° specimens and 0.054 for 10° specimens. Table 2.2 shows that the ratio of apparent to actual modulus is close to one in both cases. Thus, the selected specimen dimensions were assumed to be appropriate. Specimens dimensions for off-axis as well as longitudinal and transverse specimens are shown in Fig. 2.12.

Table 2.2: Ratio of Apparent to Actual Modulus for Off-Axis Specimens

θ (degree)	R	$\bar{S}_{12}$ (m^2/GN)	$\bar{S}_{16}$ (m^2/GN)	$\frac{E_{XA}}{E_X}$
10	0.054	0.013	0.026	1.04
45	0.048	0.028	0.045	1.02

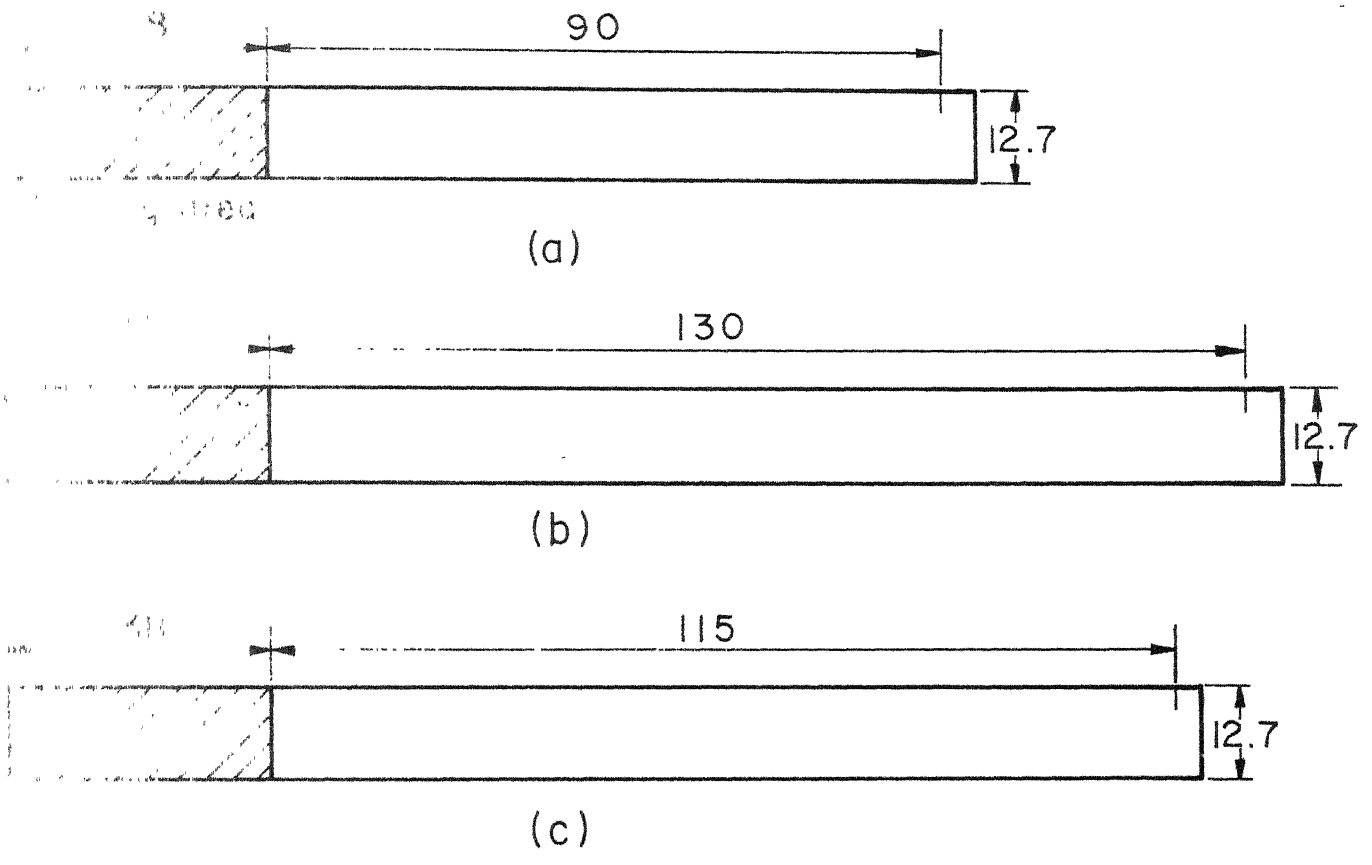

Thickness = 3.3

Dimensions are in mm

Dimensions of test specimens (a) longitudinal and transverse, (b) 45° and (c) 10°

CHAPTER III

FATIGUE TESTS: RESULTS AND DISCUSSIONS

With a view of developing understanding of fatigue behaviour of unidirectional composites in an arbitrary direction, fatigue behaviour of the glass fibre reinforced epoxy has been studied along the natural material axes (longitudinal and transverse) and along two off-axis directions. Fiber orientations selected for the off-axis tests were 10 and 45 degree. Flexural fatigue tests were performed on flat specimens prepared from the material fabricated in the laboratory. One end of the specimen was fixed while the other end was cycled between known displacement limits with zero mean displacement. For each fibre orientation, four different displacement limits were selected so that fatigue life varied from less than one thousand to more than a million cycles. When a specimen did not break at 10^6 cycles, the test was discontinued and the specimen was assumed to be a runout. Bending moment at the fixed end was measured by means of a dynamometer and was recorded at desired intervals without interrupting the fatigue tests. For each fibre orientation records of bending moment have been used to obtain several (S - N) curves each of which represents a fixed stage of fatigue damage. Fraction of the stiffness retained by the specimen during fatigue cycling has been taken a measure of fatigue damage. The

stiffness retained has been calculated from the ratio of instantaneous bending moment to the bending moment in first loading cycle.

Progressive fatigue damage of specimens has been further investigated by cycling additional specimens to different fractions of fatigue life for all displacements in each orientation. Static flexural tests to failure were conducted on these precycled specimens. The residual stiffness and the residual strength were measured to study the effect of fatigue cycling on the static properties of the specimens.

3.1 LONGITUDINAL FATIGUE BEHAVIOUR

Longitudinal fatigue strength is obtained by conducting tests on specimens having fibres parallel to the axis of the specimen. In the present investigations, longitudinal fatigue specimens (dimensions shown in Fig. 2.12) were subjected to four different displacement amplitudes namely 23.5, 27, 33 and 44 mm which produce strain amplitudes of 0.77, 0.88, 1.07 and 1.35 percent respectively at the fixed end of the specimens. The tests were performed on high capacity machine at frequencies between 6 and 8 Hz.

Results of fatigue tests on longitudinal specimens are given in Table 3.1 and shown graphically in Fig. 3.1. Each point in the figure corresponds to one specimen.

Table 3.1: Fatigue Life of Longitudinal Specimens at Different Strain Amplitudes

N_f			
ε = 0.77%	ε = 0.88%	ε = 1.07%	ε = 1.35%
1,070,000	334,508	7,320	202
940,050	332,709	6,248	178
929,021	330,040	5,863	163
722,105	320,500	4,908	150
724,758	190,502	4,553	132
	168,103	4,184	102
	110,527	3,551	93
15 Runouts	89,255	2,960	85
at one	74,848	2,698	83
million	60,114	2,187	76
cycles	53,050	1,921	74
	50,131	1,902	72
	45,540	1,498	71
	44,050	1,390	68
	43,525	1,205	64
	37,351	1,120	49
	34,509	990	46
	33,750	931	45
	33,512	853	40
	32,228	754	25

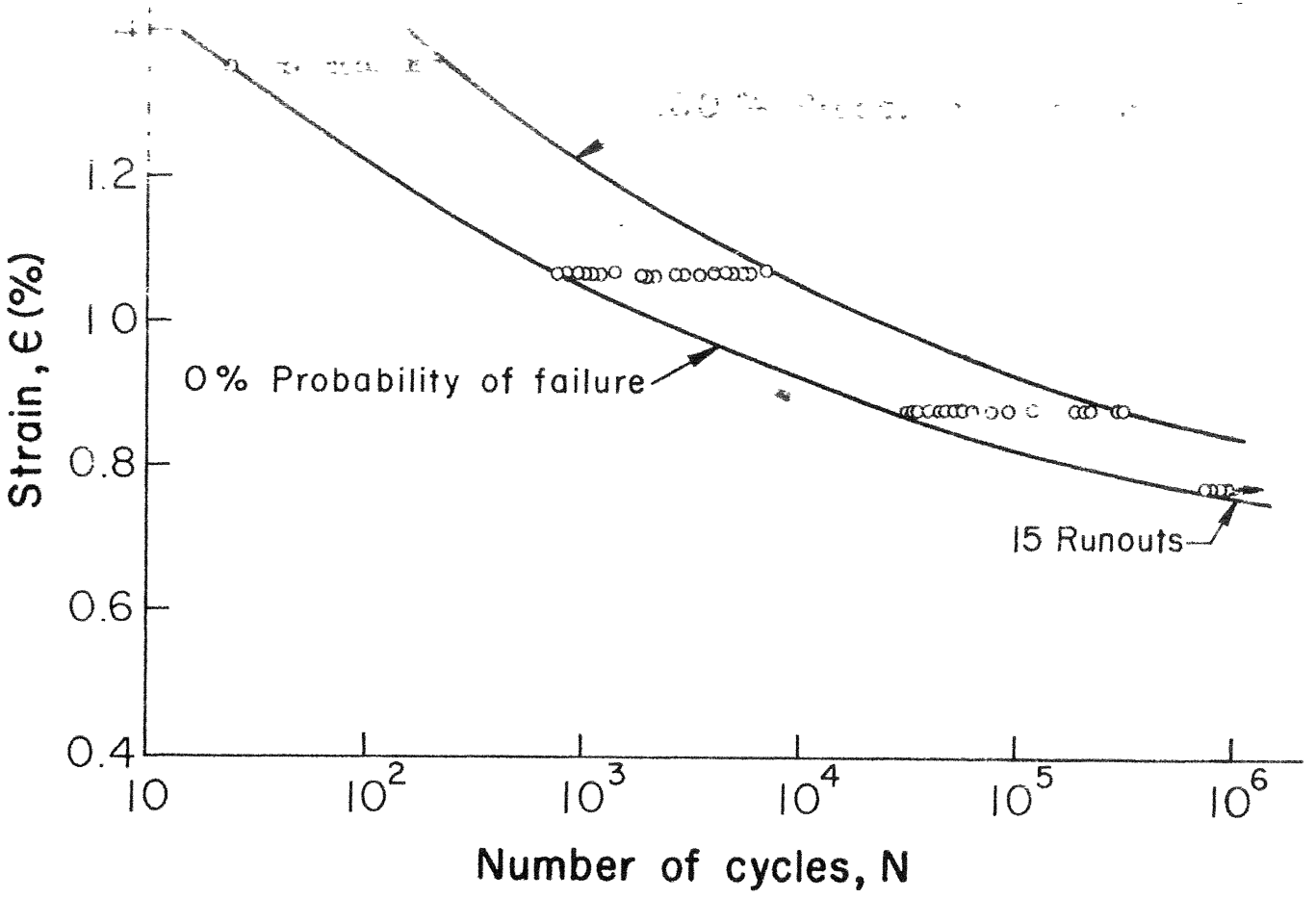

Fig. 3.1 Strain vs fatigue life curves for longitudinal specimens

and the cyclic life corresponds to total fracture or the separation of the specimen. It is observed that the fatigue life varies between twenty cycles to more than 10^6 cycles. General nature of the curve is as expected in that the fatigue life increases as the cyclic strain decreases. The two solid curves indicate 0 and 100 percent probability of failure. It is observed that the two curves are nearly one decade apart, that is, at all strain levels there is a scatter of one order of magnitude in fatigue life.

Bending moment at the fixed end of the specimens was measured at desired intervals during fatigue cycling and recorded on a Visicorder. This was done for several specimens in each set of specimen tested at a fixed strain amplitude. Typical variation in cyclic bending moment normalised with respect to the first cycle bending moment is shown in Fig. 3.2 as a function of fraction of fatigue life. It is observed that for all strain limits cyclic bending moment continuously decreases. The normalised bending moment represents fraction of stiffness retained by the specimens. Fig. 3.2 shows that the specimens subjected to smaller strain amplitudes (larger life) lose greater fraction of stiffness at relatively smaller fraction of fatigue life in the initial stages of fatigue cycling whereas the specimens subjected to larger strain amplitudes show a more gradual loss of stiffness for most part

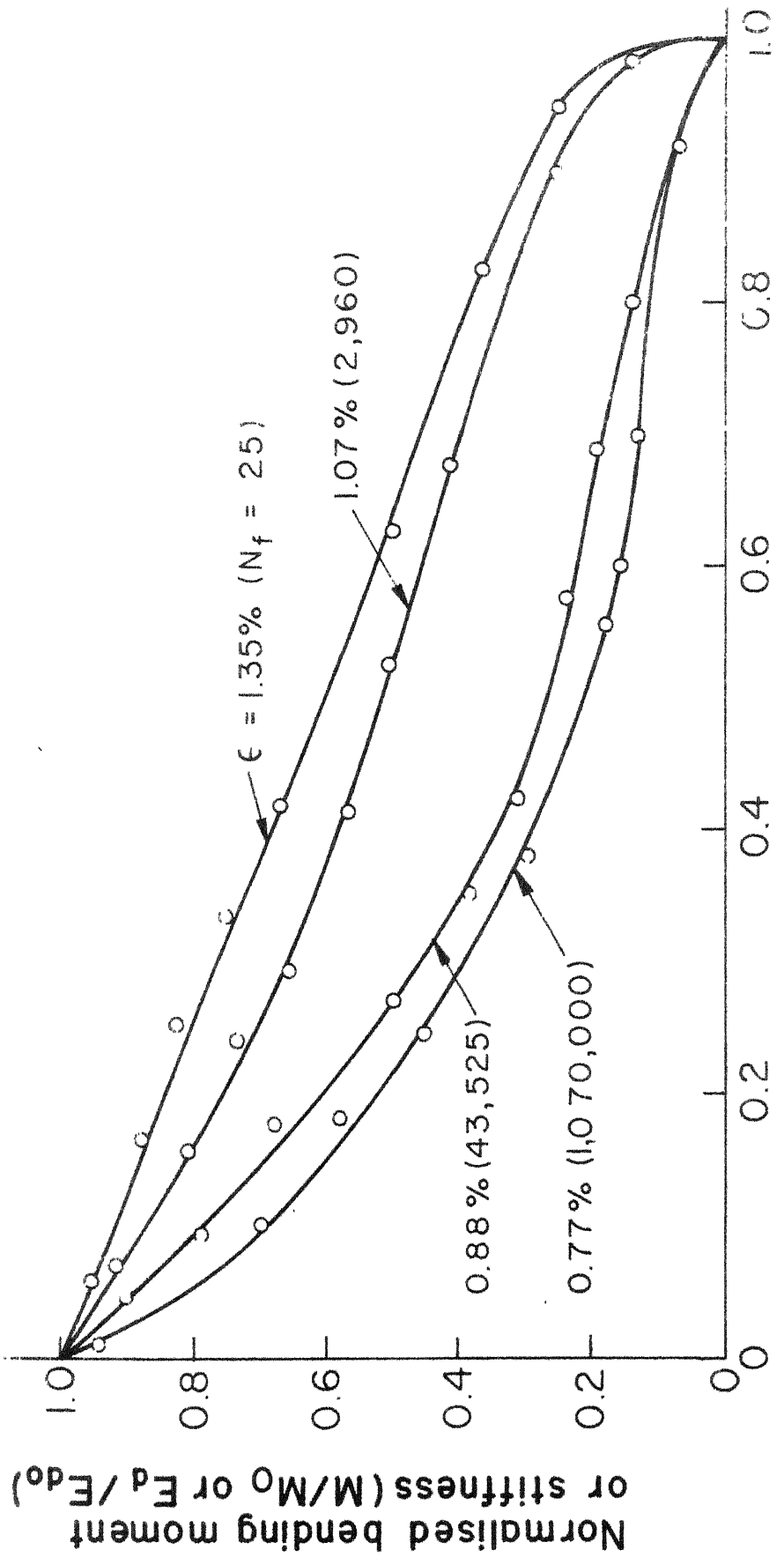

Fig. 3.2 Variation of normalised bending moment or stiffness with fraction of fatigue life for different strain limits (longitudinal specimens)

of their fatigue life. It has been observed that at strain amplitudes of 0.77 and 0.88% stiffness reduces to 25% of the initial stiffness in little more than half the fatigue cycles whereas the remaining 25% stiffness is lost in remaining cycles. For strain amplitudes of 1.07 and 1.35%, the last 25% stiffness is lost in only few cycles (less than 10% of fatigue life). The loss of stiffness can be explained as follows with the help of progressive damage occuring to the specimens.

Failure in longitudinal specimens subjected to flexural fatigue initiates by failure of fibres in the outer layers at the fixed end. The fibre failures cause a reduction in specimen stiffness. The next stage of damage is a delamination crack parallel to the surface of the specimen which further reduces effectiveness of the broken fibres. Photograph in Fig. 3.3 (a) shows this stage of damage in which the outer layer of fibres are broken and delamination crack has occurred. As the number of cycles increases, fibres in the inner layers break and more delamination cracks are formed. However, the delamination cracks in the inner layers propogate to smaller lengths compared to those in the outer layers. In specimens subjected to smaller strain amplitudes, innermost layer is able to sustain large number of cycles because the low strain requires larger number of cycles to cause final failure. In the specimens subjected to larger strain amplitudes, the innermost layer is

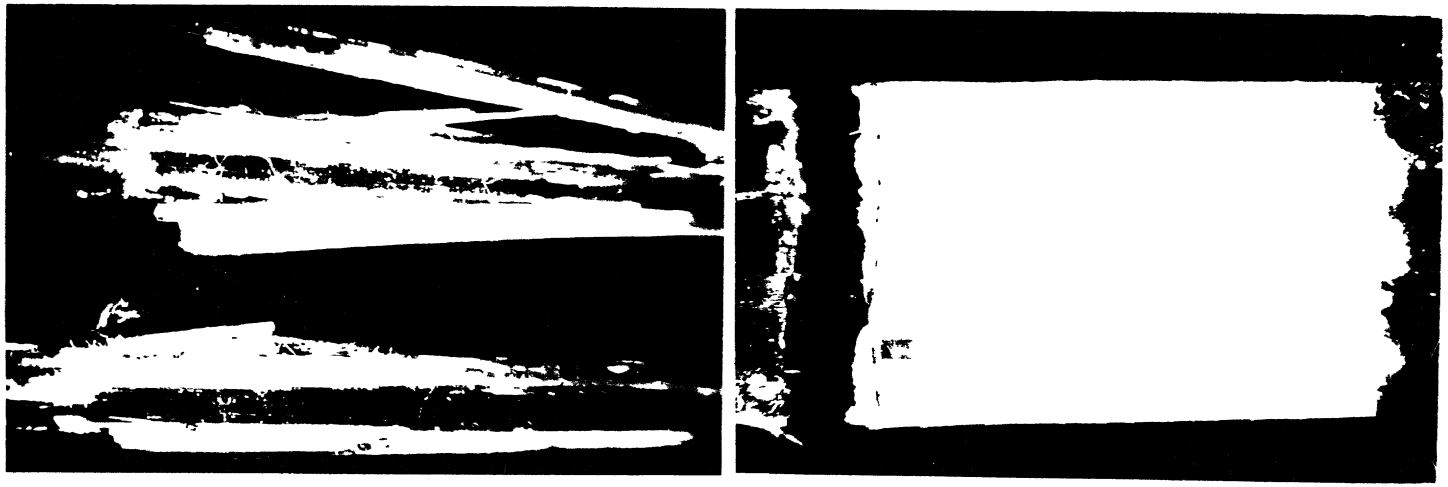

(a) (b)

Fig. 3.3 (a) Specimens showing breaking of fibres in the outermost layers and delamination in longitudinal specimens and
(b) top view of a fractured longitudinal specimen

able to sustain only a much smaller number of cycles. The overall specimen fracture appears relatively sharp because it occurs at the fixed end.(Fig. 3.3 (b)).

From the knowledge of instantaneous stiffness of specimens during fatigue cycling as indicated by the ratio of the instantaneous bending moment to the original bending moment at the fixed end, several S-N curves have been drawn, each of which indicates a fixed stage of material damage. These S-N curves are shown in Fig. 3.4. Salkind [27] has argued that this kind of representation of fatigue results is more appropriate compared to a single S-N curve. The curves shown in Fig. 3.4 have been drawn by taking average number of cycles required to reduce the stiffness by a desired value for several specimens tested at a fixed strain amplitude. It is observed that at high strain amplitudes, curves representing different stages of damage are quite far apart which indicates that the damage starts early in fatigue life and increases progressively. At low strain limits damage starts after a large number of cycles although the fraction of fatigue life at which damage initiates is still quite small (less than 10%). This observation is consistent with the results shown earlier in Fig. 3.2. At lower strain amplitudes the curves appear to be close because all of them have a much reduced slope at these strain limits.

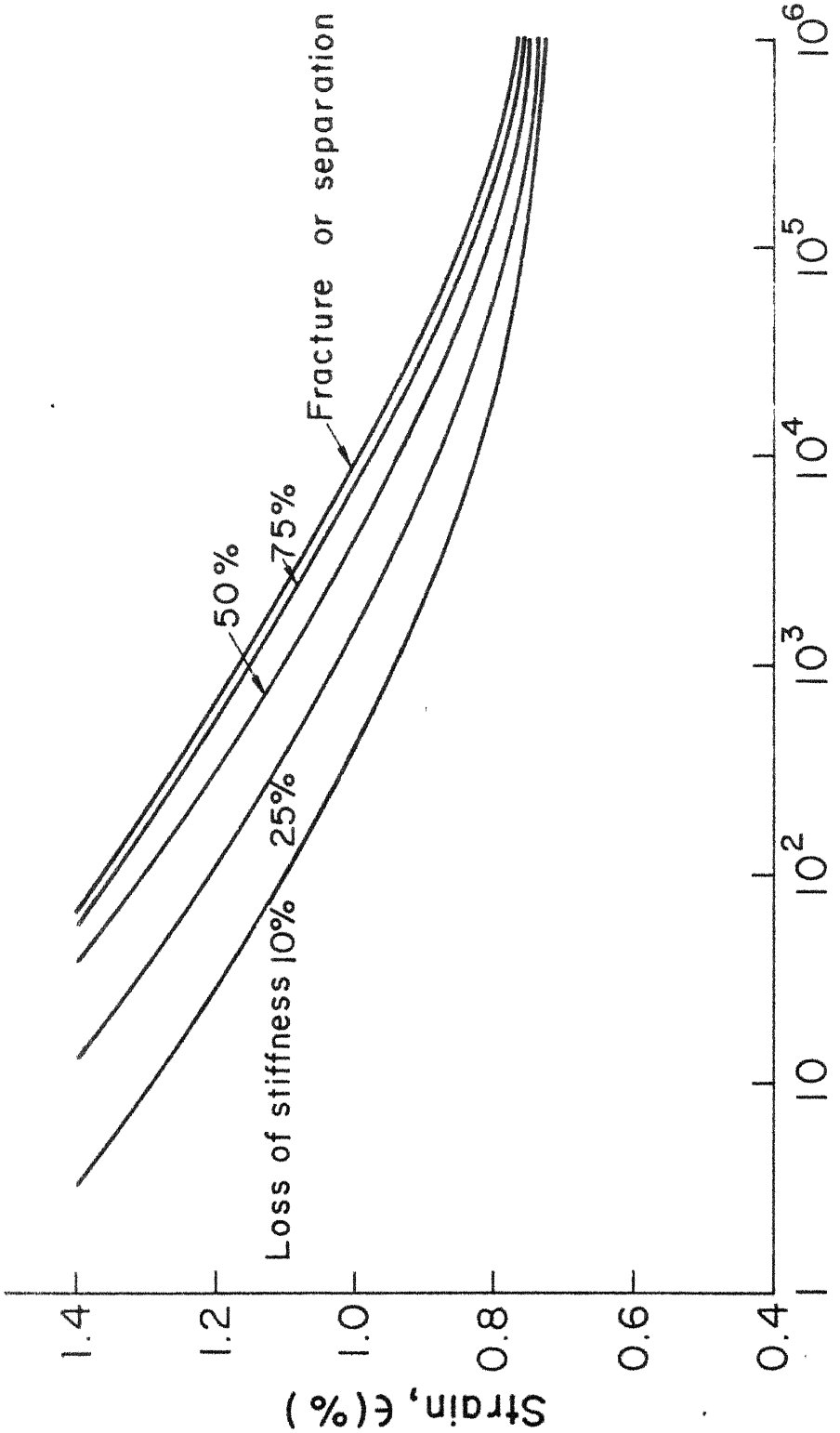

Fig. 3.4 S-N curves representing different stages of damage in longitudinal specimens

Progressive fatigue damage has been further investigated by cycling additional specimens to different fractions of fatigue life at each strain amplitude. On all these precycled specimens static flexural tests to failure have been performed. Results of static tests are shown in Figs. 3.5 to 3.8 as plots of bending moment as a function of end deflection. These plots have been used to calculate residual stiffnesses and strengths of the specimens at each stage of fatigue damage. Residual strength has been directly calculated from the bending moment at fracture of a precycled specimen. To be consistent with the concept that the ratio of instantaneous bending moment to the first cycle bending moment is same as the ratio of instantaneous dynamic stiffness to first cycle stiffness, the static stiffness has been calculated from the ratio of bending moment and deflection (M/δ) at an end deflection equal to the maximum deflection during fatigue cycling and not from the initial slope of the $M-\delta$ curve. In each of the Figs. 3.5 to 3.8 a vertical dotted line indicates the deflection at which M/δ is to be obtained for calculating static stiffness. The same procedure has been employed in later sections as well for calculating static residual stiffness of specimens with different fibre orientations.

The ratios of residual stiffness to initial stiffness ($\frac{E_R}{E_o}$) as calculated from Figs. 3.5 to 3.8 are given in Table 3.2 and have been plotted against loss of

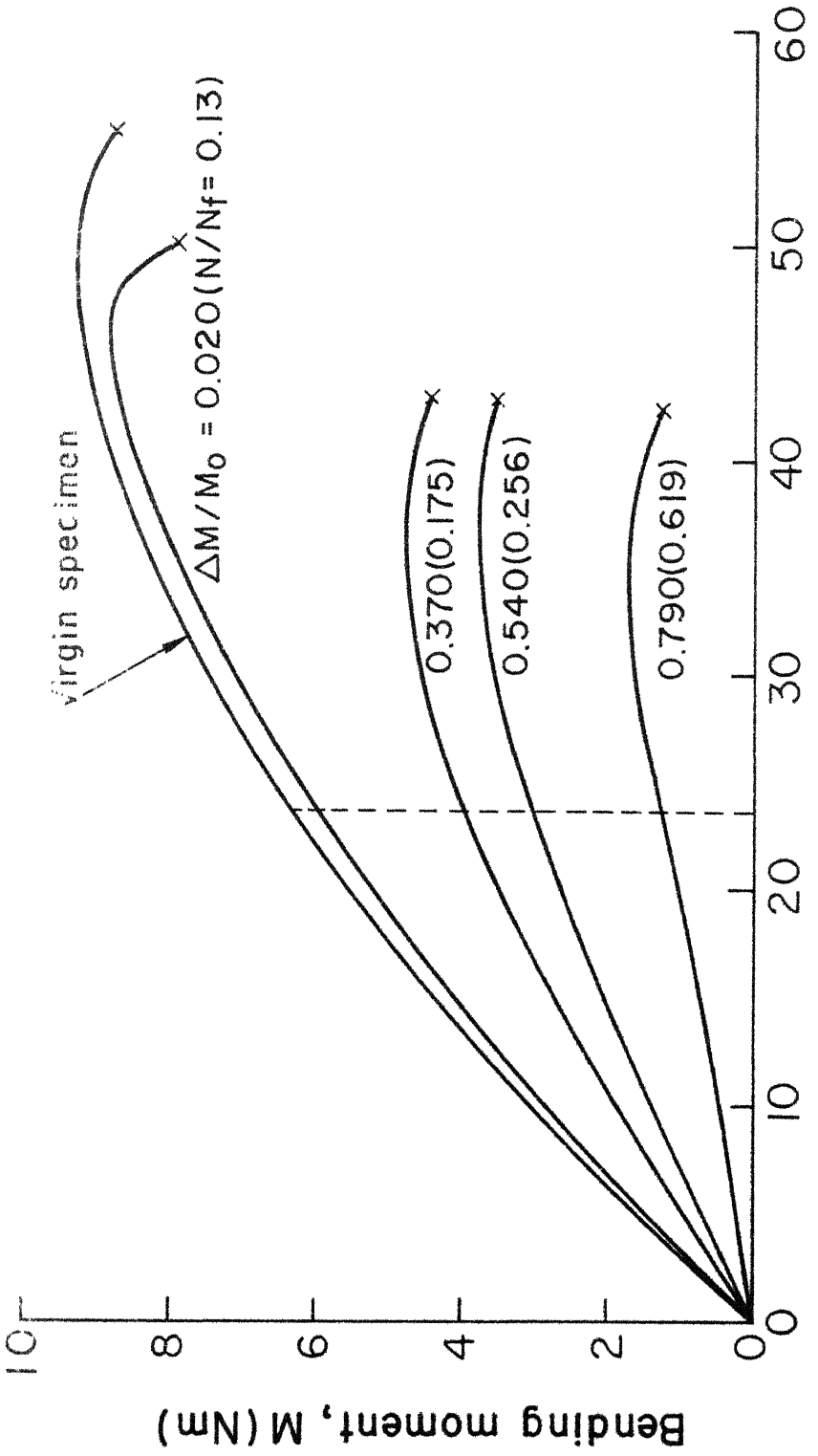

Fig.3.5 Bending moment vs deflection curves for specimens precycled to different stages of damage (longitudinal specimens, $\epsilon = 0.77\%$)

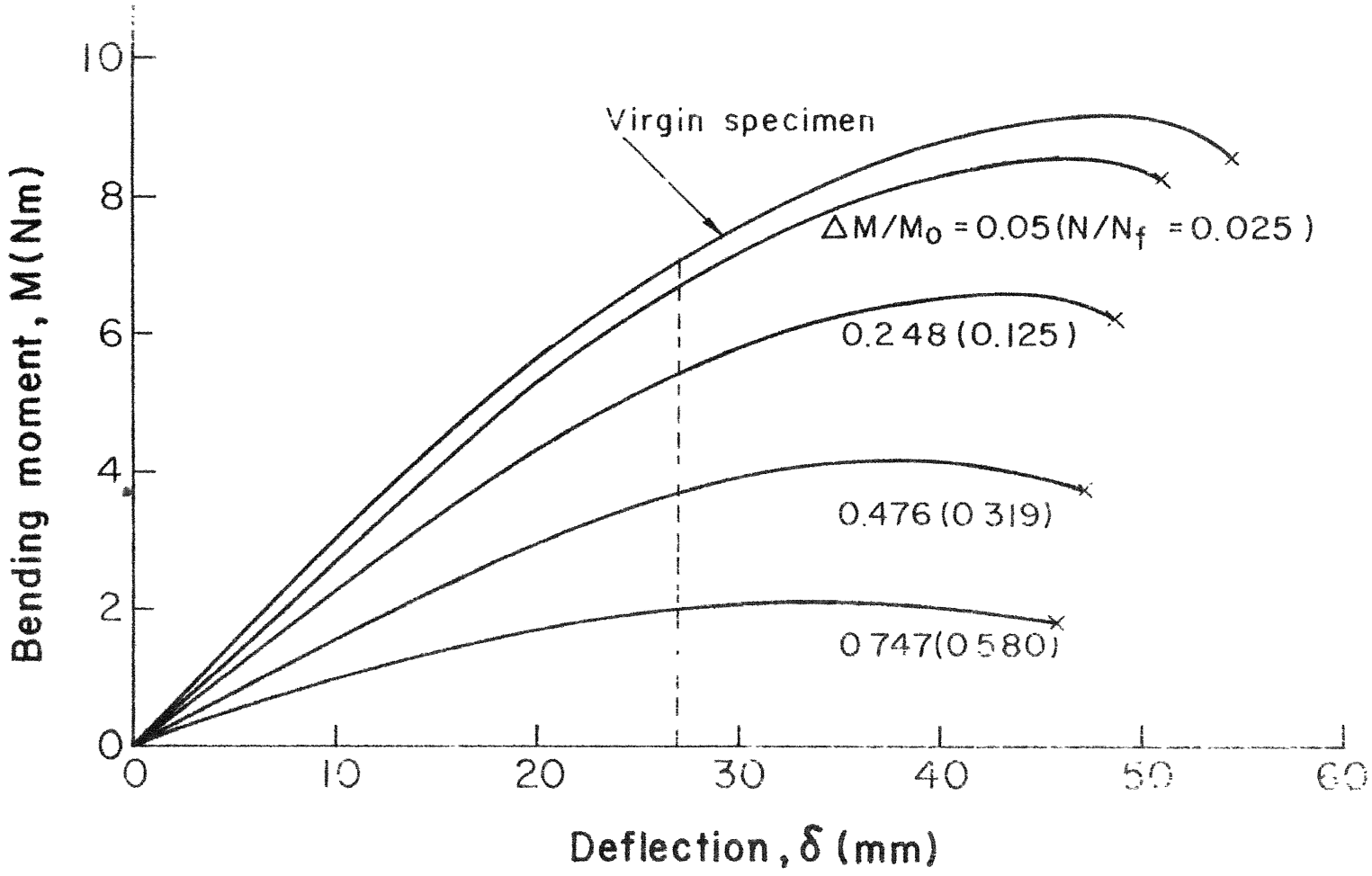

Fig. 3.6 Bending moment vs deflection curves for specimens precycled to different stages of damage (longitudinal specimens, ϵ = 0.88 %)

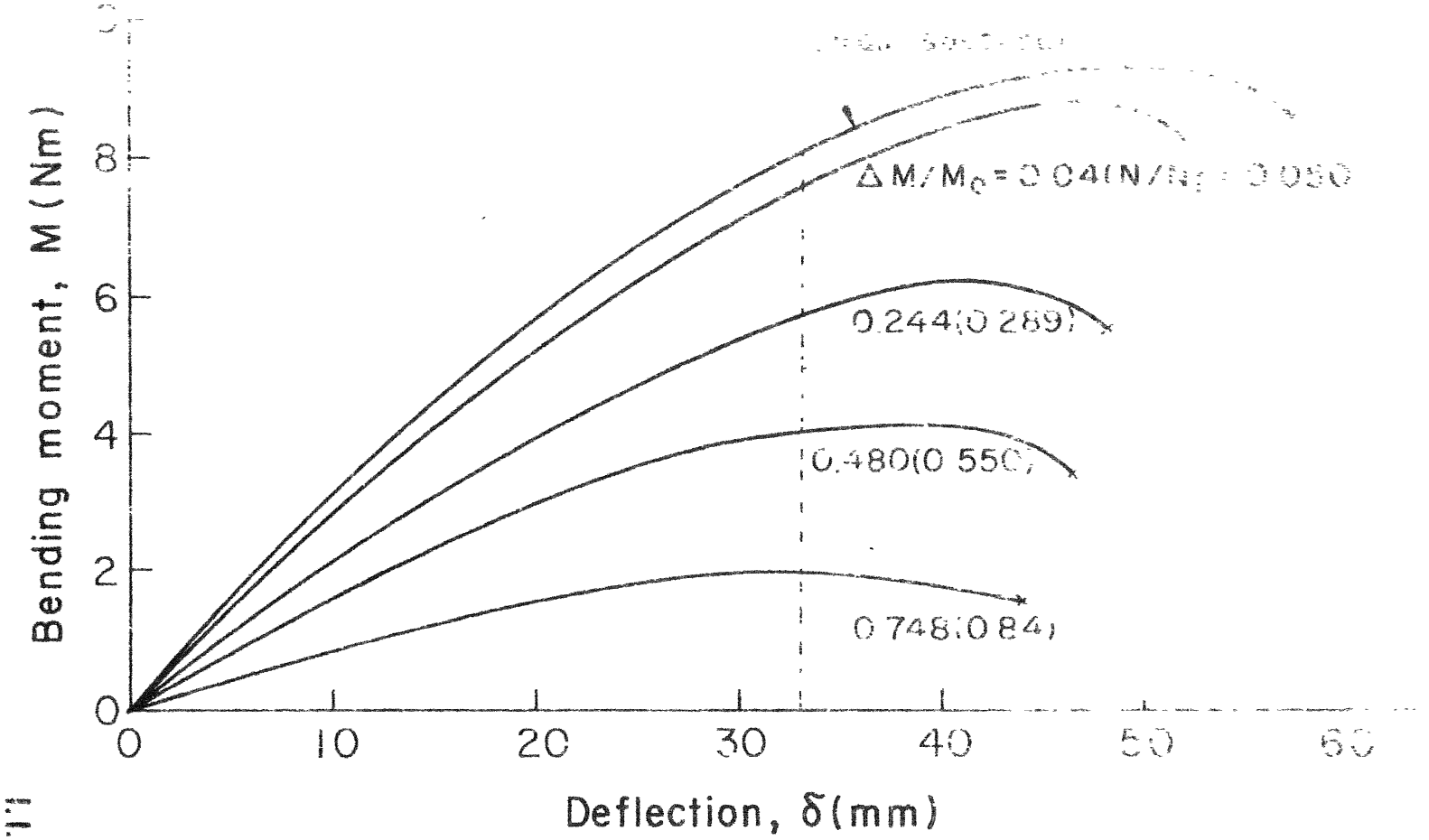

Fig. 3.7 Bending moment vs deflection curves for specimens precycled to different stages of damage (longitudinal specimens, ϵ = 1.07%)

Table 3.2: Ratio of Residual Stiffness to Stiffness of a Virgin Specimen at Different Fraction of Average Fatigue Life for Different Strain Amplitudes (Longitudinal Specimens)

$\varepsilon = 0.77\%$		$\varepsilon = 0.88\%$		$\varepsilon = 1.07\%$		$\varepsilon = 1.35\%$	
N/N_f*	E_R/E_o	N/N_f*	E_R/E_o	N/N_f*	E_R/E_o	N/N_f*	E_R/E_o
0.130	0.958	0.025	0.938	0.050	0.942	0.084	0.962
0.175	0.542	0.125	0.742	0.289	0.725	0.353	0.708
0.256	0.444	0.319	0.500	0.550	0.479	0.539	0.571
0.619	0.197	0.580	0.250	0.840	0.250	0.882	0.350

* N_f Average fatigue life

dynamic stiffness ($\frac{\Delta E_d}{E_{do}}$) in Fig. 3.9, where $\frac{\Delta E_d}{E_{do}}$ has been taken equal to $\Delta M / M_o$ and obtained from Fig. 3.2 for appropriate fraction of fatigue life. The points corresponding to different strain amplitudes have been plotted in the same figure. The points lie very close to the straight line:

$$\frac{E_R}{E_o} = 1 - \frac{\Delta E_d}{E_{do}} \qquad (3.1)$$

This indicates that the normalised static stiffness is equal to the normalised dynamic stiffness.

Residual strength as calculated from the bending moment at fracture has been plotted as a function of fraction of fatigue life in Fig. 3.10. The trends exhibited by the residual strengths at different strain limits are very similar to the ones exhibited by the normalised bending moment as shown in Fig. 3.2. Specimens subjected to smaller strain amplitudes (larger fatigue life) lose greater fraction of strength at relatively smaller fraction of fatigue life in the initial stages of fatigue cycling whereas the specimens subjected to larger strain amplitudes show a more gradual loss of strength for most part of their fatigue life.

Residual strength has been plotted as a function of loss in stiffness in Fig. 3.11. It is observed that all the points lie close to following straight line:

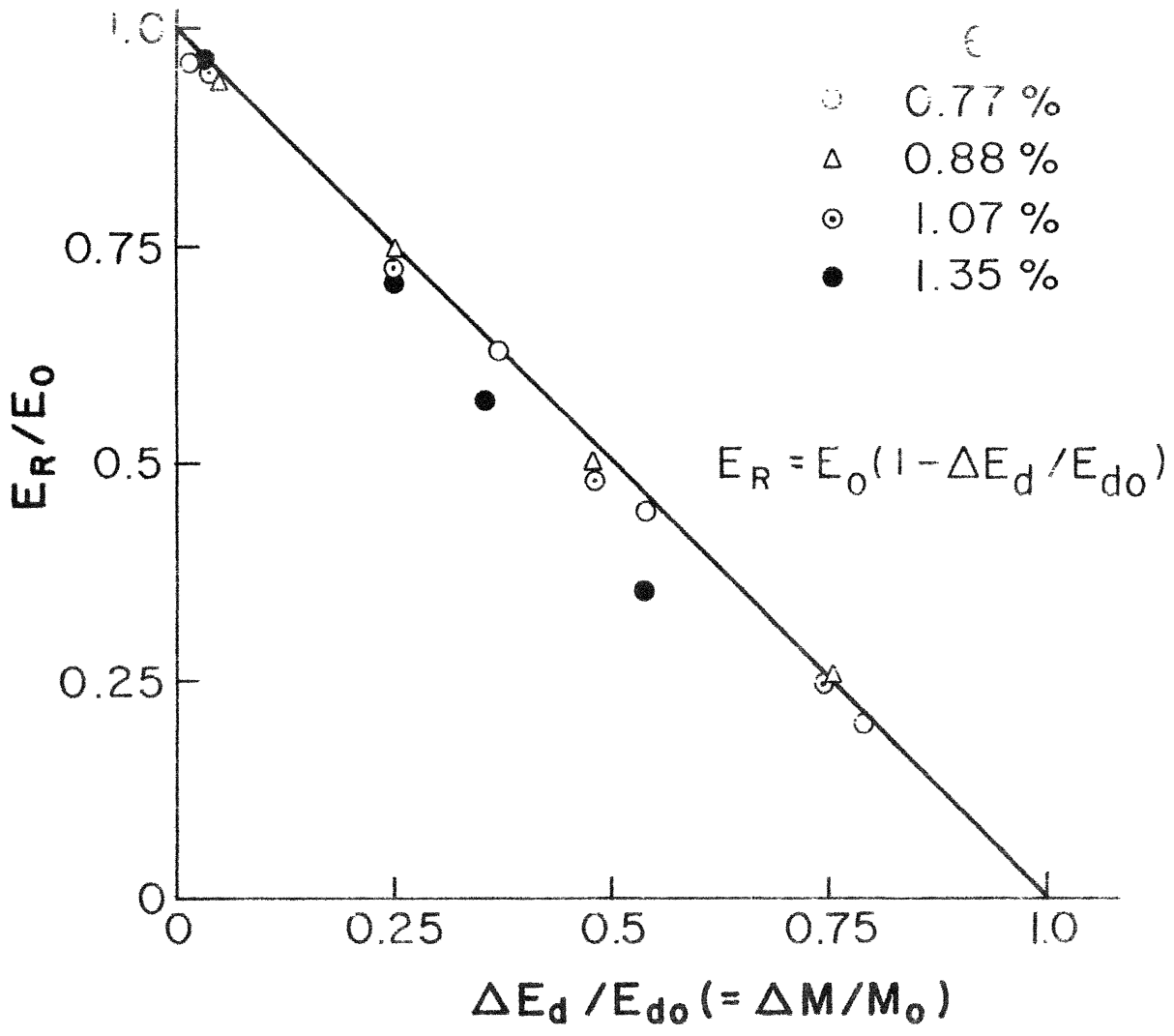

Fig.3.9 Normalised residual stiffness vs loss in dynamic stiffness (longitudinal specimens)

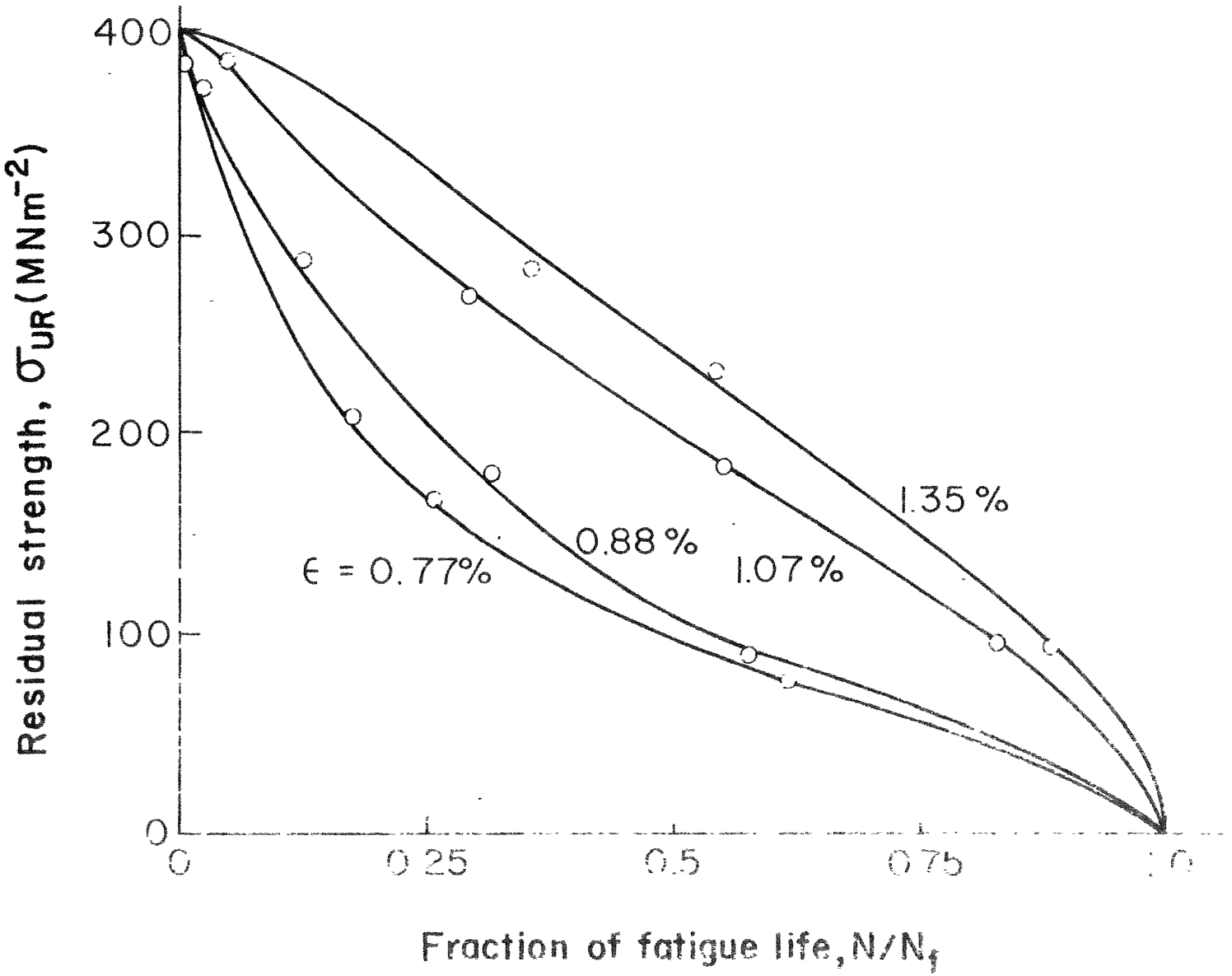

Fig. 3.10 Variation of residual strength with fraction of fatigue life (longitudinal specimens)

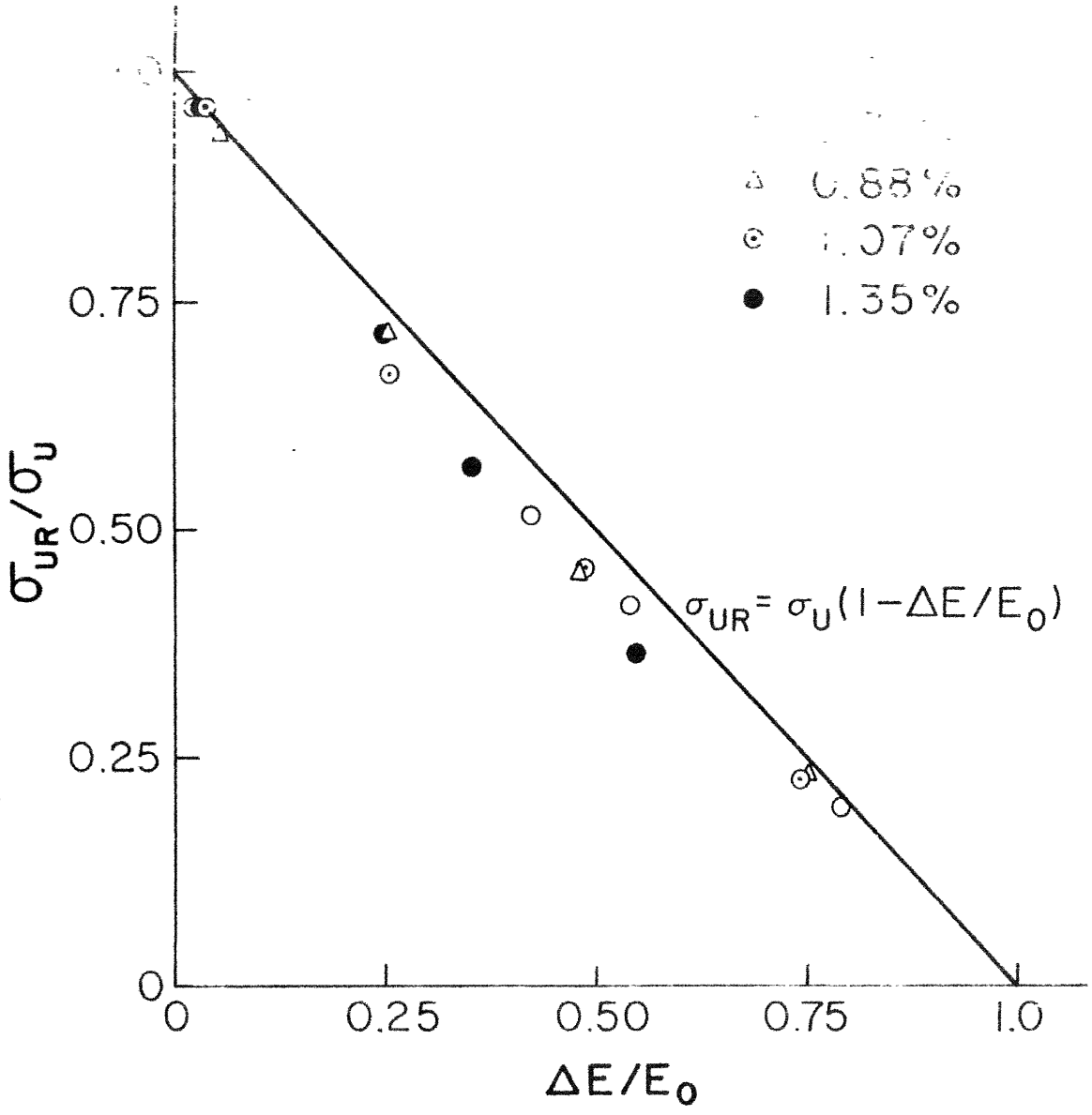

Fig. 3.11 Variation in normalised residual strength with loss in stiffness (longitudinal specimens)

$$\frac{\sigma_{UR}}{\sigma_{U}} = 1 - \frac{\Delta E}{E_o} \qquad (3.2)$$

The straight line relationship shows a good correspondence between residual strength and the residual stiffness. Further comments on this correspondence will be made in the next chapter where a comparative fatigue behaviour for different fibre orientations is presented.

3.2 TRANSVERSE FATIGUE BEHAVIOUR*

Transverse fatigue behaviour has been studied by performing tests on specimens having fibres perpendicular to the axis of the specimen. The transverse fatigue specimens (dimensions shown in Fig. 2.12) were subjected to four different displacement amplitudes namely 3.6, 4.45, 5.4 and 7.0 mm which produce strain amplitudes of 0.22, 0.27, 0.33 and 0.43 percent respectively at the fixed end of the specimens. The tests were performed on low capacity machine at a frequency of 10 Hz.

Results of fatigue tests are given in Table 3.3 and shown graphically in Fig. 3.12. Each point represents one specimen and the cyclic life corresponds to fracture

---

*A paper entitled "Flexural Fatigue Properties of Unidirectional Composites in Transverse Direction", based on a part of the results discussed in this section has been published in "Composites", Vol. 10, No. 1, Jan. 1979.

Table 3.3: Fatigue Life of Transverse Specimens at Different Strain Amplitudes

N_f			
$\varepsilon = 0.22\%$	$\varepsilon = 0.27\%$	$\varepsilon = 0.33\%$	$\varepsilon = 0.43\%$
1,000,215	511,012	225,013	31,878
720,000	490,481	210,518	28,307
609,385	450,239	203,438	27,254
450,988	464,387	181,050	23,050
412,058	440,319	173,673	21,501
349,921	430,121	170,348	20,050
	419,280	138,435	15,509
	388,719	118,348	15,000
15 Runouts	321,240	112,051	14,494
at one	290,043	85,050	12,059
million	274,285	79,997	11,503
cycles	261,348	77,511	6,182
	253,435	76,074	6,047
	232,151	74,057	5,897
	219,790	69,502	5,108
	185,311	62,505	4,402
	173,056	46,000	4,278
	159,343	42,053	4,139
	92,318	28,255	4,053
	81,034	22,519	3,192

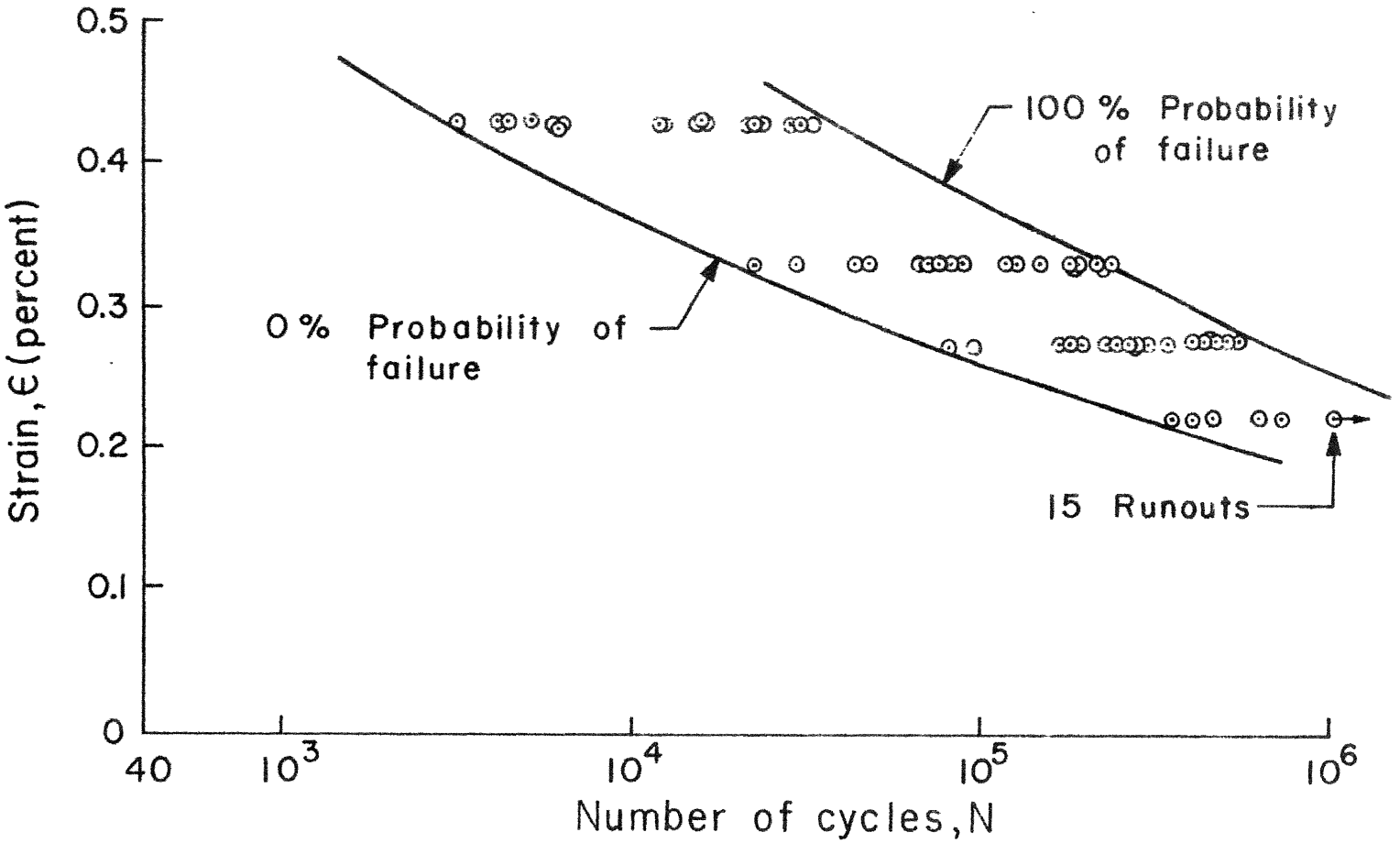

Fig.3.12 Strain vs fatigue life curves for transverse specimens

or separation. It is observed that fatigue life varies from 3000 to 10^6 cycles. General nature of curve is as expected in that fatigue life increases as maximum strain decreases. Scatter in fatigue life of transverse specimens is also of one order of magnitude as was observed for the longitudinal specimens.

Bending moment at the fixed end of the specimens was measured at desired intervals during fatigue cycling and recorded on a Visicorder. This was done for several specimens in each set of specimens tested at a fixed strain amplitude. Typical variation in cyclic bending moment normalised with respect to the first cycle bending moment is shown in Fig. 3.13 as a function of fraction of fatigue life on a log scale. Logarithmic scale has been preferred in this case to appropriately illustrate significant variation in the bending moment at small number of cycles. The ratio of bending moment to initial bending moment represents fraction of stiffness retained by the composite during fatigue loading. It is observed from Fig. 3.13 that the specimens retain their original stiffness only for a very small fraction (less than 5%) of expected fatigue life. A sudden drop in specimen stiffness occurs between 0.2 to 5% of cyclic life. Due to this downward drop, the stiffness reduces to only about 30% of the specimen stiffness in the first loading cycle. The sudden drop in stiffness is accompanied by a clearly audible sound. The sound and

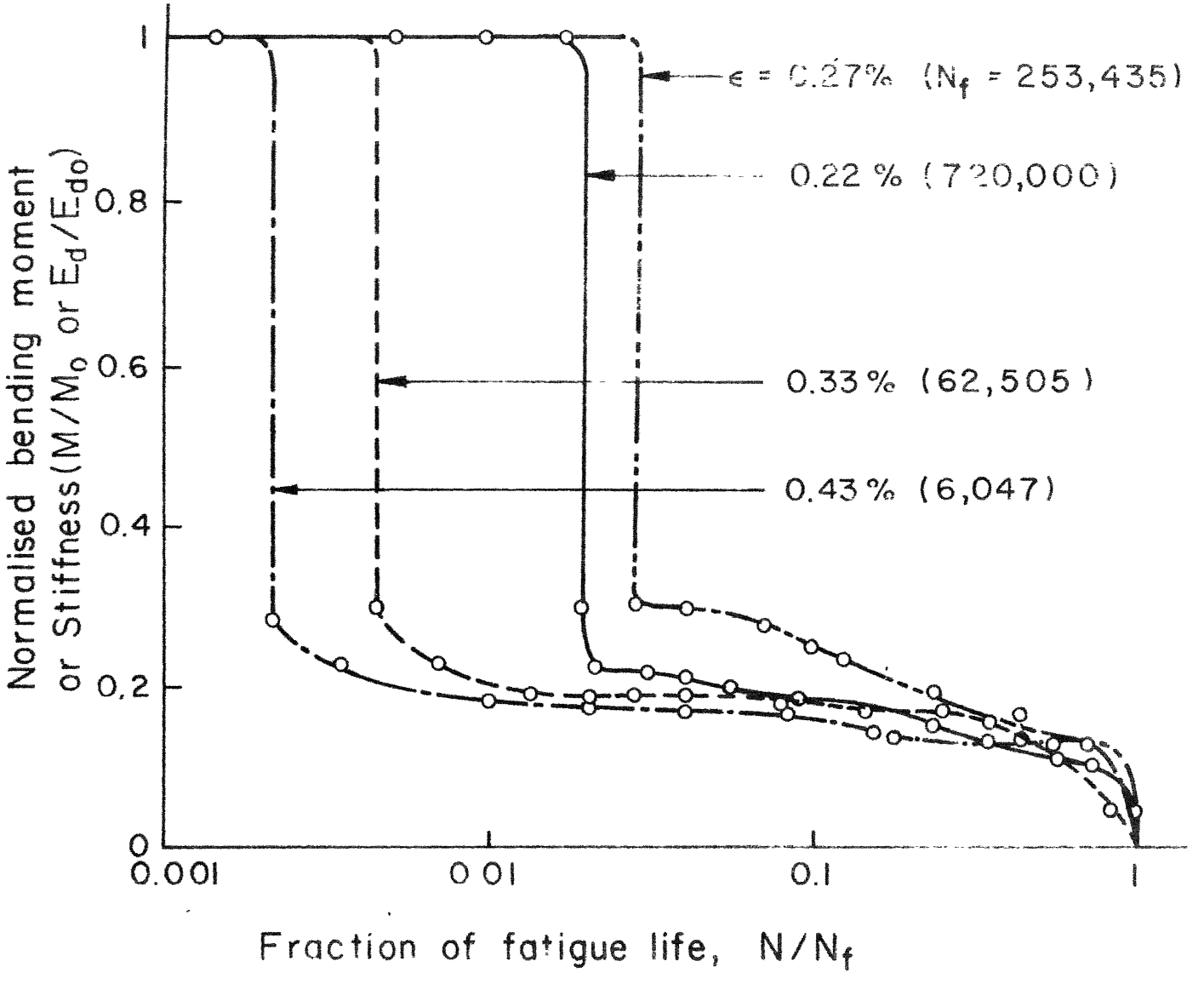

Fig 3.13 Variation of normalised bending moment or stiffness with fraction of fatigue life for different strain amplitudes (transverse specimens)

accompanying loss of stiffness are caused due to interface failure near the fixed end of the specimen. This behaviour is different from the one observed for longitudinal specimens in which no sudden drop in stiffness occurs. However, sudden drop in stiffness has been observed for 45 degree specimens as will be discussed later. Similar drops in stiffness have been reported by other investigators also [33]. Even beyond the downward drop, stiffness rapidly reduces to about 15% of the original stiffness within 25% of fatigue life. After this, the loss in stiffness is extremely slow. The loss of stiffness can be explained as follows with the help of damage occurring to the specimens.

Failure in the transverse specimens initiates at the fixed end by debonding of fibres in the surface layers. This debonding occurs very early in fatigue life due to large stress concentrations produced by the transverse fibres. The debonding crack propogates through the entire width of the specimen almost instantly. In an undebonded specimen, the stresses are maximum in the outermost layers and account for a large fraction of total bending moment at the section. Due to debonding crack the stresses in the outermost layers are relieved so that a sudden drop in bending moment is observed. In other words, effective stiffness of the specimen is reduced suddenly. The debonding cracks then propagate from the outer layers to the

neutral plane (i.e. mid plane) due to stress concentrations at the tips of the cracks. This rapid crack propagation accounts for rapid drop in stiffness beyond the sudden drop. The crack propagation stops at a point near the neutral plane where the stresses are very small. Figure 3.14 is a photograph of three specimens showing cracks along the entire width of the specimens. Beyond this stage the overall specimen stiffness is only about 15% of the original stiffness and the stresses in the undebonded portion of the cross-section are very small so that further damage requires a very large number of load cycles.

S - N curves representing different stages of material damage have been drawn in this case also (Fig. 3.15). The left most curve represents sudden drop in stiffness to about 30% of the initial stiffness. The curves representing sudden drop and 15% stiffness are quite far apart because the loss in transverse stiffness beyond the sudden drop is extremely slow. Since the stiffness drop (to only 30% of the original stiffness)is quite severe, the left most curve may be taken as the failure curve (to be used for design purposes).

Static tests on precycled specimens were performed to further investigate progressive fatigue damage. Fractions of fatigue life selected for precycling were such that the dynamic stiffness of specimens was in both

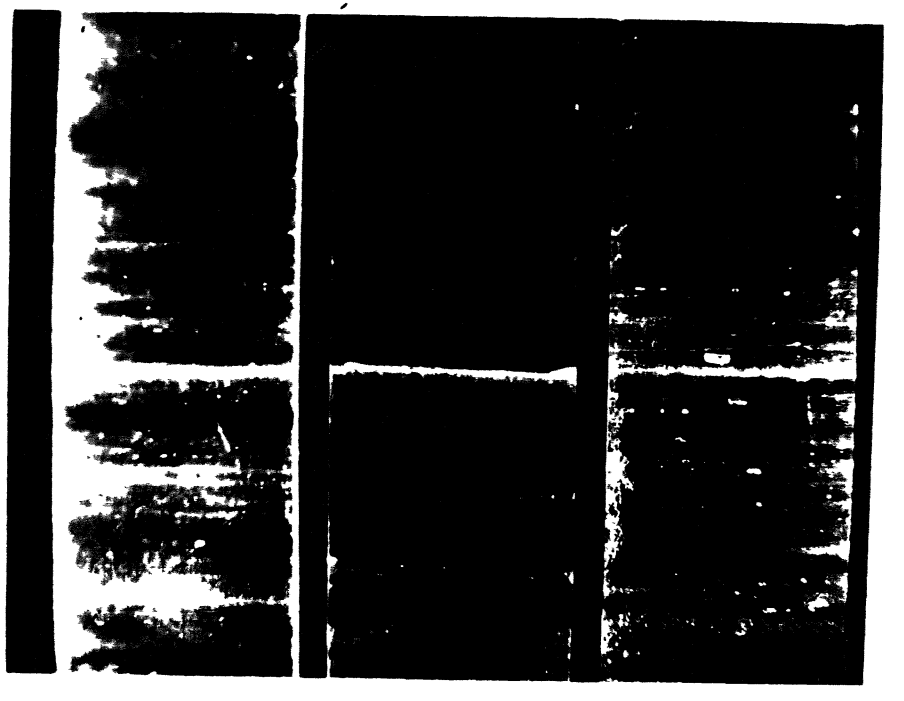

Fig. 3.14 Cracks across the width in three transverse specimens after sudden drop in stiffness

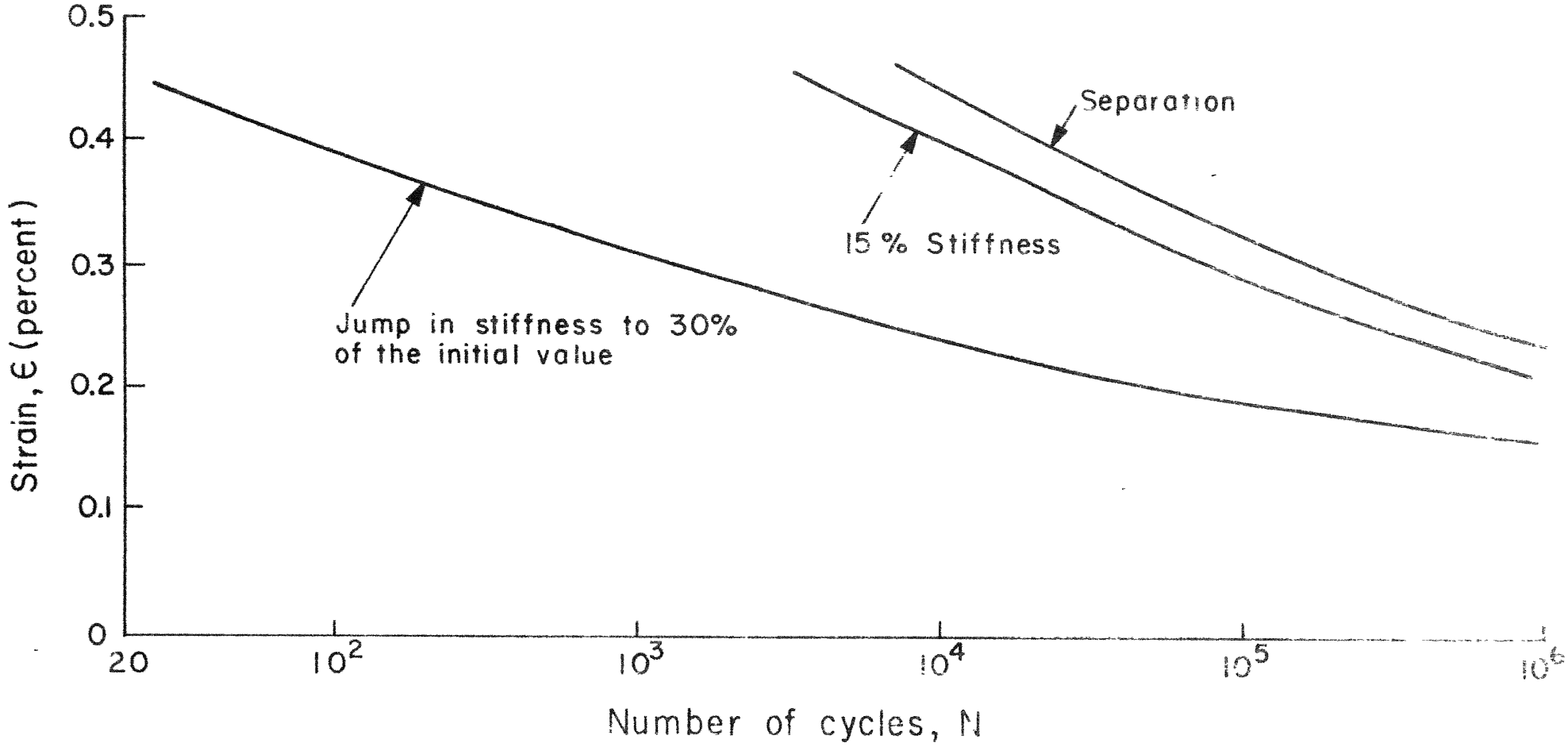

Fig. 3.15 S-N curves representing different stages of damage in transverse specimens

ranges i.e. before and after the sudden drop. Due to poor strength of unidirectional composites in the transverse direction, the specimens required additional care in handling. Results of the static tests to failure are shown in Figs. 3.16 to 3.19 as plots of bending moment versus end deflection. It is observed that the bending moment vs deflection curve for a specimen precycled to a point before sudden drop cannot be distinguished from the bending moment vs deflection curve of a virgin specimen. This shows that there is little damage to the specimen before sudden drop in stiffness occurs. This observation is true for all strain amplitudes. The ratios of residual stiffness to intial stiffness $(\frac{E_R}{E_o})$ as calculated from Figs. 3.16 to 3.19 are given in Table 3.4 and have been plotted against loss in dynamic stiffness $(\frac{\Delta E_d}{E_{do}})$ in Fig. 3.20 for all strain limits. Data could not be obtained for normalised dynamic stiffness loss between 0 and 0.7 due to sudden drop in stiffness which was observed in all cases. The available data points in this case also are close to the straight line given by Eq. (3.1) obtained in the case of longitudinal fatigue behaviour. The dotted portion of straight line in Fig. 3.20 corresponds to the range of stiffness in which data could not be taken. Thus, normalised static stiffness equals the normalised dynamic stiffness in this case also.

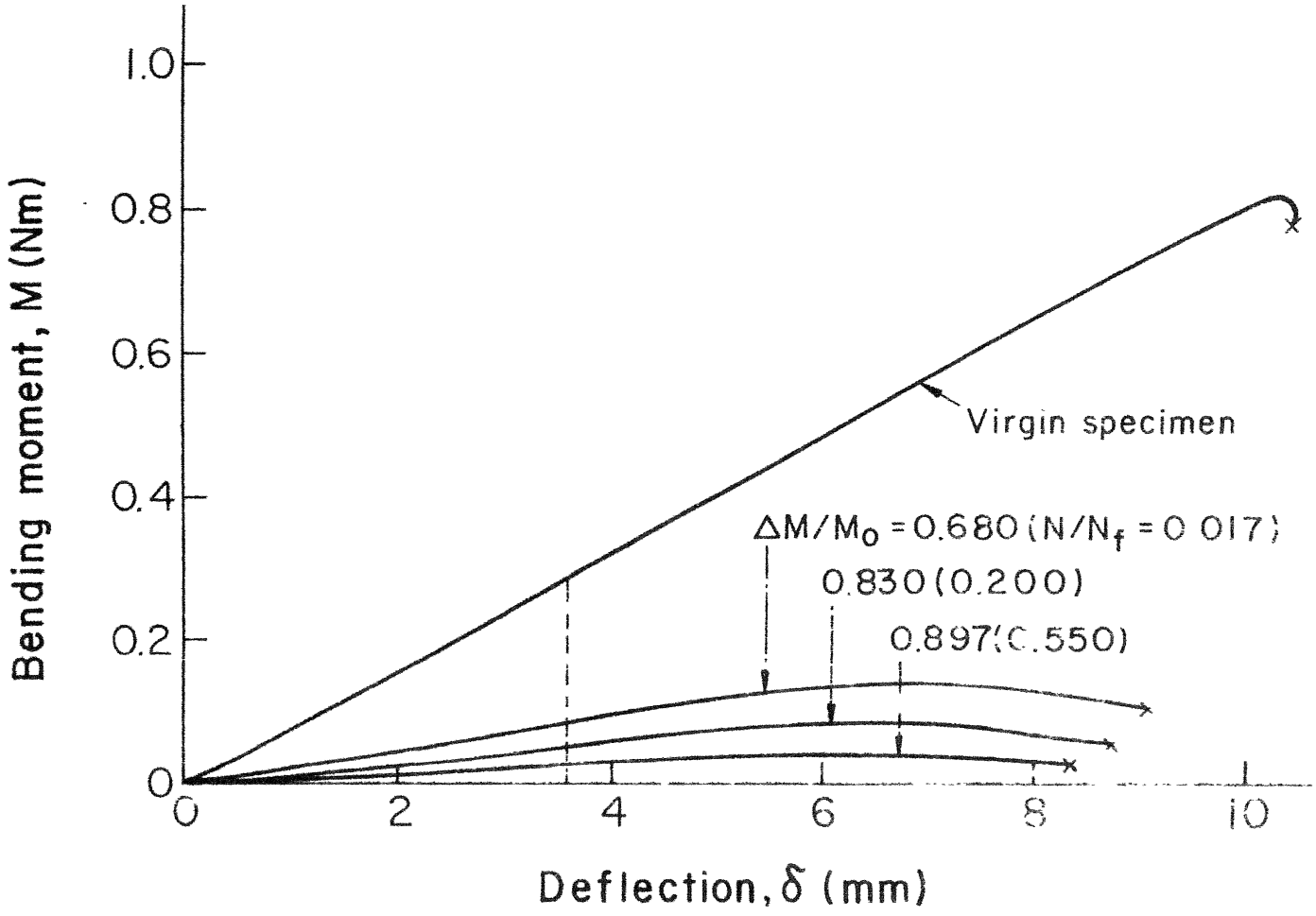

Fig. 3.16 Bending moment vs deflection curves for specimens precycled to different stages of damage (transverse specimens, ϵ = 0.22%)

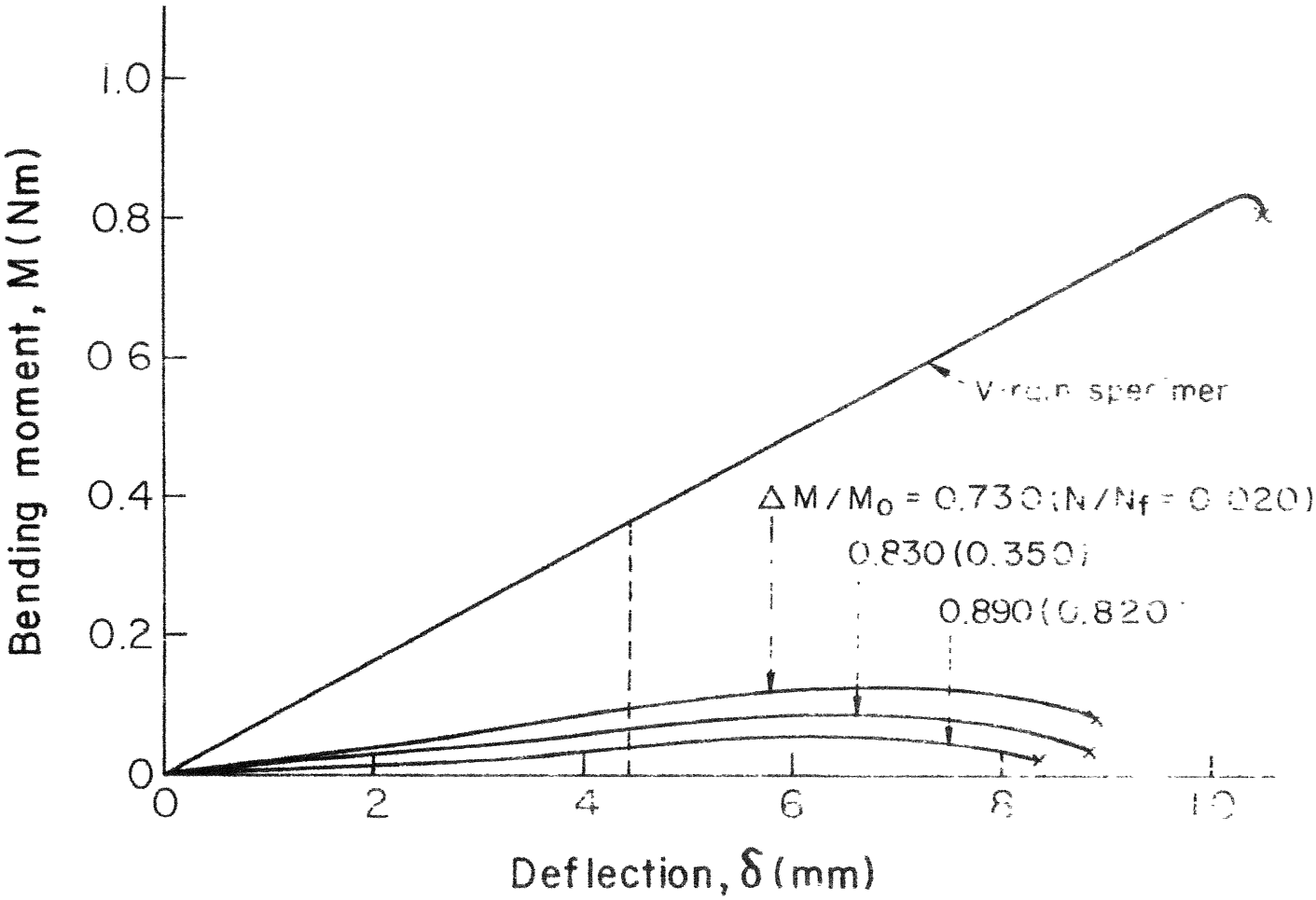

Fig. 3.17 Bending moment vs deflection curves for specimens precycled to different stages of damage (transverse specimens, $\epsilon = 0.27\ \%$)

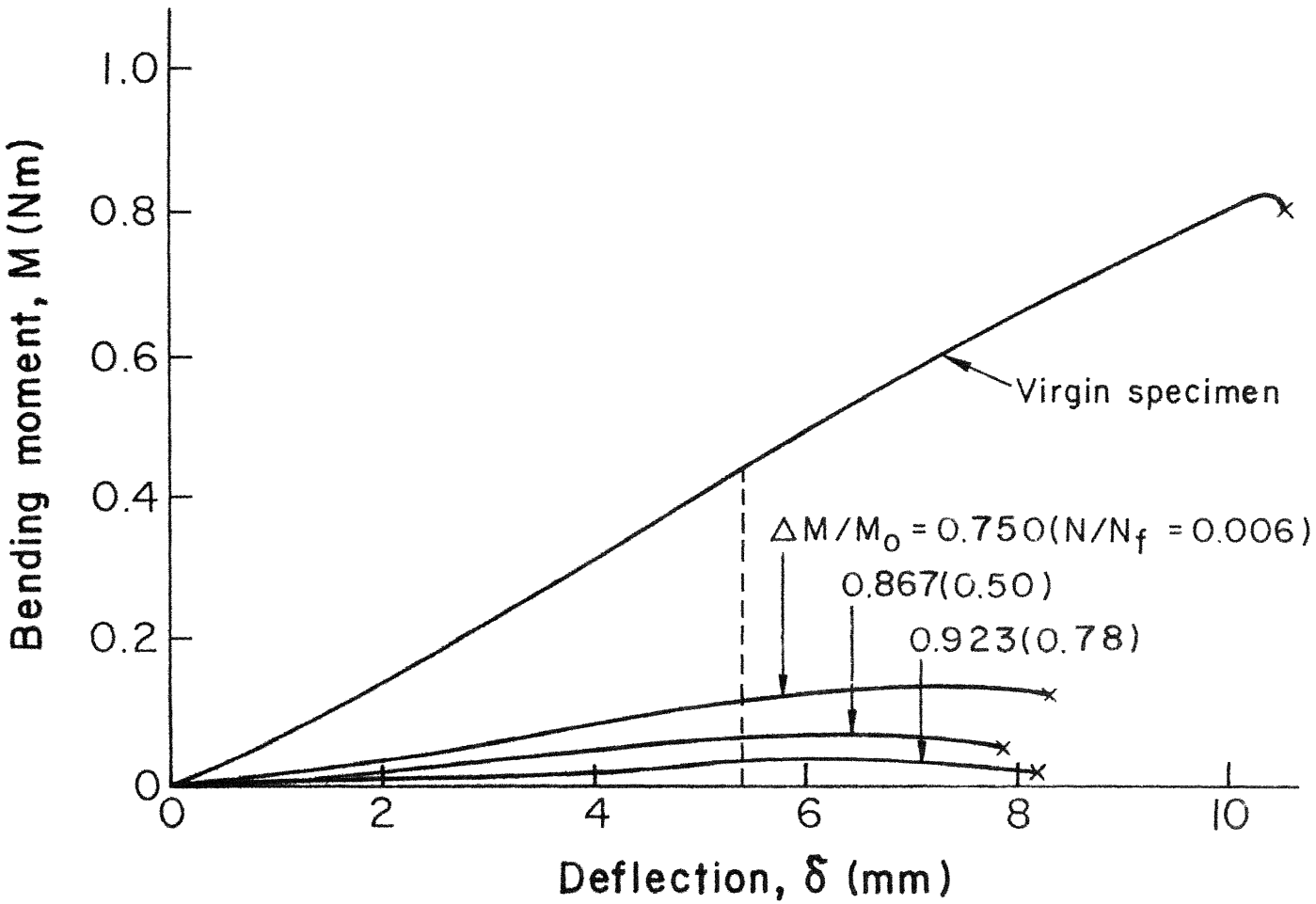

Fig. 3.18 Bending moment vs deflection curves for specimens precycled to different stages of damage (transverse specimens, $\epsilon = 0.33\%$)

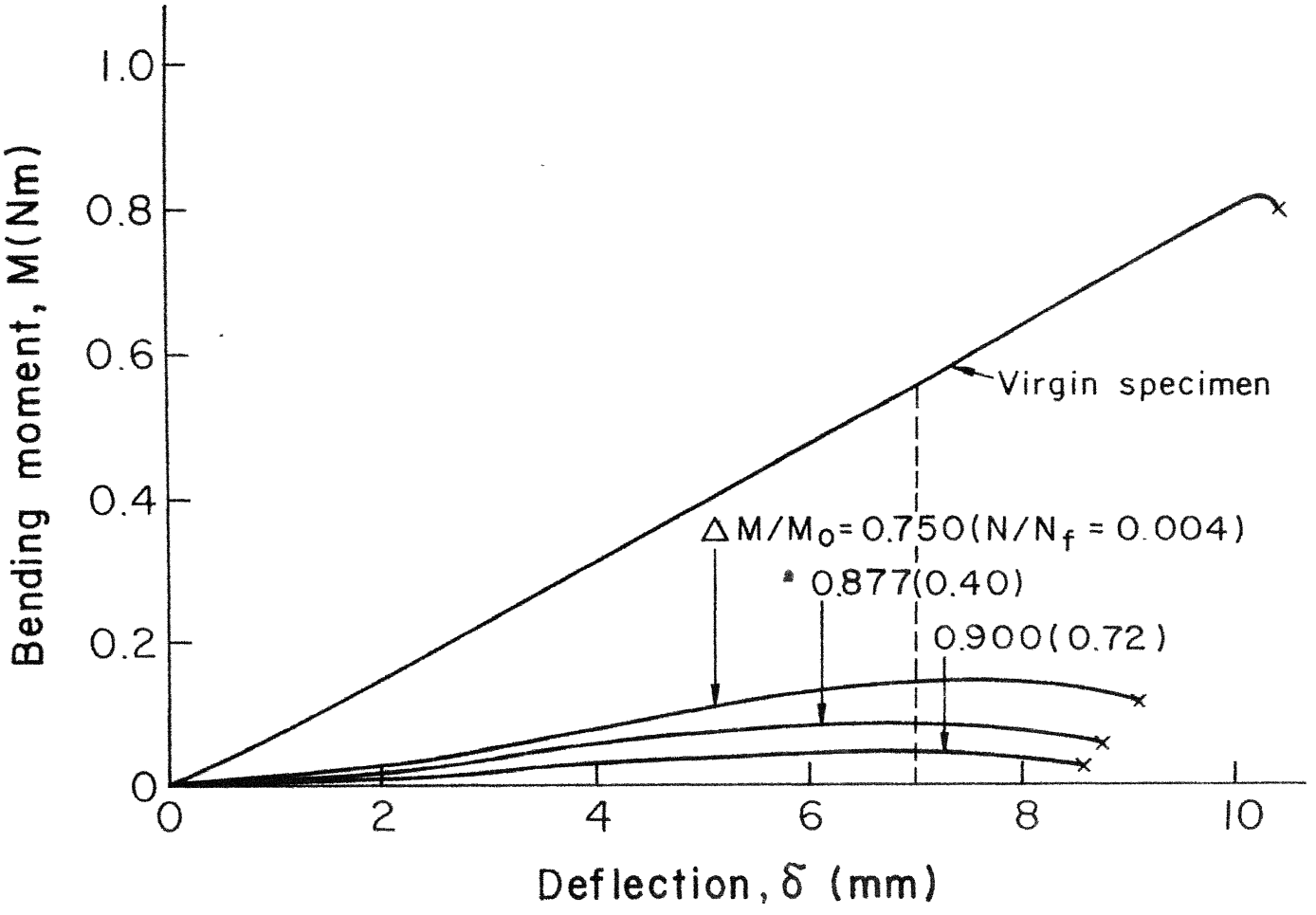

Fig. 3.19 Bending moment vs deflection curves for specimens precycled to different stages of damage (transverse specimens, $\epsilon = 0.43\%$)

Table 3.4: Ratio of Residual Stiffness to Stiffness of a Virgin Specimen at Different Fraction of Average Fatigue Life for Different Strain Amplitudes (Transverse Specimens).

$\varepsilon = 0.22\%$		$\varepsilon = 0.27\%$		$\varepsilon = 0.33\%$		$\varepsilon = 0.43\%$	
N/N_f*	E_R/E_o	N/N_f*	E_R/E_o	N/N_f*	E_R/E_o	N/N_f*	E_R/E_o
0.0075	1.0	0.0054	1.0	0.0025	0.990	0.0017	0.984
0.0170	0.30	0.020	0.250	0.006	0.242	0.004	0.250
0.2000	0.15	0.350	0.158	0.500	0.133	0.400	0.125
0.5500	0.10	0.820	0.096	0.780	0.075	0.720	0.083

*N_f Average fatigue life

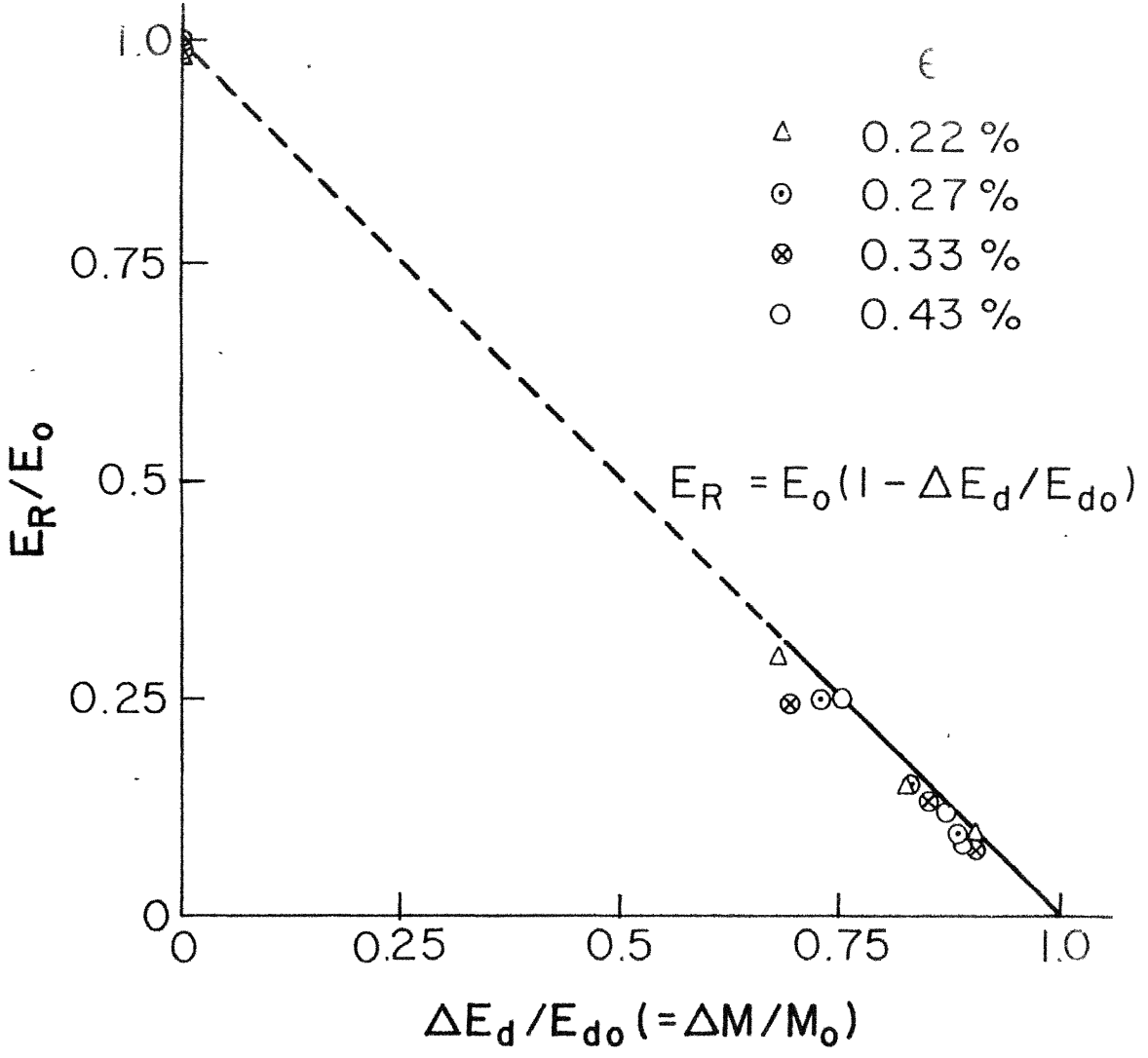

Fig. 3.20 Normalised residual stiffness vs loss in dynamic stiffness (transverse specimens)

Residual strength as calculated from the bending moment at fracture has been plotted as a function of fatigue life in Fig. 3.21. The trends exhibited by the residual strength at different strain limits are very similar to the ones exhibited by the normalised bending moment shown in Fig. 3.13. It is again observed that before sudden drop there is little loss in strength. After the sudden drop residual strength gradually decreases with fraction of cyclic life in a manner similar to the stiffness retained. Residual strength has been plotted as a function of loss in stiffness in Fig. 3.22. Once again it is observed that the residual strength is close to that predicted by Eq. (3.2) obtained in the case of longitudinal fatigue behaviour. The dotted portion of line again represents the range of stiffness in which data could not be obtained due to sudden drop.

3.3 FATIGUE BEHAVIOUR OF 45° SPECIMENS*

Fatigue tests have been performed on specimens having fibres oriented at 45 degree to the specimen axis. Displacement amplitudes in fatigue tests were 7.5, 9.5, 13 and 18 mm which produce strain amplitudes 0.22, 0.28,

*A paper entitled "Progressive Damage in GFRP under constant deflection flexural fatigue" based on part of the work described in this section has been accepted for publication in Fibre Science and Technology.

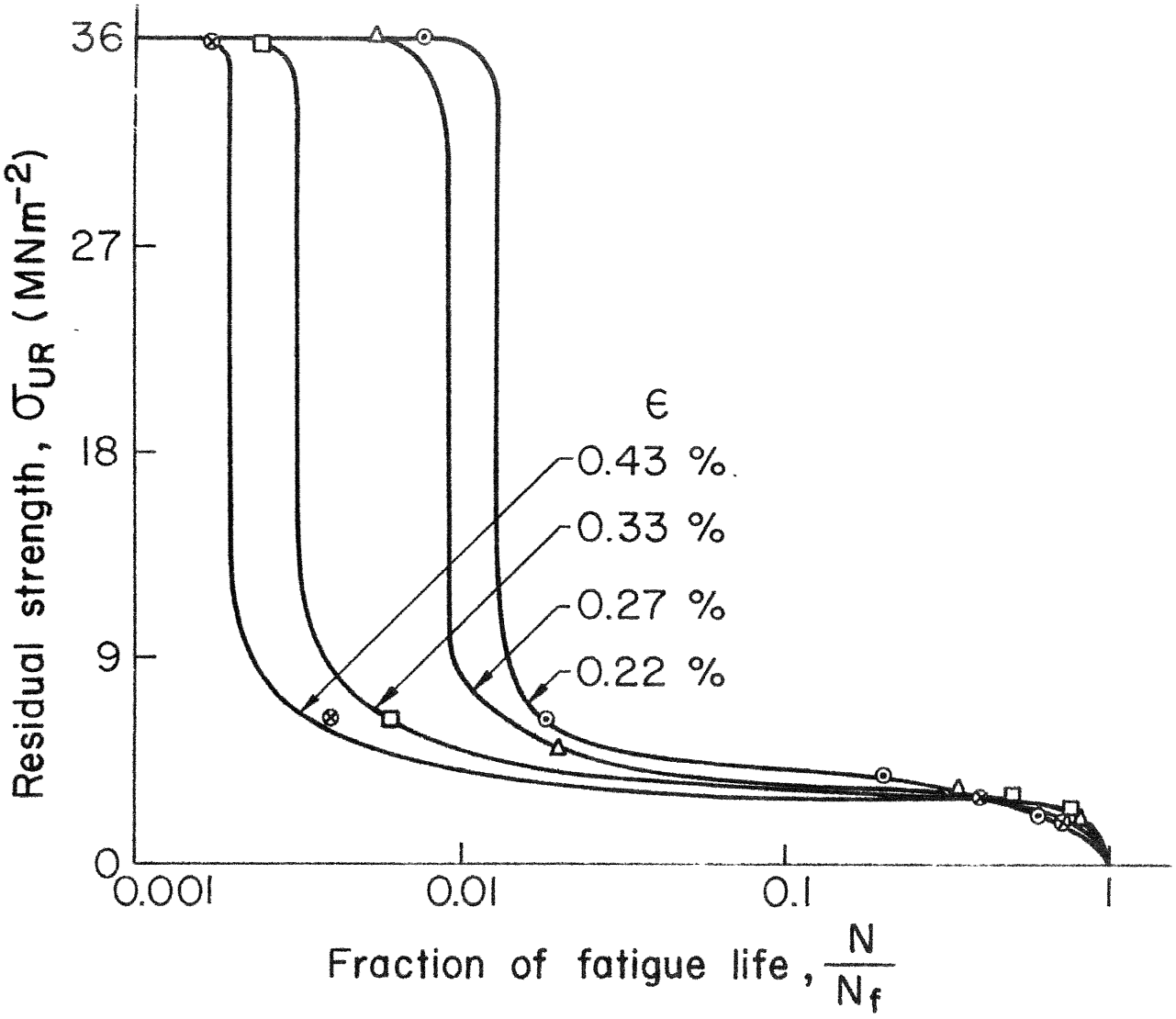

Fig.3.21 Variation of residual strength with fraction of fatigue life (Transverse specimens)

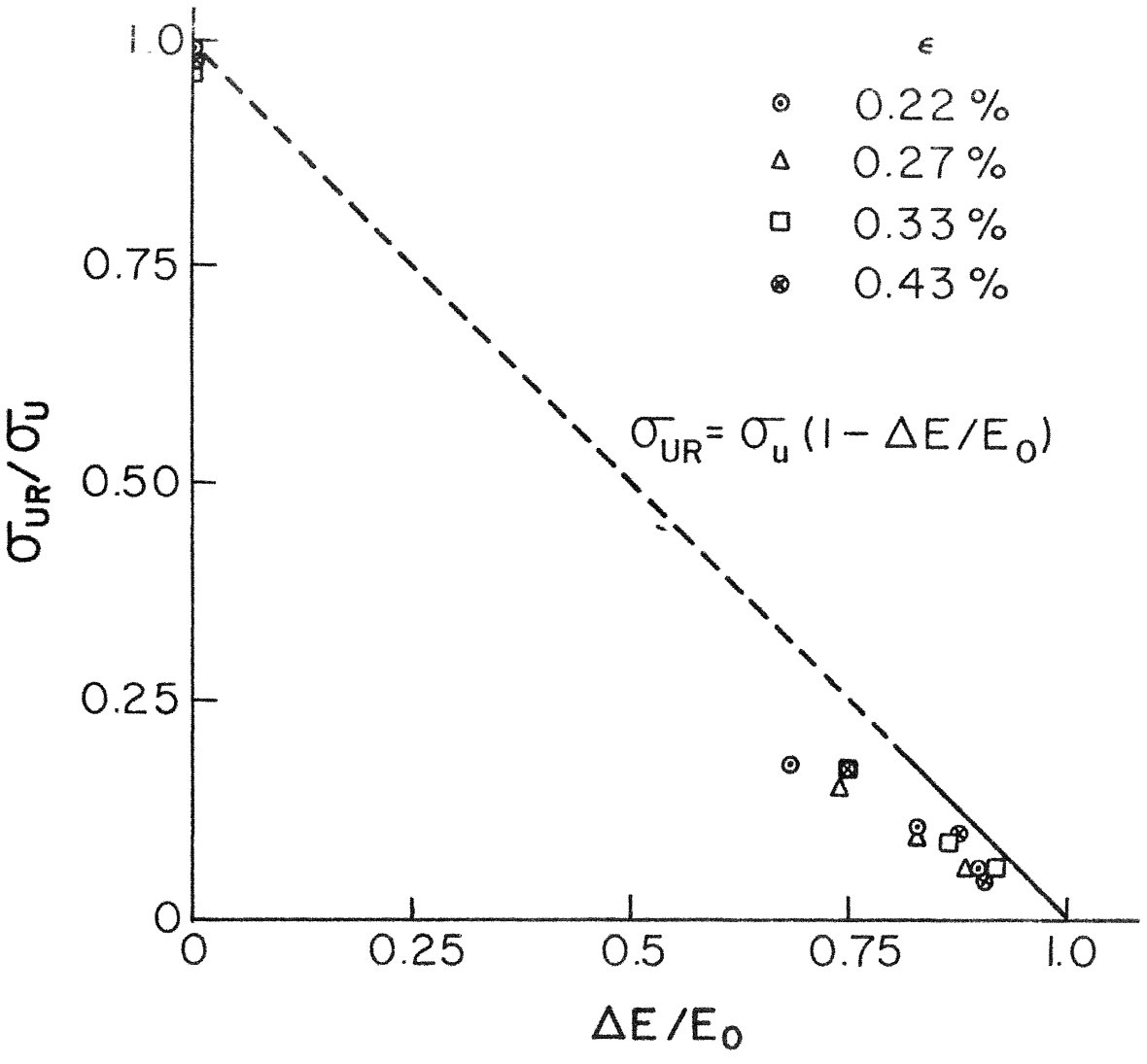

Fig.3.22 Variation of normalized residual strength with loss in stiffness (transverse specimens)

0.38 and 0.53 percent respectively at the fixed end of the specimen. The tests were performed on low capacity machine at a frequency of about 10 Hz.

Results of fatigue tests are given in Table 3.5 and shown graphically in Fig. 3.23. Each point in the figure represents fatigue life corresponding to fracture or separation of the specimen. It is observed that fatigue life of specimen varies from less than 100 cycles to more than 10^6 cycles. Scatter in the fatigue life in this case has also been observed to be of one order of magnitude as was observed in the two cases discussed earlier.

Bending moment at the fixed end of the specimens was measured at desired intervals for several specimens in each set of specimens tested at a fixed strain amplitude. Typical variation in the cyclic bending normalised with respect to the first cycle bending moment is shown in Fig. 3.24. It is observed that the loss of stiffness in the first half of fatigue life is only very marginal. The first significant change in stiffness takes place by a sudden drop which occurs between 60 to 90% of fatigue life. As strain amplitude decreases, the occurance of sudden drop tends to shift to higher fraction of fatigue life. At the end of the sudden drop the stiffness reduces to approximately half of its first cycle stiffness. The stiffness drop is accompanied by a clearly audible sound over an interval of few cycles. The sound emanates due to release

Table 3.5: Fatigue Life of 45° Specimens at Different Strain Amplitudes

N_f			
$\varepsilon = 0.22\%$	$\varepsilon = 0.28\%$	$\varepsilon = 0.38\%$	$\varepsilon = 0.53\%$
998,780	153,528	15,678	897
910,325	140,028	13,892	806
845,680	125,438	10,737	785
834,500	116,357	10,215	621
824,725	102,342	8,978	585
817,510	98,505	8,250	402
810,220	91,137	7,818	391
692,715	85,346	7,624	362
620,050	79,892	7,411	338
520,120	75,630	6,522	303
510,070	71,500	6,000	290
450,728	61,037	5,638	281
435,890	58,316	5,227	265
425,750	52,050	4,915	245
320,050	47,538	4,527	226
	44,370	4,218	143
5 Runouts	42,358	3,492	131
at one	39,893	3,259	122
million	31,839	2,506	117
cycles	22,453	1,215	90

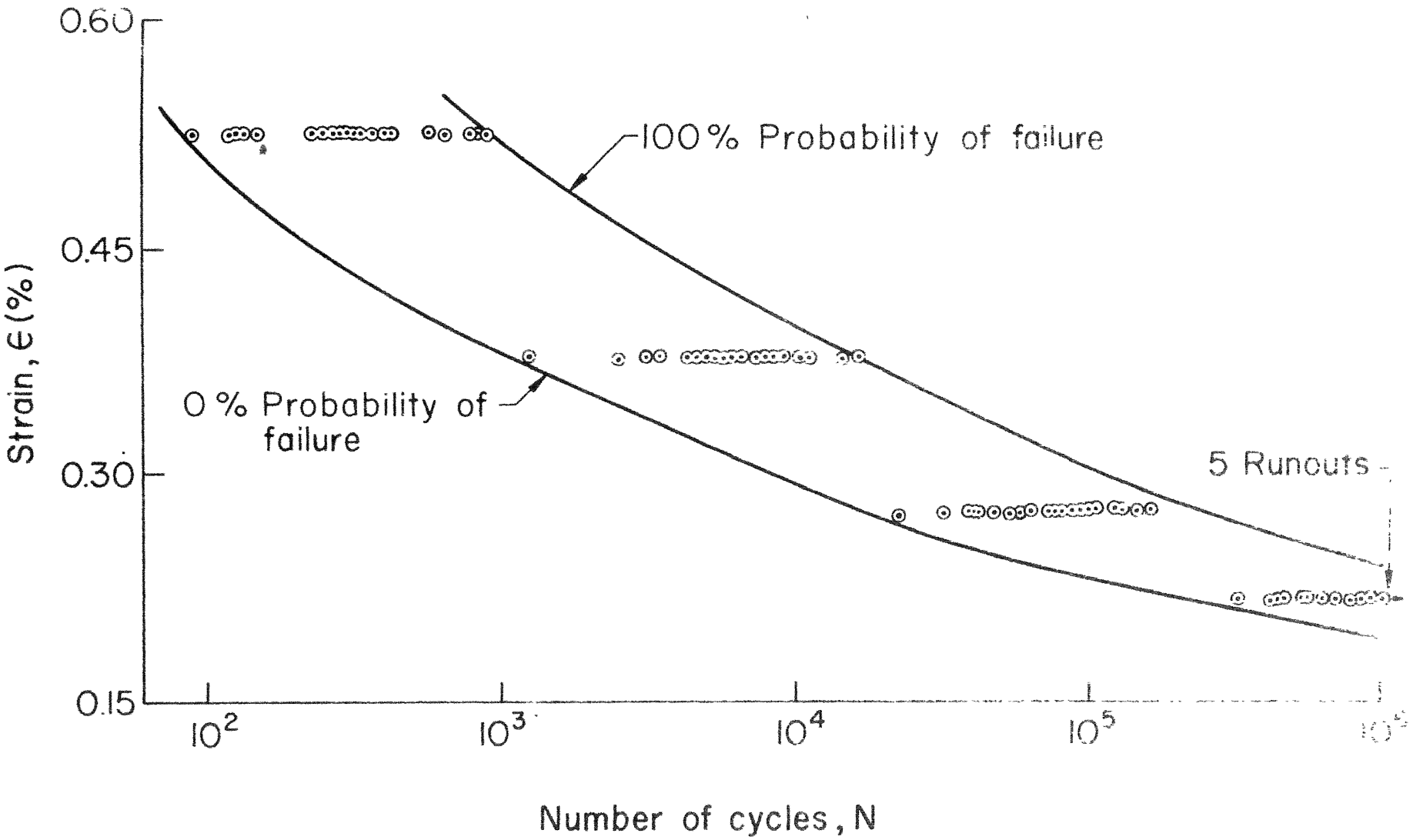

Fig.3.23 Strain vs fatigue life curves for 45° specimens

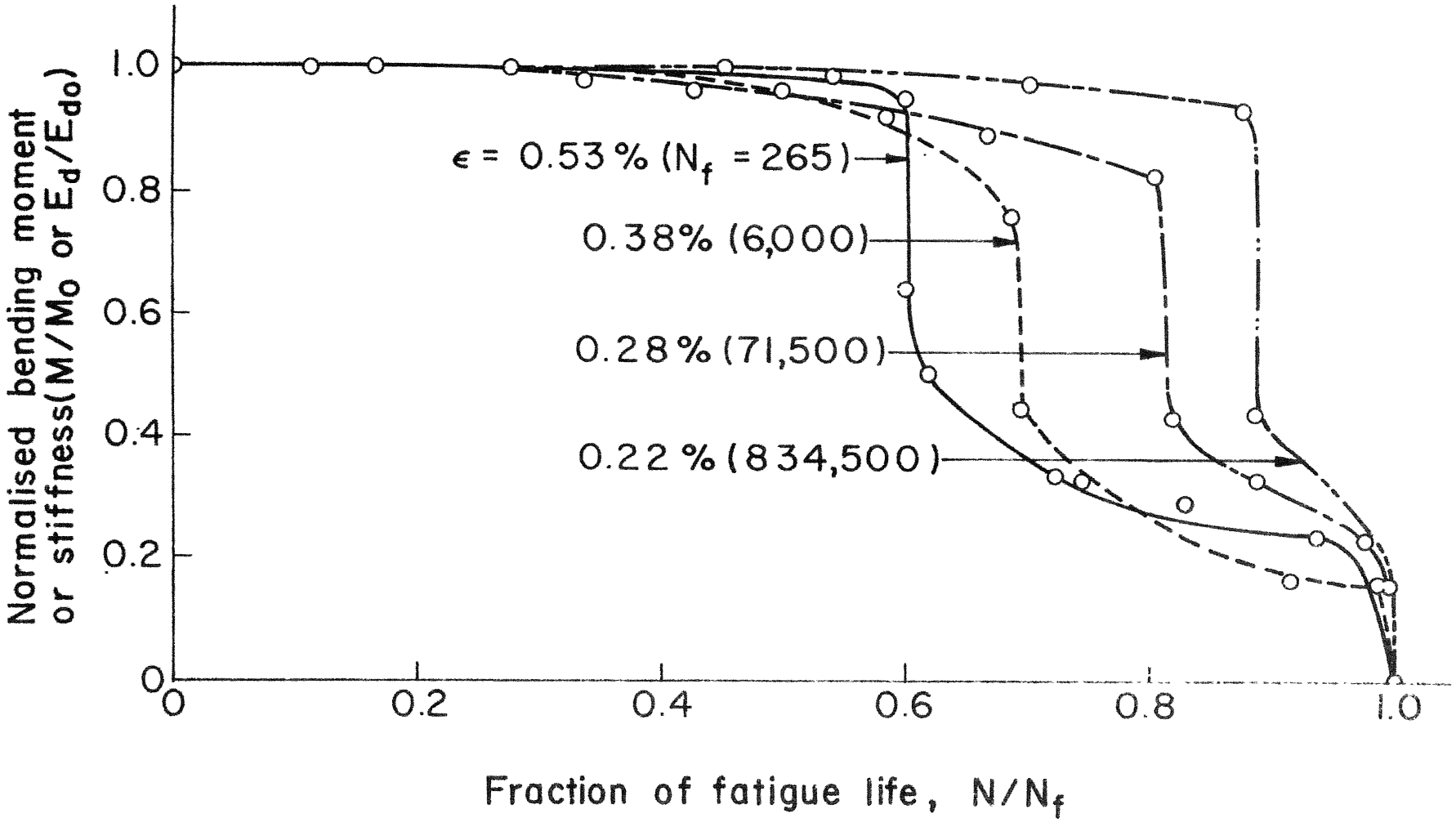

Fig. 3.24 Variation of normalized bending moment or stiffness with fraction of fatigue life for different strain limits (45° specimens)

of energy during formation of crack. The crack initiates at the fixed end and forms along the length of the fibres due to shear failure of the matrix and/or interface failure and causes reduction in stiffness. The crack becomes visible at the end of the sudden drop in stiffness. Figure 3.25 shows a photograph of a specimen with a crack and a photomicrograph shows the crack path. Beyond the sudden drop, stiffness gradually decreases to 25% of the first cycle stiffness. At this stage, stiffness decreases very rapidly and complete separation takes place within few cycles.

The observations concerning loss of stiffness in 45 degree specimen are qualitatively the same but quantitatively different from those observed in the case of transverse specimens. In both cases a significant drop in stiffness occurs by a sudden drop which is not observed in longitudinal specimens. In 45 degree specimens, the sudden drop occurs after half the fatigue life whereas in the transverse specimens it occurs at less than 5% of expected fatigue life. Moreover the sudden drop is very severe in the case of transverse specimens reducing stiffness to about 30% of the original stiffness whereas in the case of 45° specimens sudden drop reduces the stiffness to about 50%. The difference in behaviour can be explained through failure mechanisms in the two cases. In case of transverse specimen, failure occurs due to interface

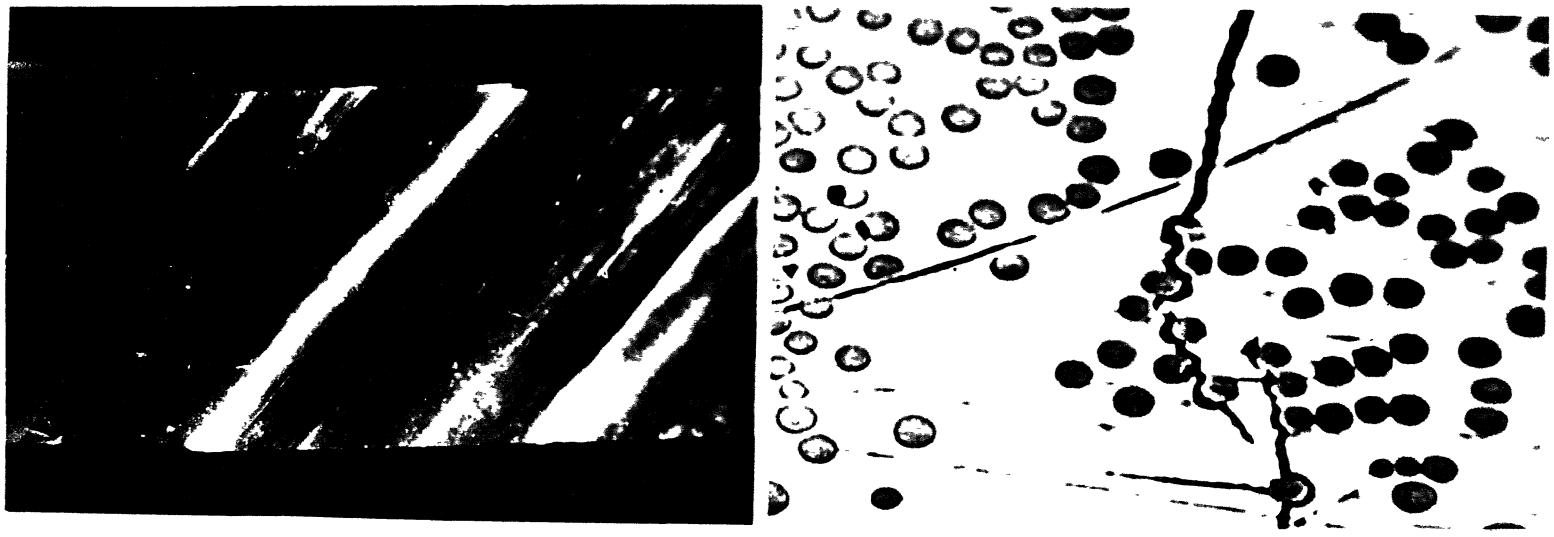

(a) (b)

Fig. 3.25 (a) Crack along the fibre-matrix interface and (b) photo-micrograph showing crack path just after the sudden drop in stiffness in a 45° specimen

failure. The crack once initiated propagates very fast in thickness direction. It is arrested only near the middle plane where the stress is very small. This crack at the fixed end runs across the entire width of the specimen; thus making the fibres near the surface completely ineffective and consequently a severe sudden drop in stiffness occurs. In the 45° specimens failure occurs due to combined effect of interface failure and matrix shear failure. Crack at the fixed end initiates on one of the longitudinal edges and propagates along the length of the fibres. Thus crack propagation occurs along the length also. Strain is decreasing along the direction of the crack propagation. It is therefore expected that depth of crack is decreasing in the direction of crack propagation. Therefore, the sudden drop is less severe.

S-N curves representing different stages of material damage have been shown in Fig. 3.26. Since the three curves representing marginal and 50% loss in stiffness and complete separation are very close to each-other, curves for other stiffnesses have not been shown. The curves are expected to be close to each other because sudden drop in stiffness occurs after half the fatigue life and on a log scale the later half gets squeezed. In view of the closeness of the curves it may be suggested that the left most curve be taken as the failure curve without being unduly conservative.

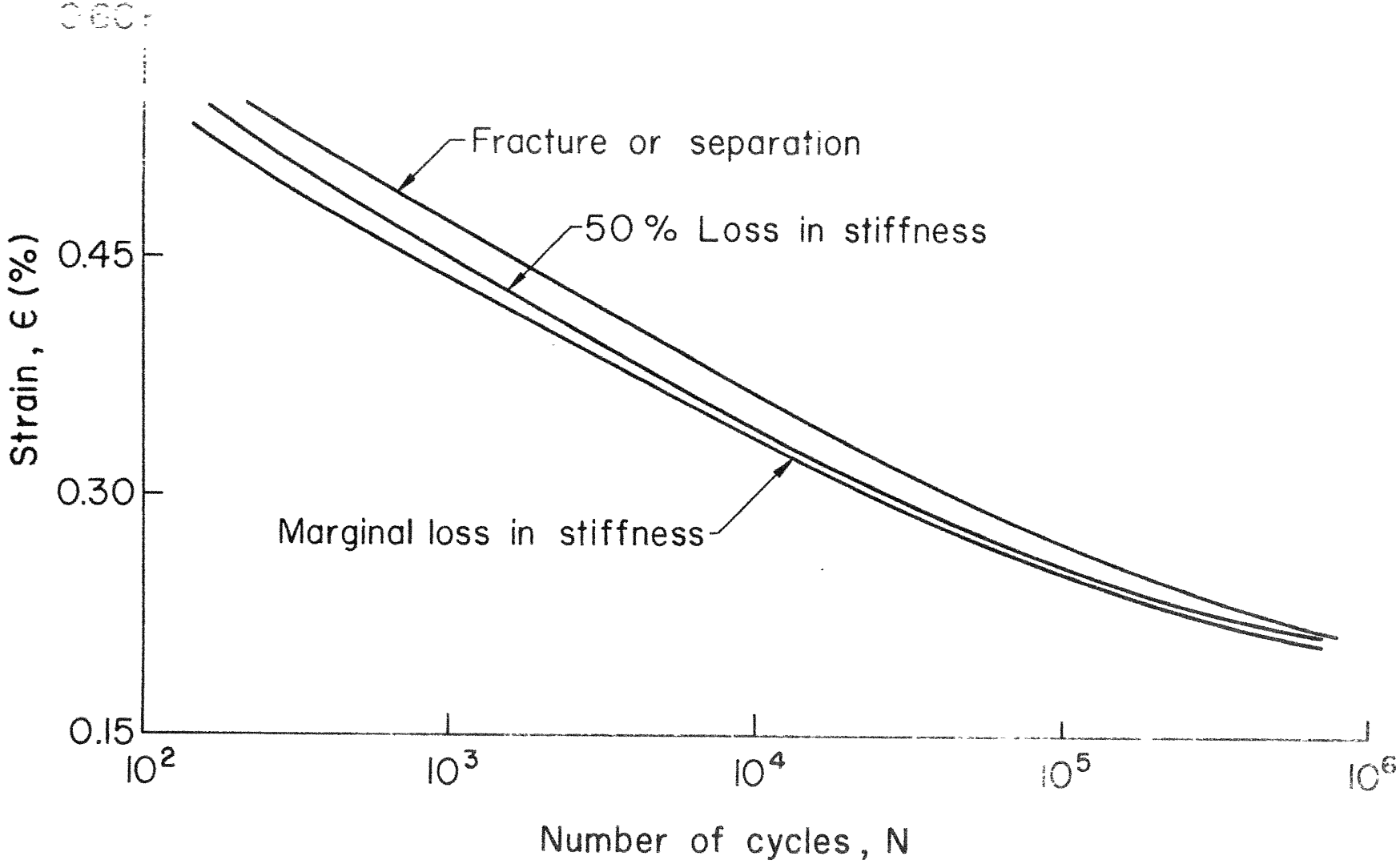

Fig.3.26 S-N curves representing different stages of damage in 45° specimens.

Static tests on precycled specimens were performed to further investigate the progressive damage. Fractions of fatigue life selected for precycling were such that the dynamic stiffness of the specimens were in both ranges, that is, before and after the sudden drop. Records of bending moment versus end deflection in these static tests are shown in Figs. 3.27 to 3.30. It is observed that the bending moment versus deflection curve for a specimen precycled to a point before sudden drop cannot be distinguished from the curve for a virgin specimen as in the case of transverse specimens. The ratio of residual stiffness to initial stiffness (E_R/E_o) as calculated from Figs. 3.27 to 3.30 are given in Table 3.6 and have been plotted against loss in dynamic stiffness ($\Delta E_d/E_{do}$) in Fig. 3.31. The points for all strain amplitudes have been plotted on the same graph. Data could not be obtained for normalised dynamic stiffness loss between 0 and 0.5 due to sudden drop in stiffness which was observed in all cases. The available data pointsin this case also are close to the straight line given by Eq. (3.1) as was observed in the two previous cases. The dotted part of straight line in Fig. 3.31 corresponds to the range of stiffness in which data could not be obtained. Thus normalised static stiffness equals the normalised dynamic stiffness in this case also.

Residual strength has been plotted as a function of fraction of fatigue life in Fig. 3.32. The trends

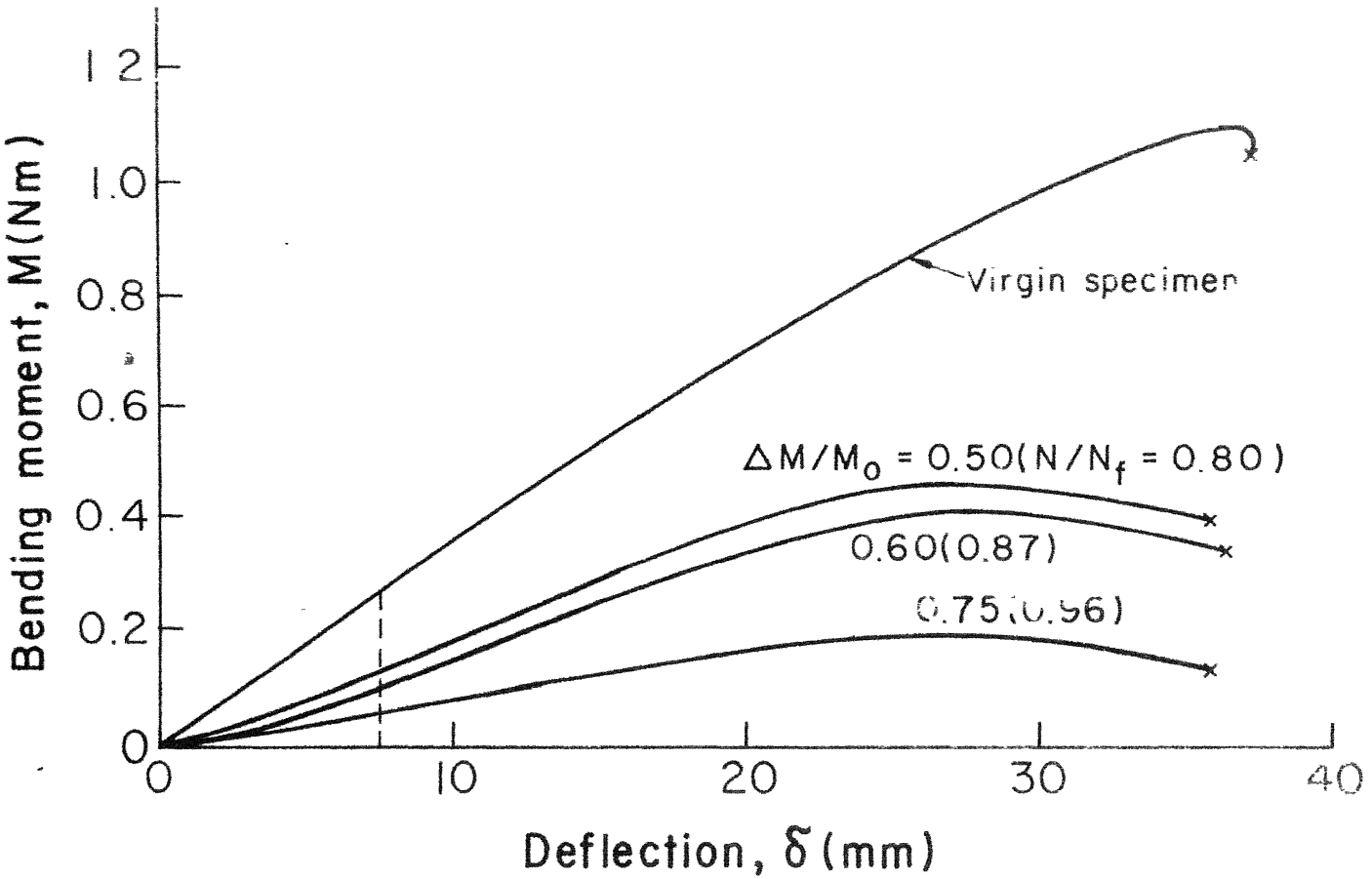

Fig. 3.27 Bending moment vs deflection curves for specimens precycled to different stages of damage (45° specimens, $\epsilon = 0.22\%$)

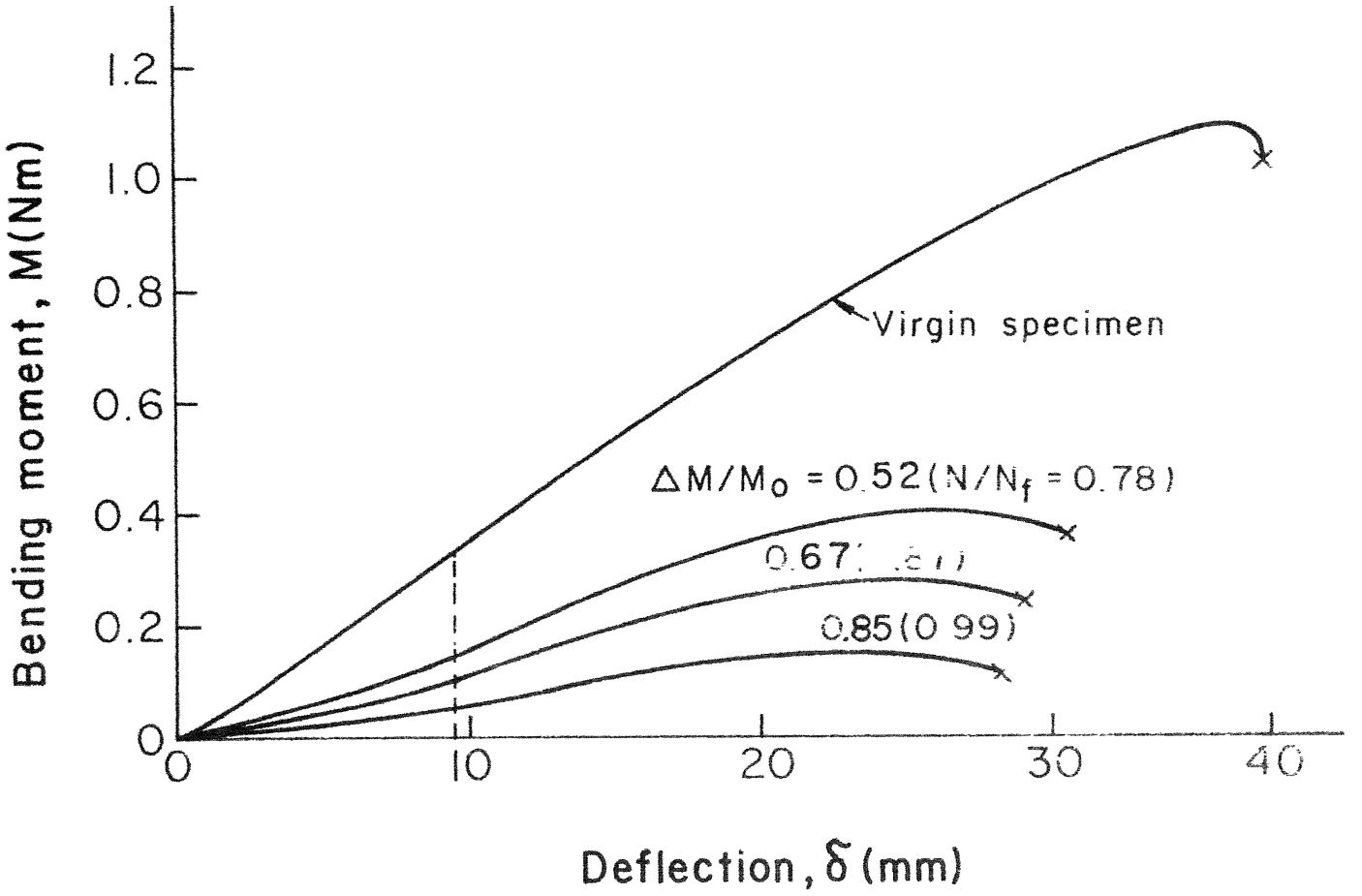

Fig. 3.28 Bending moment vs deflection curves for specimens precycled to different stages of damage (45° specimens, $\epsilon = 0.28\%$)

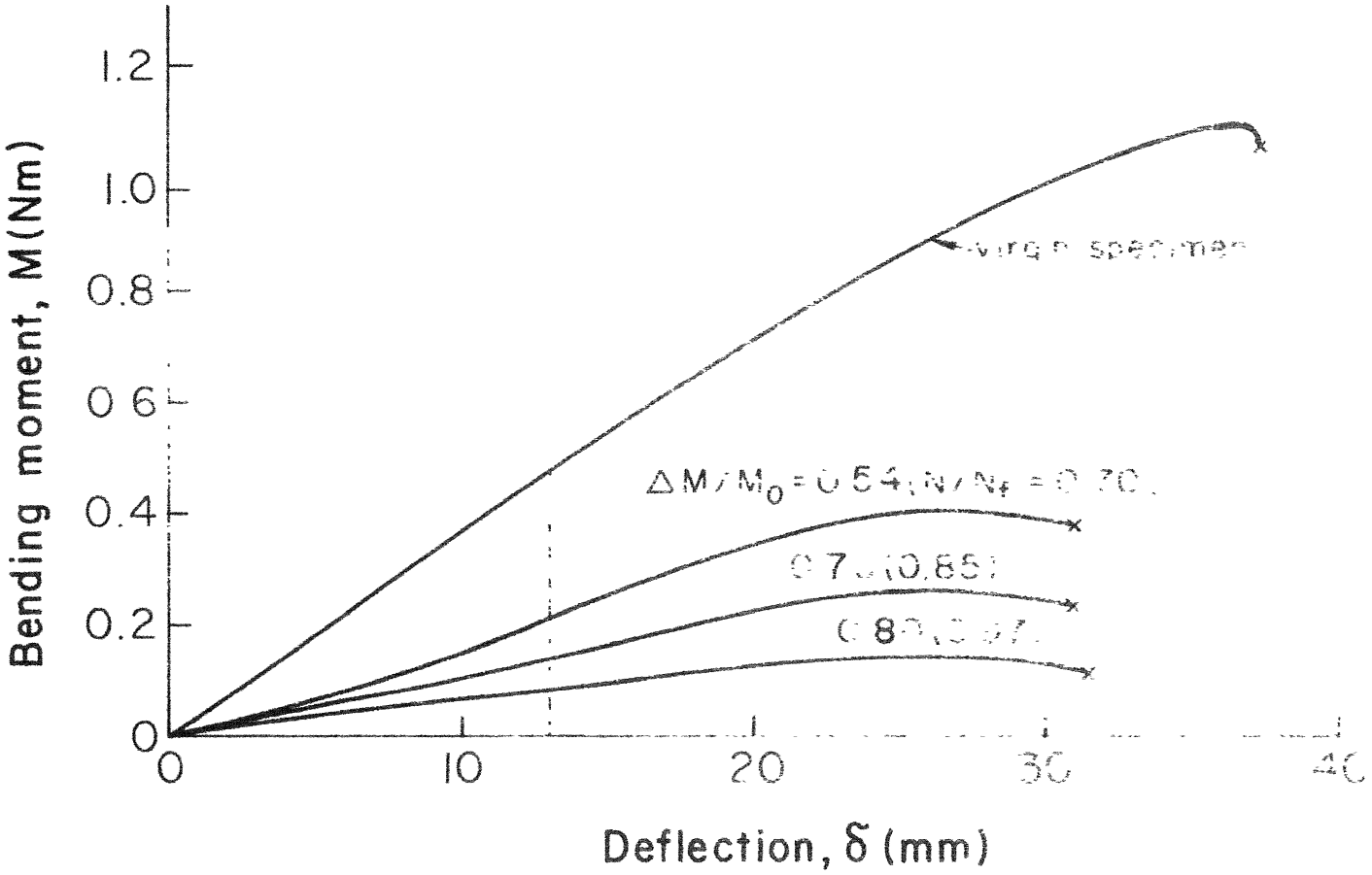

Fig.3.29 Bending moment vs deflection curves for specimens precycled to different stages of damage (45° specimens, ϵ = 0.38 %)

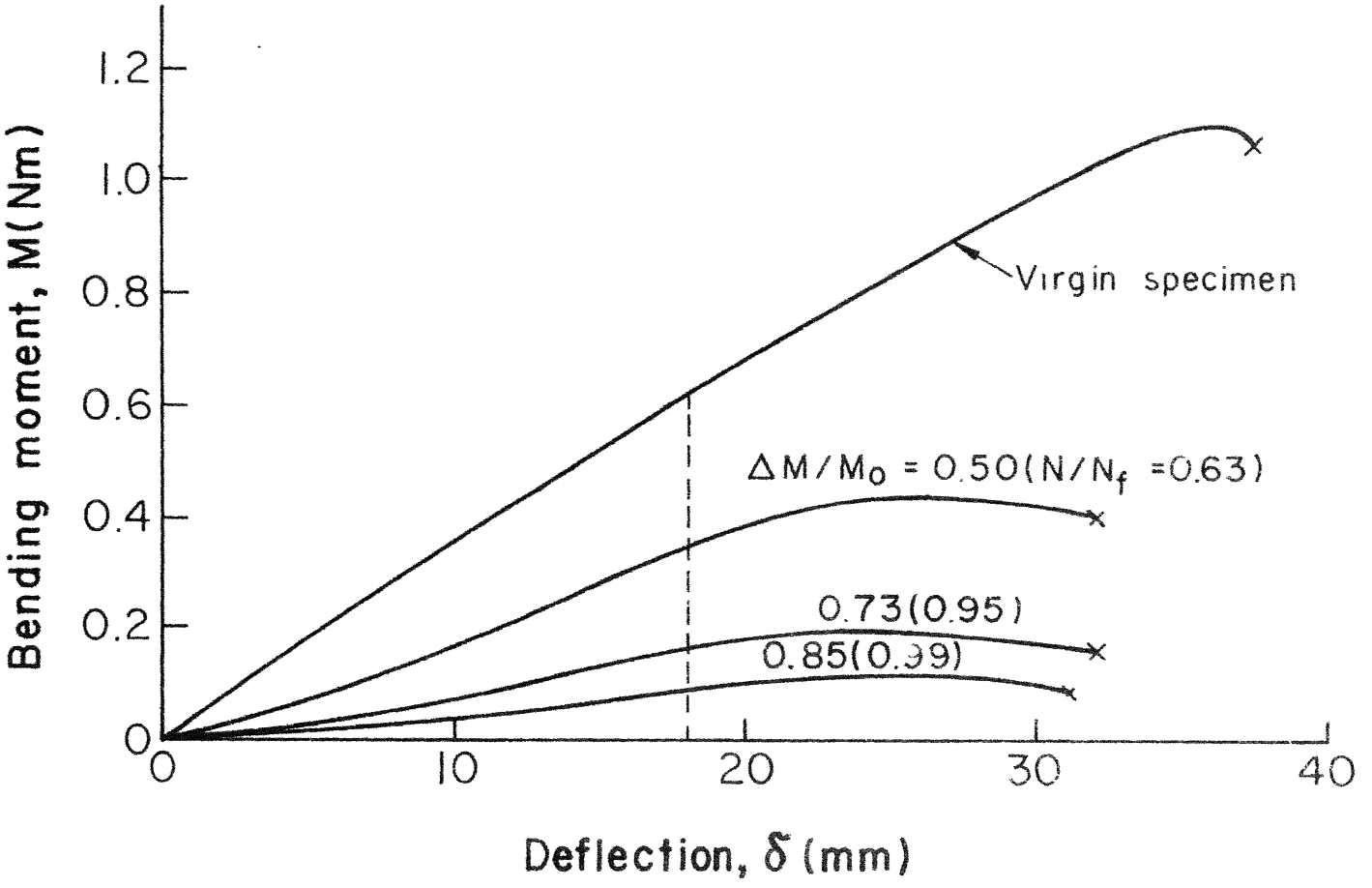

Fig. 3.30 Bending moment vs deflection curves for specimens precycled to different stages of damage (45° specimens, $\epsilon = 0.53\ \%$)

Table 3.6: Ratio of Residual Stiffness to Stiffness of a Virgin Specimen at Different Fraction of Average Fatigue Life for Different Strain Amplitudes (45 Specimens).

$\varepsilon = 0.22\%$		$\varepsilon = 0.28\%$		$\varepsilon = 0.38\%$		$\varepsilon = 0.53\%$	
N/N_f*	E_R/E_o	N/N_f*	E_R/E_o	N/N_f*	E_R/E_o	N/N_f*	E_R/E_o
0.475	1.0	0.635	0.973	0.375	0.985	0.245	0.965
0.80	0.479	0.78	0.450	0.70	0.433	0.63	0.450
0.87	0.375	0.87	0.317	0.85	0.276	0.95	0.250
0.96	0.196	0.99	0.137	0.97	0.179	0.99	0.143

* N_f Average fatigue life

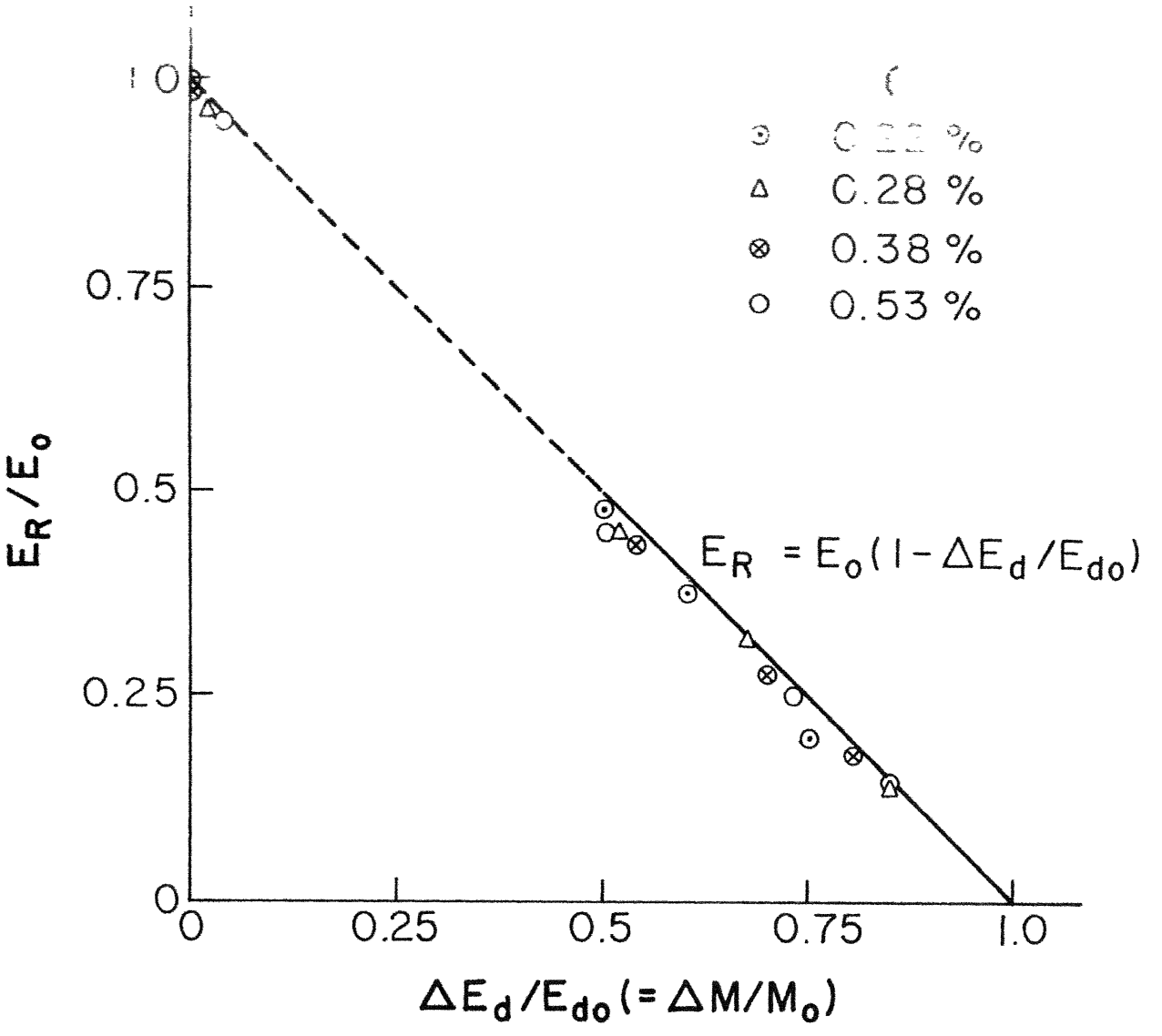

Fig. 3.31 Normalised residual stiffness vs. loss in dynamic stiffness (45° specimens)

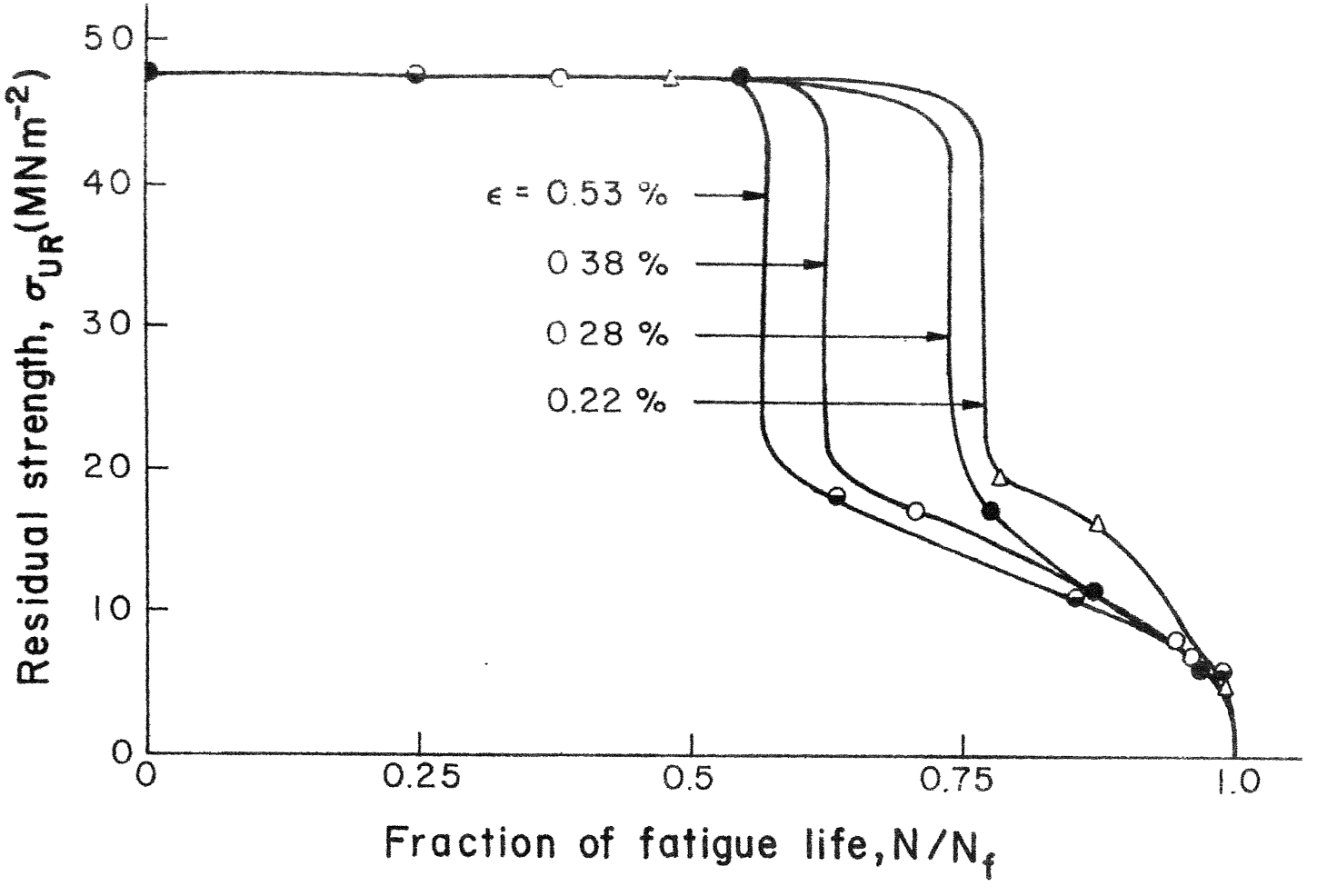

Fig. 3.32 Variation of residual strength with fraction of fatigue life (45° specimens)

exhibited by the residual strength at different strain limits are very similar to the ones exhibited by the normalised bending moment shown in Fig. 3.24. It is again observed that before sudden drop, like stiffness, there is little loss in strength. After the sudden drop, residual strength gradually decreases with fraction of cyclic life in a manner similar to the stiffness retained. Residual strength has been plotted as a function of loss in stiffness in Fig. 3.33. Once again it observed that the residual strength is close to that predicted by Eq. (3.2) as in the previous cases. The dotted portion of line again represents the range of stiffness in which data could not be obtained due to sudden drop in the stiffness.

3.4 FATIGUE BEHAVIOUR OF 10° SPECIMENS*

The second fibre orientation selected to study the off-axis fatigue behaviour was 10°. Significance of 10° specimens lies in the fact that when subjected to uniaxial stress they fail under shear mode of failure and many investigators [33, 34] have suggested the use of 10° specimens to study in-plane shear behaviour of unidirectional composites. Displacement amplitudes employed in these tests were 25, 30, 35 and 44 mm which produce strain amplitudes of 0.53, 0.61, 0.71 and 0.90% respectively

* A paper entitled "Crack Propagation in Off-Axis (10°) Unidirectional Glass-Epoxy Composite During Flexural Fatigue" based on part of the work discussed in the section was presented at the International Conference on Fracture Mechanics in Engineering Applications held on 26-30 March 1979 at Bangalore, India.

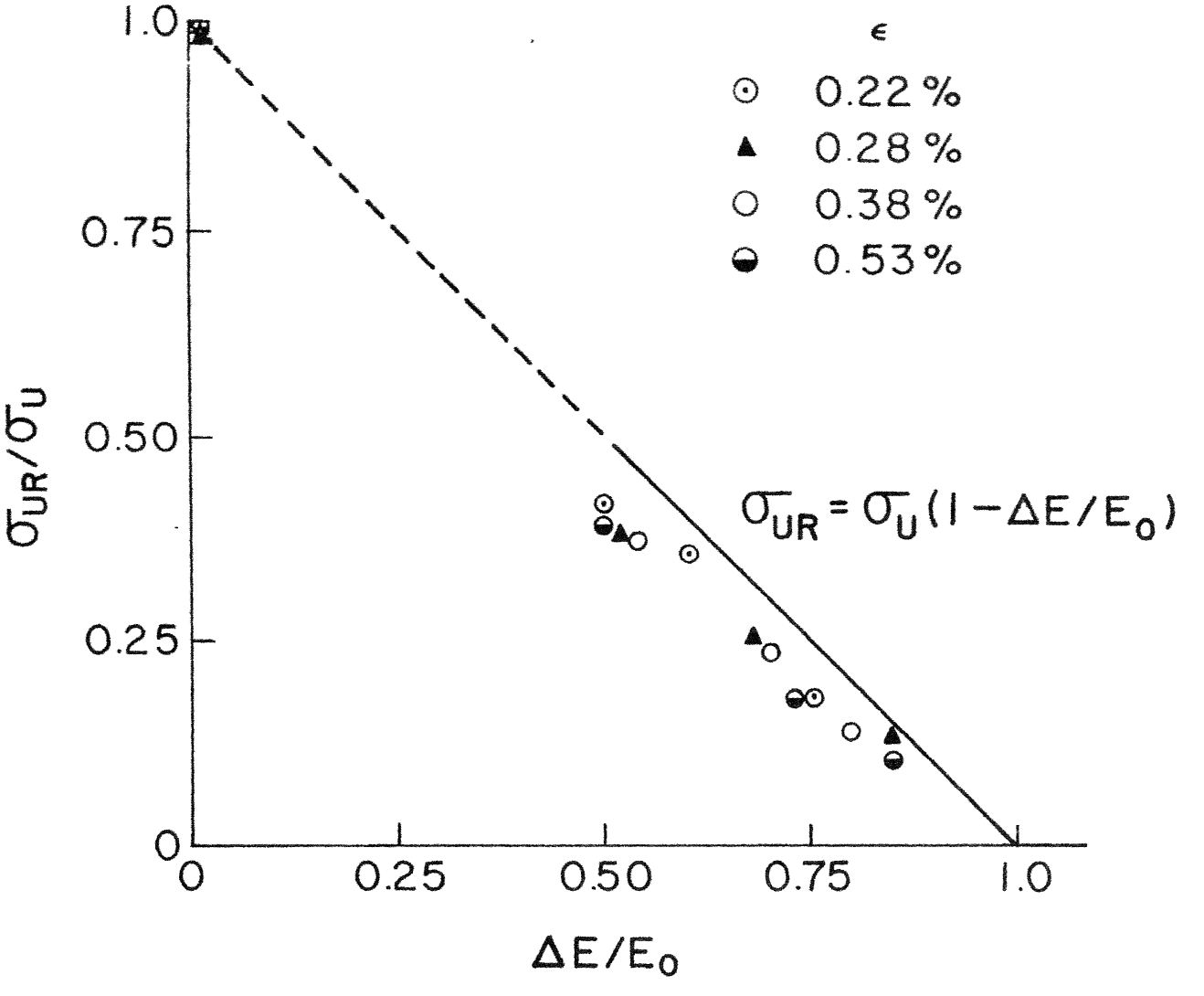

Fig. 3.33 Variation in normalized residual strength with loss in stiffness (45° specimens)

at the fixed end of the specimens. Tests were performed on the high capacity machine at frequencies between 6 and 8 Hz.

A peculiar behaviour has been observed in the constant deflection fatigue of 10° specimens. Initially, stiffness of these specimens gradually decreases with fatigue cycling and later appears to stabilise at a value lower than the first cycle stiffness (at about 50%). Typical variations in normalised stiffness with number of cycles are shown in Fig. 3.34. When these specimens are further cycled, no further drop in stiffness occurs and no separation is observed. In many specimens no change occurred even when the additional cycles were twice the number of cycles in which the stabilised stiffness was first observed. Nearly zero slope of the curves in Fig. 3.34 at the stabilised stiffness indicates that further fatigue cycling at constant deflection does not produce additional damage to the specimens. Therefore failure by separation is not expected to occur in this case. This behaviour will be further explained later in this section through observed crack propagation and strain field in the specimens. In view of this peculiar behaviour, it was decided to assume the failure to have occurred when the stiffness is first observed to be 50% of its initial value. The minimum number of cycles corresponding to this stiffness were taken as a fatigue life (N_f) for 10° specimens.

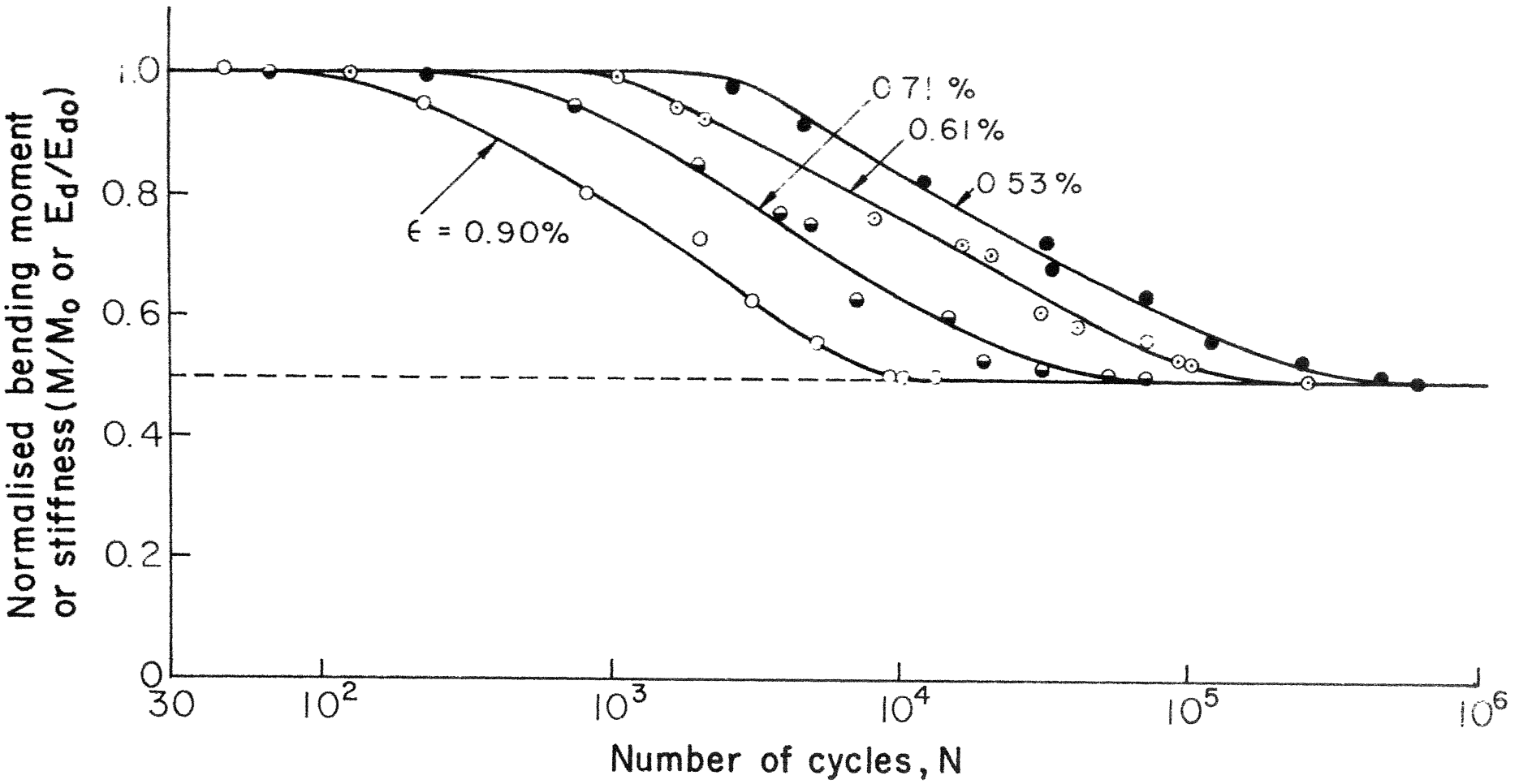

Fig.3.34 Variation in normalised stiffness with number of cycles for different strain limits (10^6 specimens)

It may be pointed out that the behaviour is peculiar because of the deflection controlled tests. In the case of stress or bending moment controlled tests, a continued damage to the material and consequently failure by separation may be expected.

The results of fatigue tests are given in Table 3.7 and shown graphically in Fig. 3.35. It is observed that the fatigue life of specimens varies between 3000 to 10^6 cycles. General nature of the fatigue curves is similar to the one observed in earlier cases. Scatter in fatigue life appears to be less than one order magnitude.

Bending moment at the fixed end was measured at desired intervals for several specimens in each set of specimens tested at a fixed strain amplitude. Typical variation of cyclic bending moment normalised with respect to the first cycle bending moment is shown as a function of fraction of fatigue life in Fig. 3.36. It is observed that for each strain amplitude loss in stiffness is progressive. There is no sudden drop as was observed in transverse and 45° specimens. As explained earlier, stiffness stabilises to 50% of the first cycle stiffness. This behaviour is different from that of longitudinal specimens where stiffness reduces to zero and complete fracture takes place. This peculiar behaviour can be explained as follows through the crack propagation in these specimens.

Table 3.7: Fatigue Life of 10° Specimens at Different Strain Amplitudes

N_f			
ε = 0.53%	ε = 0.61%	ε = 0.71%	ε = 0.90%
980,350	301,250	71,200	10,000
905,758	292,560	65,000	8,900
860,870	286,460	50,000	7,320
810,325	255,000	49,050	5,800
785,000	249,000	48,090	4,700
745,780	240,125	46,980	4,300
610,350	232,256	45,150	4,100
520,128	220,205	42,200	3,610
399,787	205,650	39,050	3,102
298,790	192,070	37,152	3,050
	180,050	35,000	2,890
10 Runouts	159,758	34,700	2,810
at one	141,034	30,210	2,565
million	124,917	26,500	2,500
cycles	90,875	22,050	2,350
	89,035	20,500	2,300
	85,780	19,000	2,200
	83,878	17,490	2,150
	69,980	16,500	2,100
	55,725	15,050	2,050

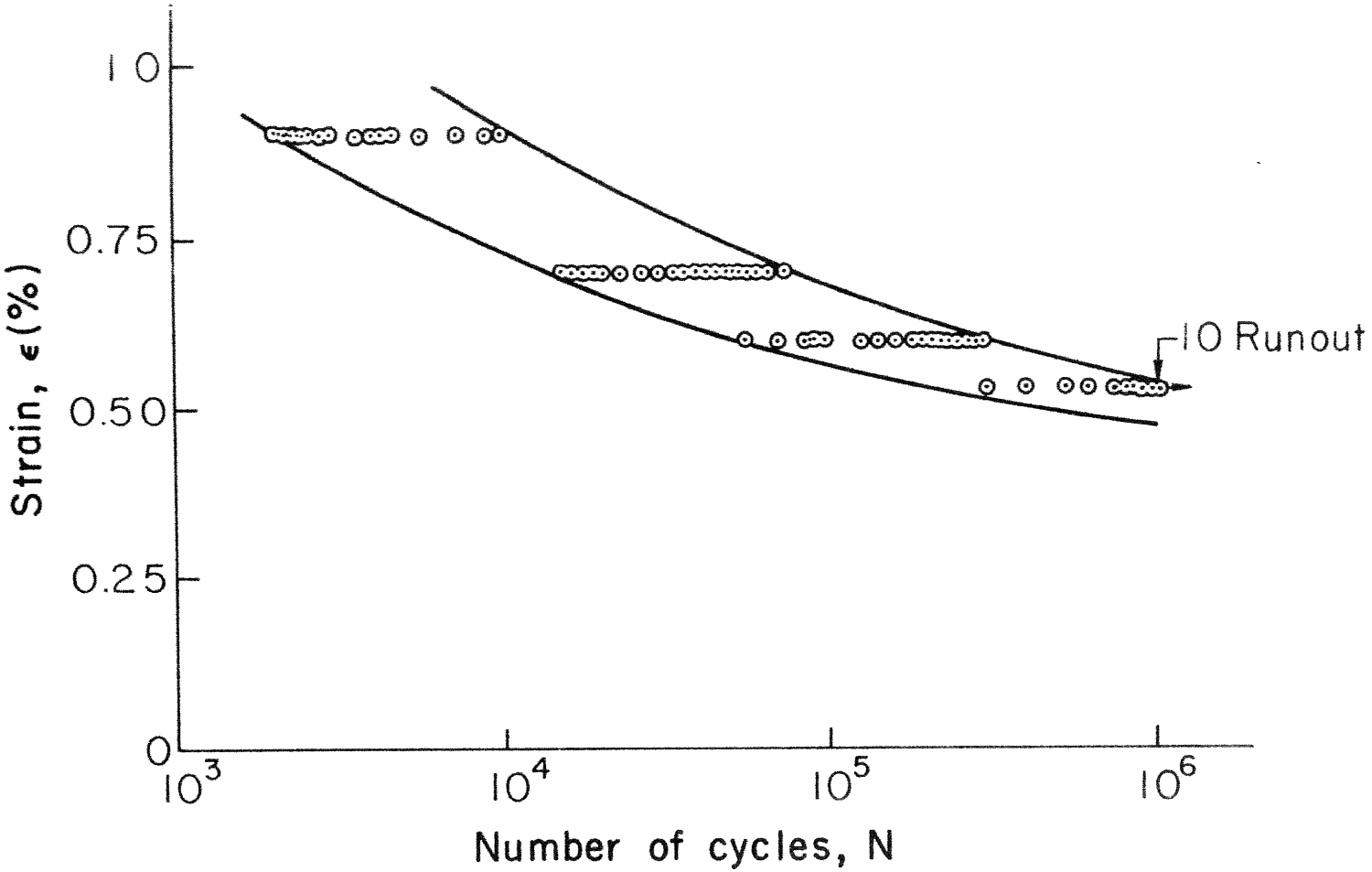

Fig. 3.35 Strain vs fatigue life curves for 10° specimens

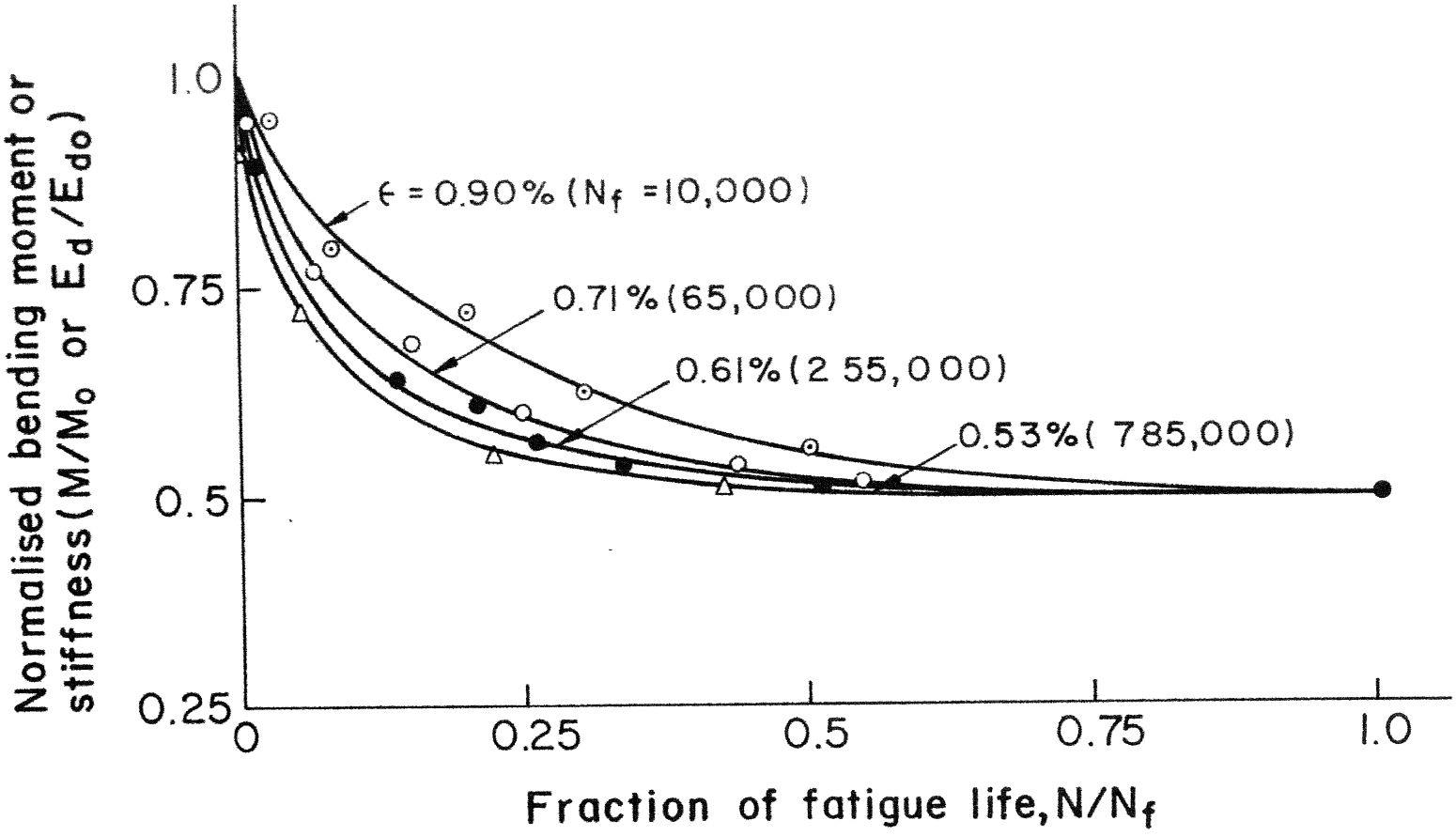

Fig.3.36 Variation of normalised bending moment or stiffness with fraction of fatigue life for different strain limits (10° specimens)

Fatigue damage in the 10 degree specimens initiates by initiation of a crack at the fixed end on one of the longitudinal edges of the specimen. Crack propagates towards the free end along the fibre matrix interface (at 10 degree to the longitudinal edge) due to interface failure and/or shear failure of the matrix. In the initial stages crack propagates with a faster rate because of the high strain value near the fixed end. Rate of crack propagation decreases as the crack tip advances towards the free end where the crack tip strain is small. In most specimens crack is unable to propagate across the full width of the specimen due to the crack tip strain becoming too small to cause further failure. It has been further observed that the crack front is a three dimensional curve so that as the crack propagates in the width and length directions (10^{o} to the longitudinal edge), it also propagates in the thickness direction over a small length. However, once the crack reaches middle plane of the specimen, it does not propagate in the thickness direction. Further propagation of the crack takes place with decrease in the depth of the crack again due to decrease in strain towards the free end. A schematic diagram of the propagation of crack front is shown in Fig. 3.37. Thus, in the specimens in which the crack does propagate across the full width of the specimen, it does not propagate over the entire thickness and consequently full separation of the specimens does not take place.

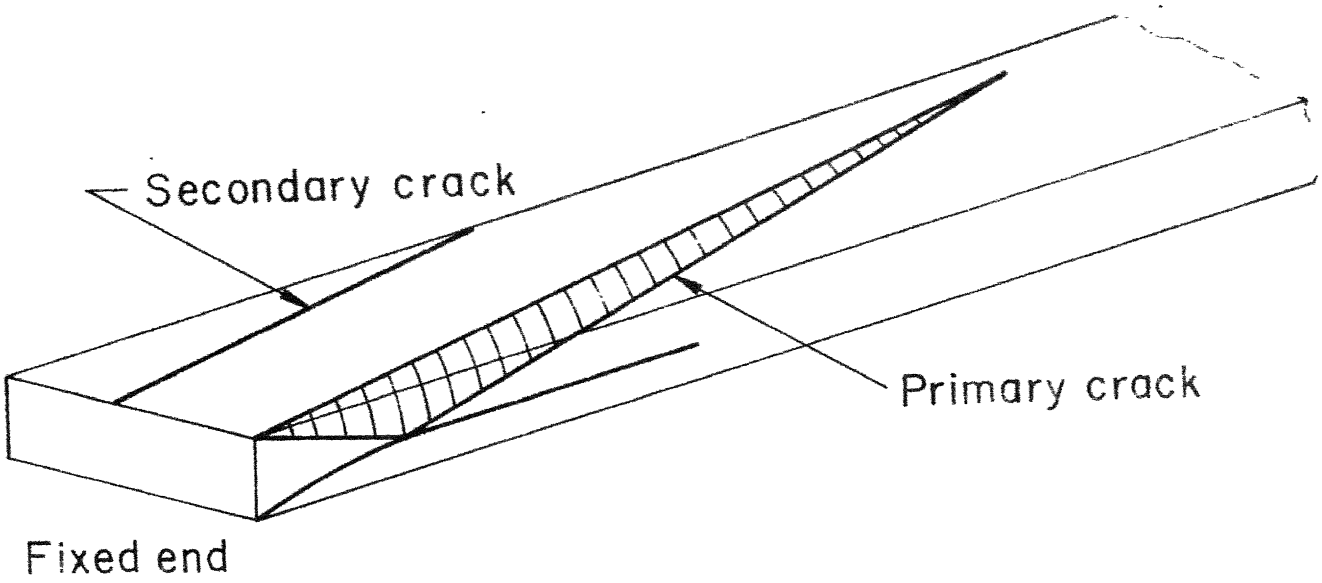

Fig. 3.37 Schematic representation of crack propagation in 10° specimens.

The cracks which initiate at the fixed end and propagate towards the free end of the specimen are formed first and therefore, have been referred to as the primary cracks. As a primary crack propagates, the effective width and the load carrying capacity of the cross-sections decrease. They cause reduction in stiffness of the specimen. Another consequence of this is that the secondary cracks initiate at the second longitudinal edge of the specimen and propagate in a direction opposite to the direction of primary crack propagation. That is, the secondary cracks propagate towards the fixed end. Photographs in Fig. 3.38 show three stages of primary and secondary cracks in a specimen. It has been observed that the secondary cracks propagate at a much faster rate because they are propagating into an increasing strain field. Further, like primary cracks, depth of the secondary cracks near the fixed end is more than that away from it.

S-N curves representing different stages of material damage have been shown in Fig. 3.39. Since stiffness stabilises at 50% of the original stiffness, curves for stiffness losses of more than 50% could not be drawn in this case.

Static tests were performed on specimens precycled to different fractions of fatigue life at different

Fig. 3.38 Three stages of primary and secondary cracks in a 10° specimen

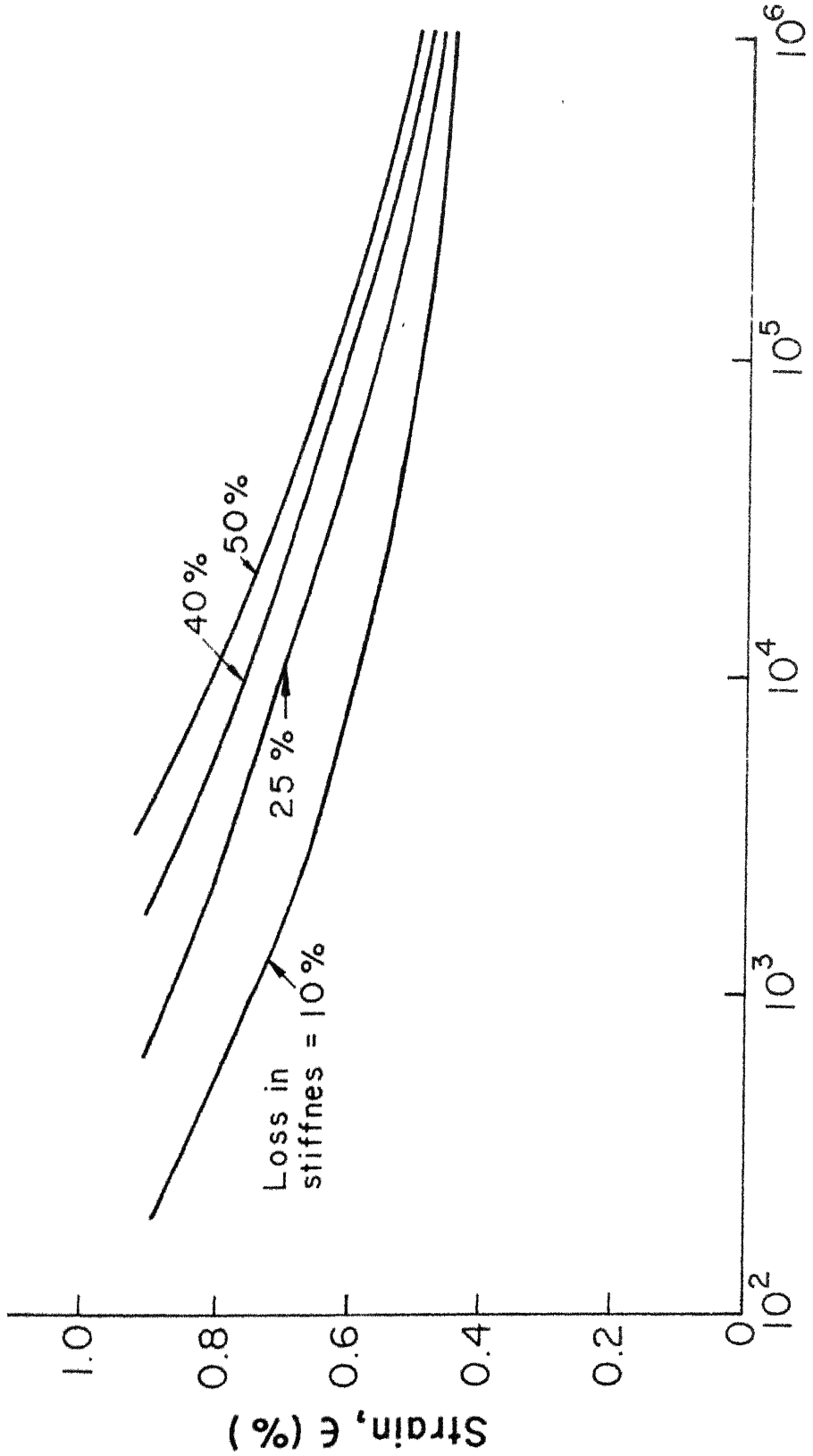

Fig.3.39 S-N curves representing different stages of damage in 10° specimens

strain amplitudes. Records of bending moment versus deflection obtained in these tests are shown in Figs. 3.40 - 3.43. The ratios of residual stiffness to initial stiffness, E_R/E_o, as calculated from Figs. 3.40 to 3.43 are given in Table 3.8 and have been plotted against loss in dynamic stiffness, $\Delta E_d/E_{do}$ in Fig. 3.44. The points for different strain amplitudes have been plotted on the same graph. The data could not be obtained for the loss in stiffness by more than 50% of the original value. As observed in the previous cases, the available data points in this case also are close to the straight line given by Eq. (3.1). The dotted part of straight line corresponds to the range of loss of stiffness in which data could not be obtained. Thus in this case also normalised static stiffness equals the normalised dynamic stiffness.

Residual strength has been plotted as a function of fraction of fatigue life in Fig. 3.45. The trends exhibited by the residual strength at different strain amplitudes are similar to the ones exhibited by the normalised bending moment shown in Fig. 3.36. However, one difference may be noted that the bending moment stabilises at 50% of the first cycle bending moment where as the strength drops to about 40% of the virgin static strength. Normalised residual strength has been plotted as a function of loss in stiffness in Fig. 3.46. Once again it is observed that available data points are close to that

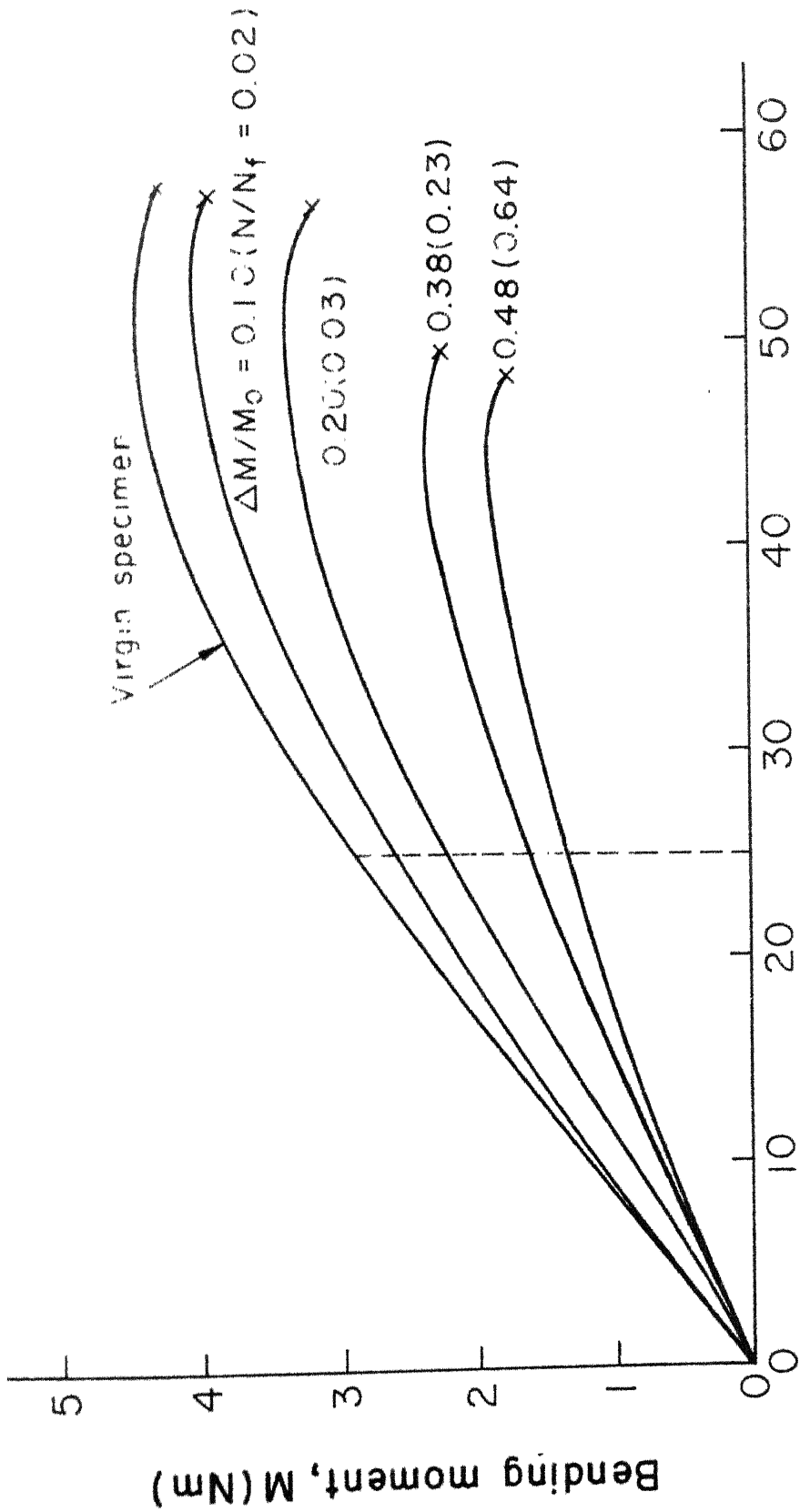

Fig. 3.40 Bending moment vs deflection curves for specimens precycled to different stages of damage (10^6 specimens, ϵ = 0.53 %)

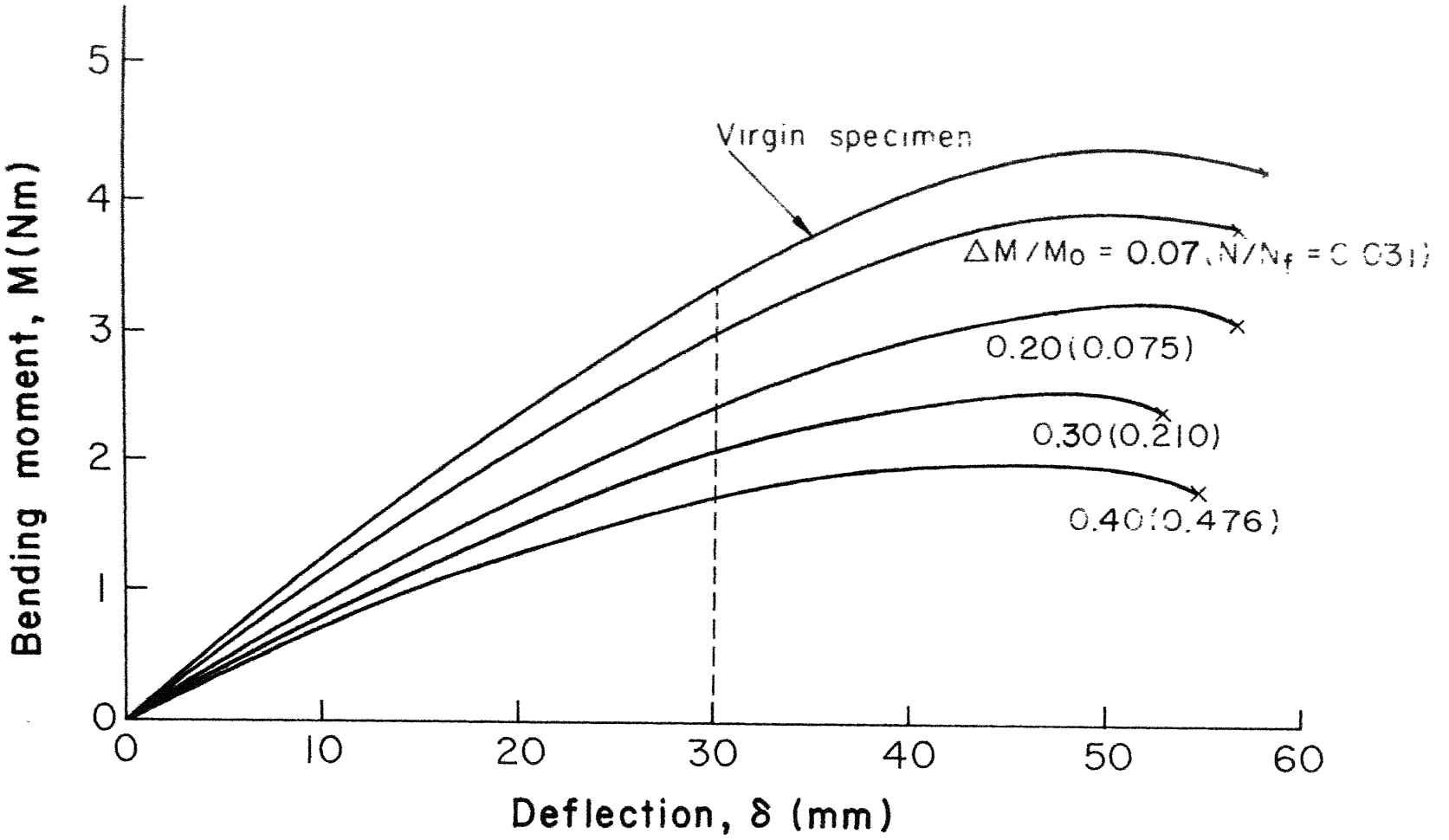

Fig. 3.41 Bending moment vs deflection curves for specimens precycled to different stages of damage (10° specimens, ϵ = 0.61%)

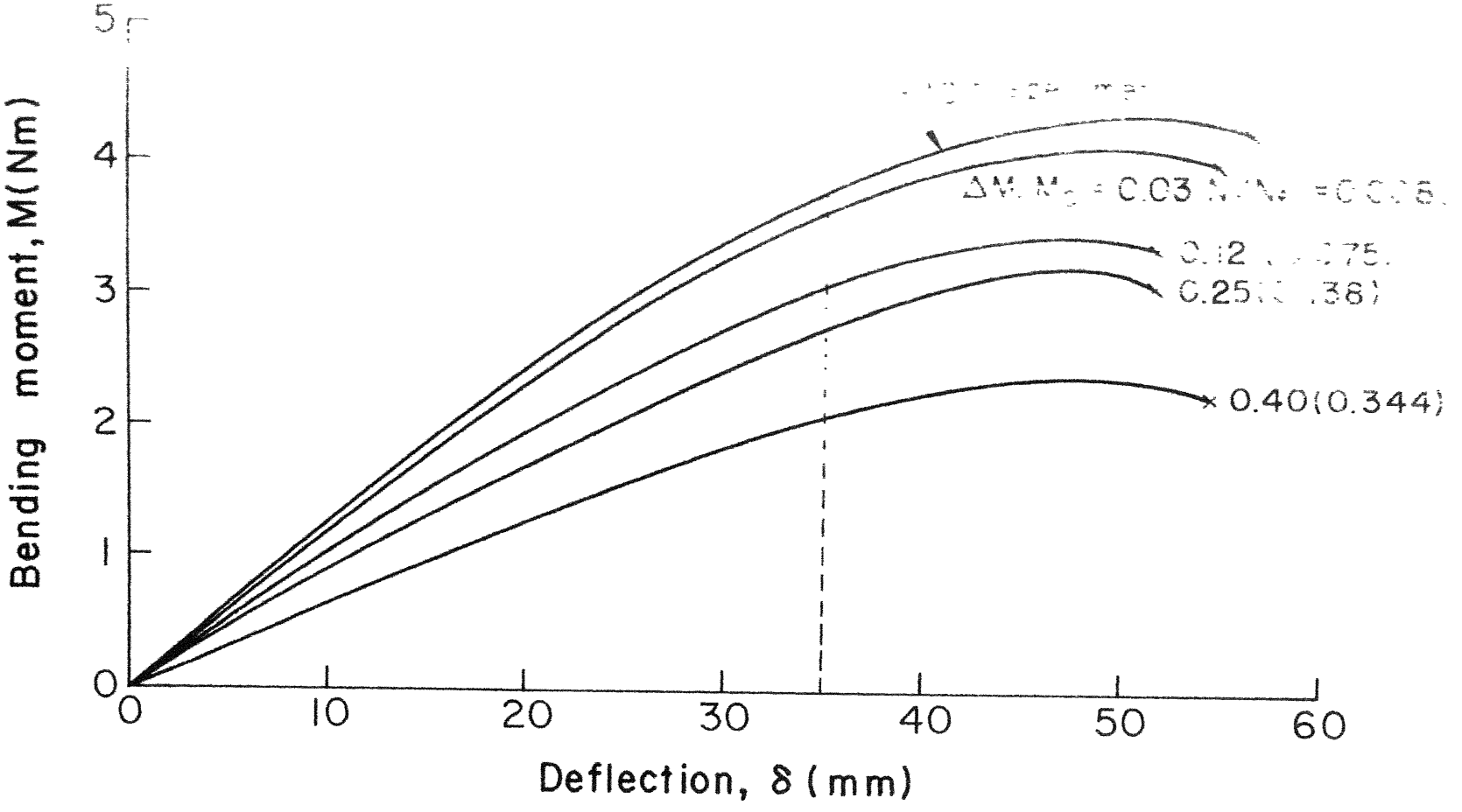

Fig. 3.42 Bending moment vs deflection curves for specimens precycled to different stages of damage (10° specimens, ϵ = 0.71 %)

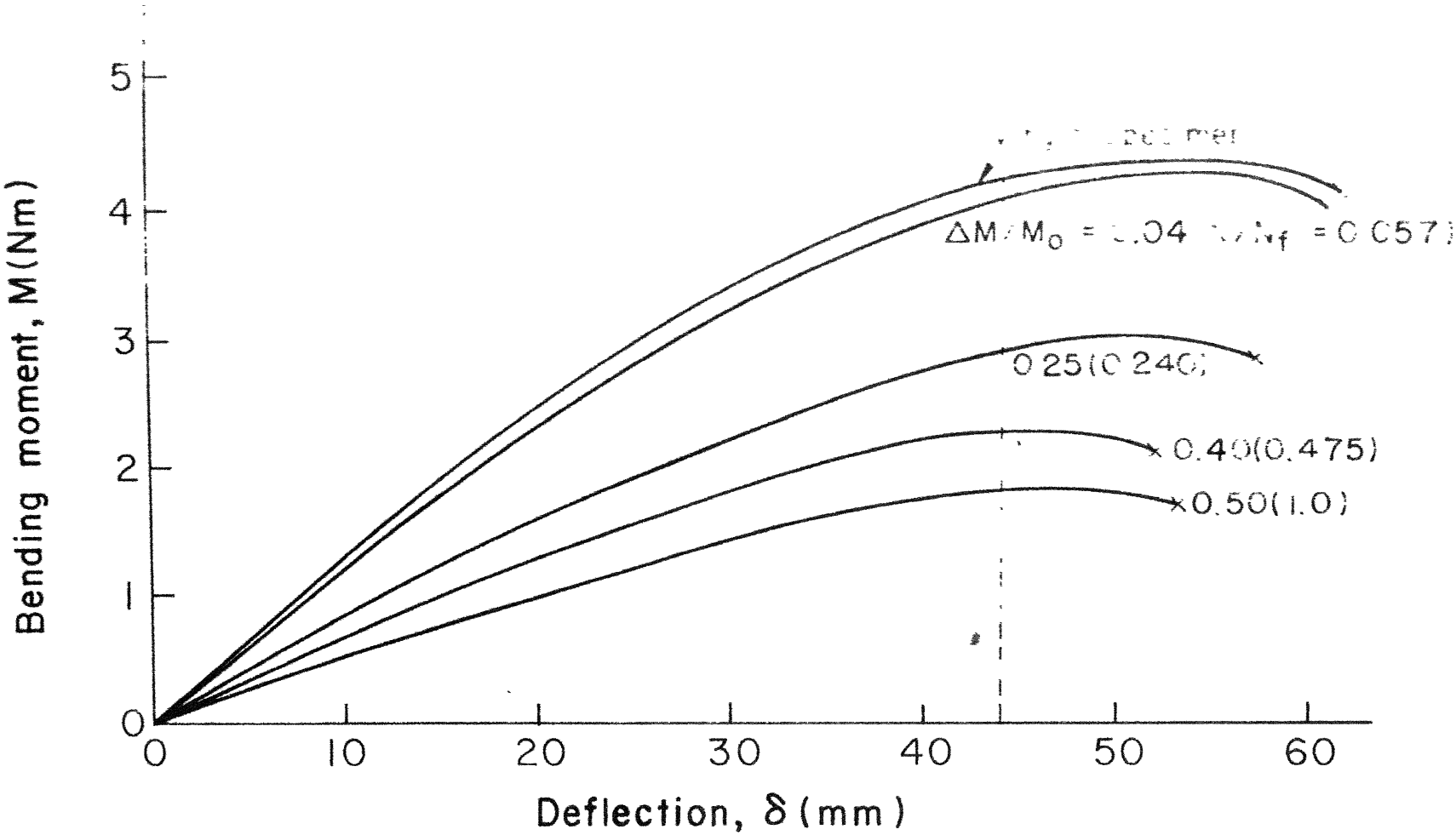

Fig. 3.43 Bending moment vs deflection curves for specimens precycled to different stages of damage (10° specimens, ϵ = 0.90%)

Table 3.8: Ratio of Residual Stiffness to Stiffness of a Virgin Specimen at Different Fraction of Average Fatigue Life for Different Strain Amplitudes (10 Specimens).

ε = 0.53%		ε = 0.61%		ε = 0.71%		ε = 0.90%	
N/N_f*	E_R/E_o	N/N_f*	E_R/E_o	N/N_f*	E_R/E_o	N/N_f*	E_R/E_o
0.02	0.892	0.031	0.908	0.008	0.967	0.057	0.946
0.03	0.850	0.075	0.742	0.075	0.808	0.240	0.692
0.23	0.567	0.210	0.642	0.138	0.721	0.475	0.534
0.64	0.467	0.470	0.530	0.344	0.550	1.0	0.445

* N_f Average value of fatigue life at stiffness to be 50% of its initial value.

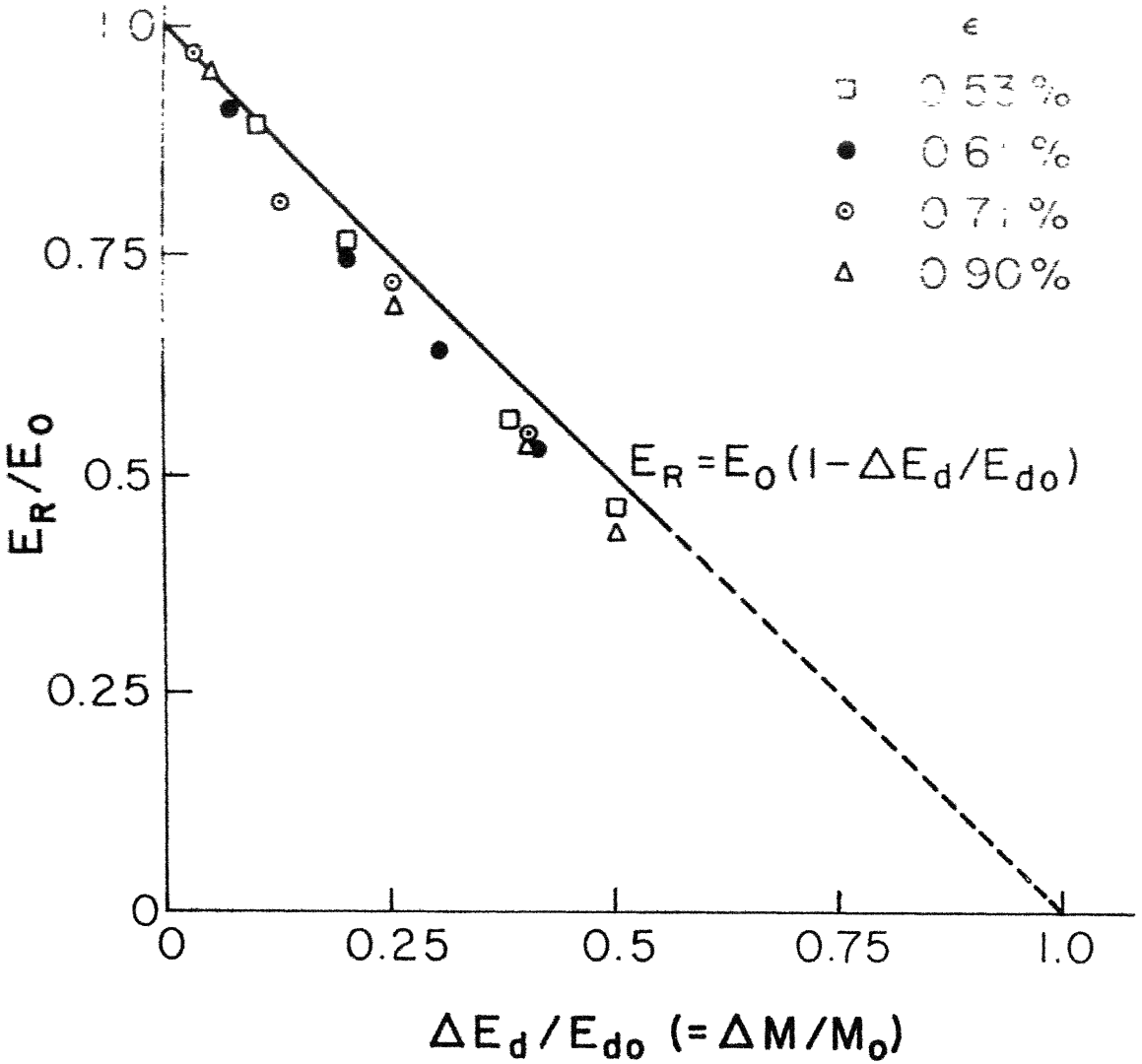

Fig. 3.44 Normalised residual stiffness vs loss in dynamic stiffness (10° specimens)

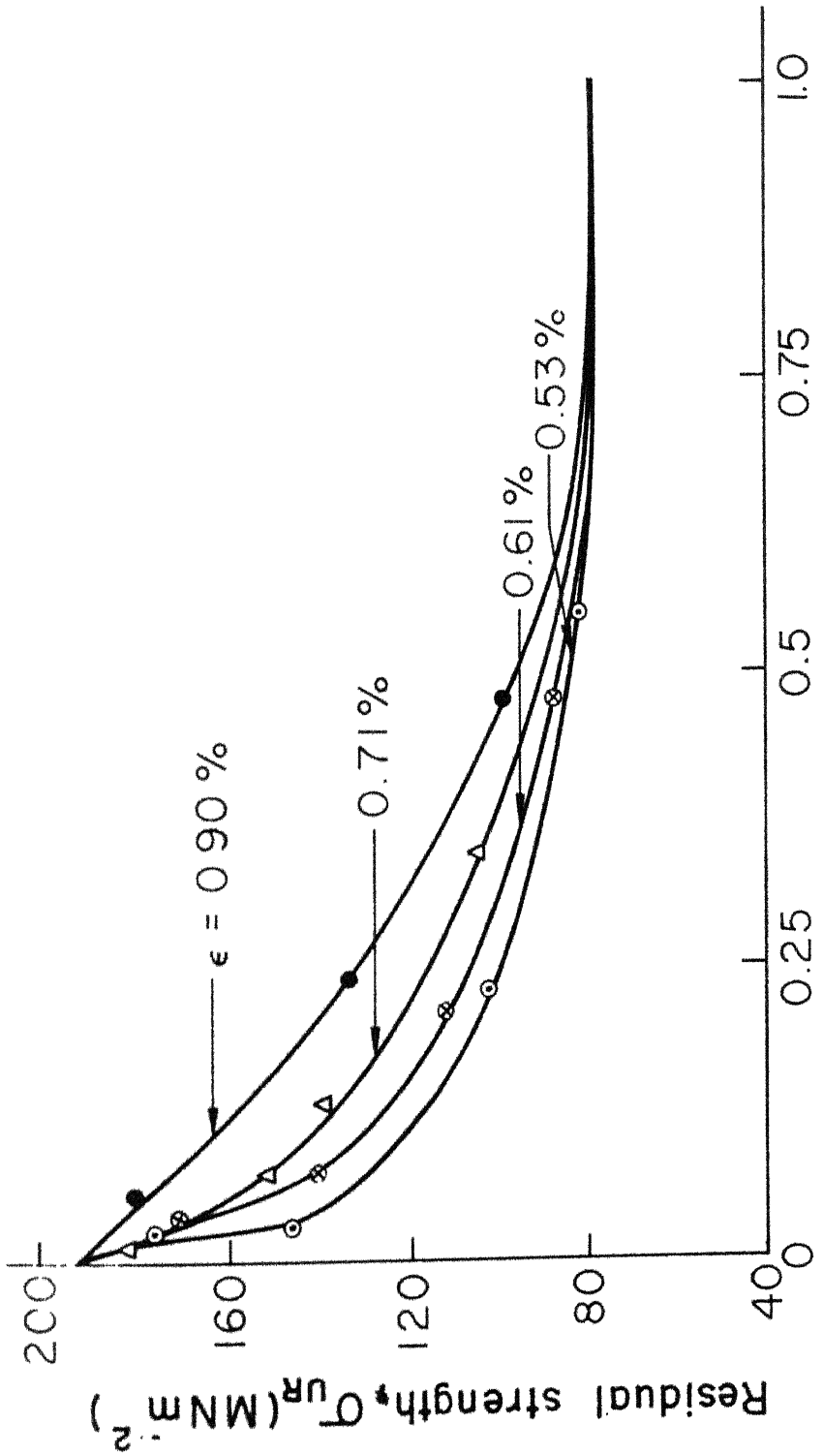

Fig. 3.45 Variation of residual strength with fraction of fatigue life (10^6 specimens)

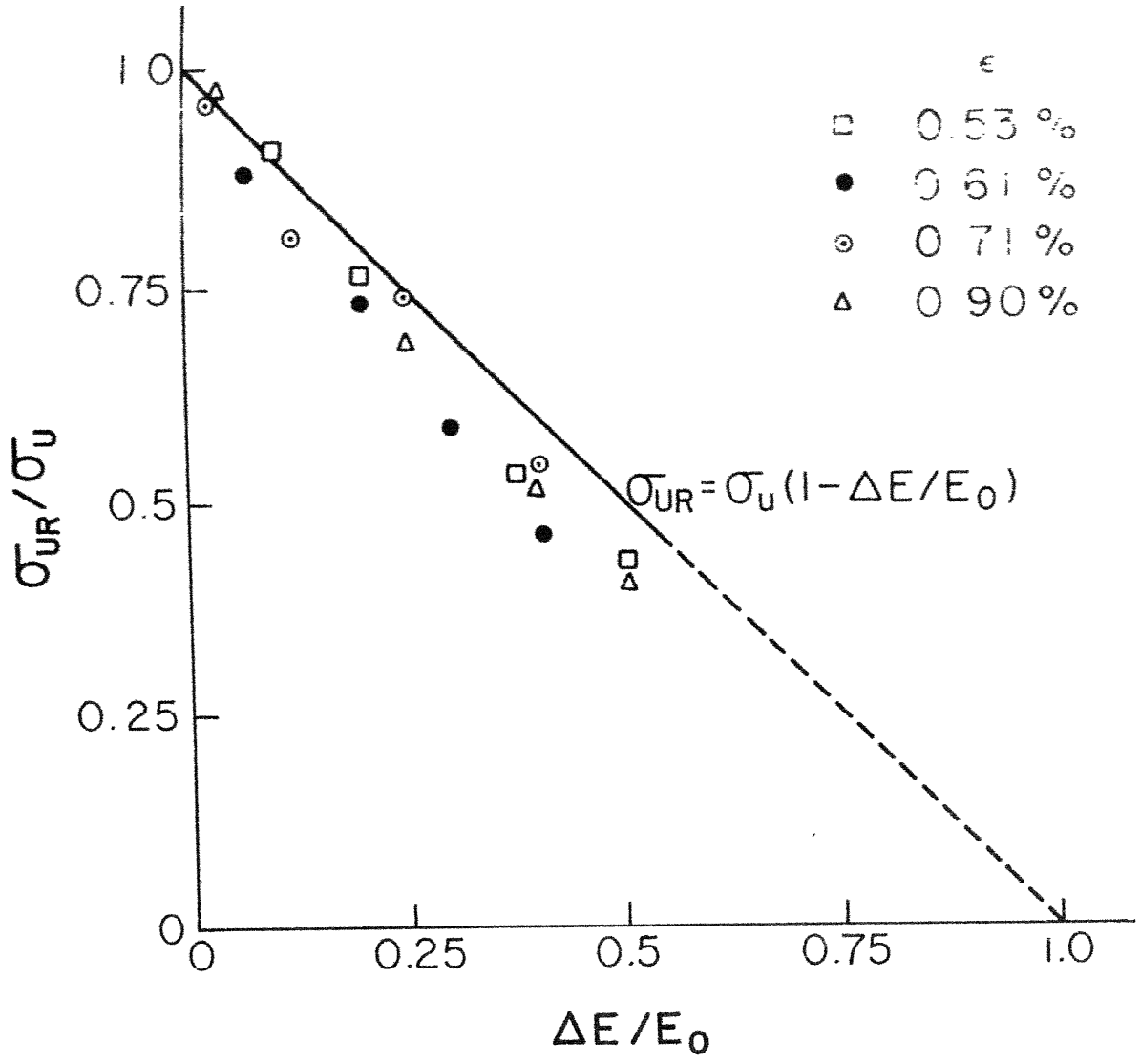

Fig.3.46 Variation in normalised residual strength with loss in stiffness (10° specimens)

predicted by Eq. (3.2) as in previous cases. The dotted portion of the straight line again represents the range of stiffness in which data could not be obtained due to stabilization of the residual stiffness.

3.5 REMARKS

Fatigue behaviour of unidirectional composite has been discussed for the different fibre orientations in this chapter. Fatigue behaviour has been observed to depend upon the fibre orientation. In each case consistency of observations has been explained. Further, analysis of results will be presented in the next chapter. Based on the analysis, two theories to predict fatigue strength have also been proposed.

CHAPTER IV

ANALYSIS OF RESULTS AND THEORIES OF FATIGUE FAILURE

4.1 ANALYSIS OF RESULTS

Fatigue behaviour of the unidirectional composite for different fibre orientations has been discussed in the preceeding chapter. For each fibre orientation, qualitative behaviour has been found consistent with the observed failure mechanism. For a better and quantitative understanding of material behaviour an overall picture is necessary. A critical examination of the results for different fibre orientations and their comparative study reveals the following:

1. The failure initiation and propagation strongly depend upon the fibre orientation. In longitudinal specimens failure occurs by fracture of fibres whereas in transverse specimens failure is predominantly interface failure. At intermediate angles failure occurs due to combined effect of shear failure and interface failure. Fibre fracture is not observed even for small fibre orientation of 10 degree. At small angles (e.g., 10^{o}) shear failure plays more predominant role than the interface failure whereas at increasing angles

(e.g., 45^{o}), interface failure also becomes an important factor.

2. Interface failure is sudden whereas the fracture of fibres and shear failure are relatively gradual. Therefore, specimens in which interface plays an important role in transmitting the load, such as the transverse specimens, lose stiffness and strength very rapidly upon failure initiation. This is why no sudden drop occurs in longitudinal and 10 degree specimens, whereas sudden drops are observed in 45 degree and transverse specimens. Moreover, due to predominance of interface in the transverse specimens, sudden drop in stiffness and strength occurs earlier in fatigue life and is more severe compared to that observed in the 45 degree specimens.

3. Strain amplitude versus average fatigue life curves for different fibre orientations are shown in Fig. 4.1. Failure criteria adopted for drawing this figure are consistent with the suggested fatigue design curves for different fibre orientations as discussed in the previous chapter. This means that the failure criterion for the longitudinal specimen is complete separation, stabilisation of stiffness for 10 degree specimens and sudden drop in stiffness for transverse and 45 degree specimens. The experimental points shown in the

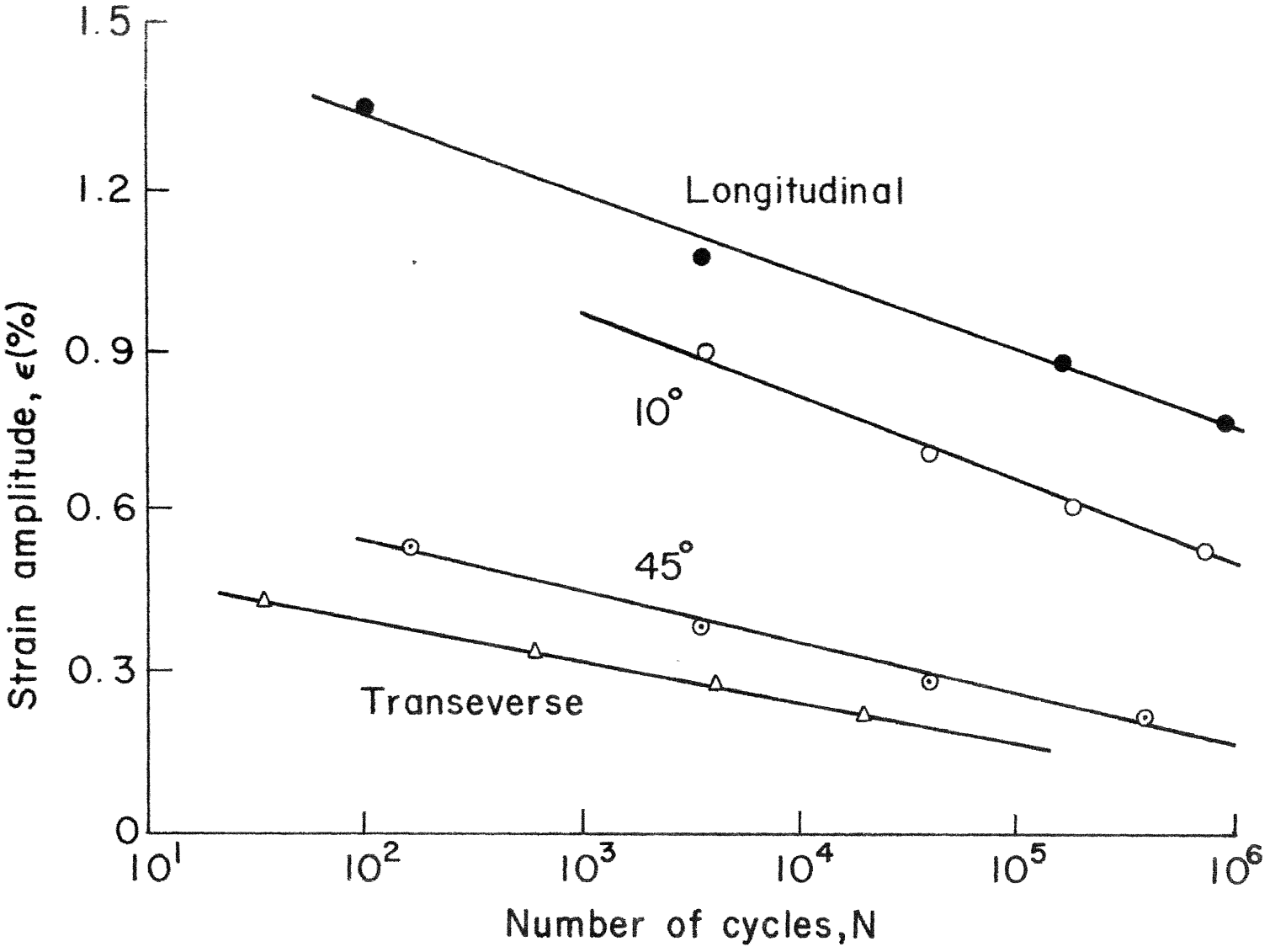

Fig. 4.1 Strain amplitude vs average fatigue life for different fibre orientations

figure represent average fatigue life at the indicated strain amplitude. In each case a straight line shows a good fit to the data. Further quantitative discussion on these straight lines will be presented in a later section.

4. Through cross plotting of the results of Fig. 4.1, fatigue strengths (strain amplitudes) at different cyclic lives are shown as functions of fibre orientation in Fig. 4.2. Also shown in the figure is a plot of static fracture strain as a function of fibre orientation. It is observed that the variations in the fatigue strength at different cyclic lives are similar to the variation in static strength (strength decreasing with increasing fibre orientation). This indicates that a theory which predicts off-axis static strength of unidirectional composites, may, with minor modifications, be adopted to predict fatigue strength at a fixed cyclic life as has been proposed by Sims and Brogdon [25]. However, in the present case, the strengthsare given as a fracture strains. The only existing static strength theory in terms of strain, the maximum strain theory, has not been found to represent the result adequately because this theory assumes that the failure modes do not interact.

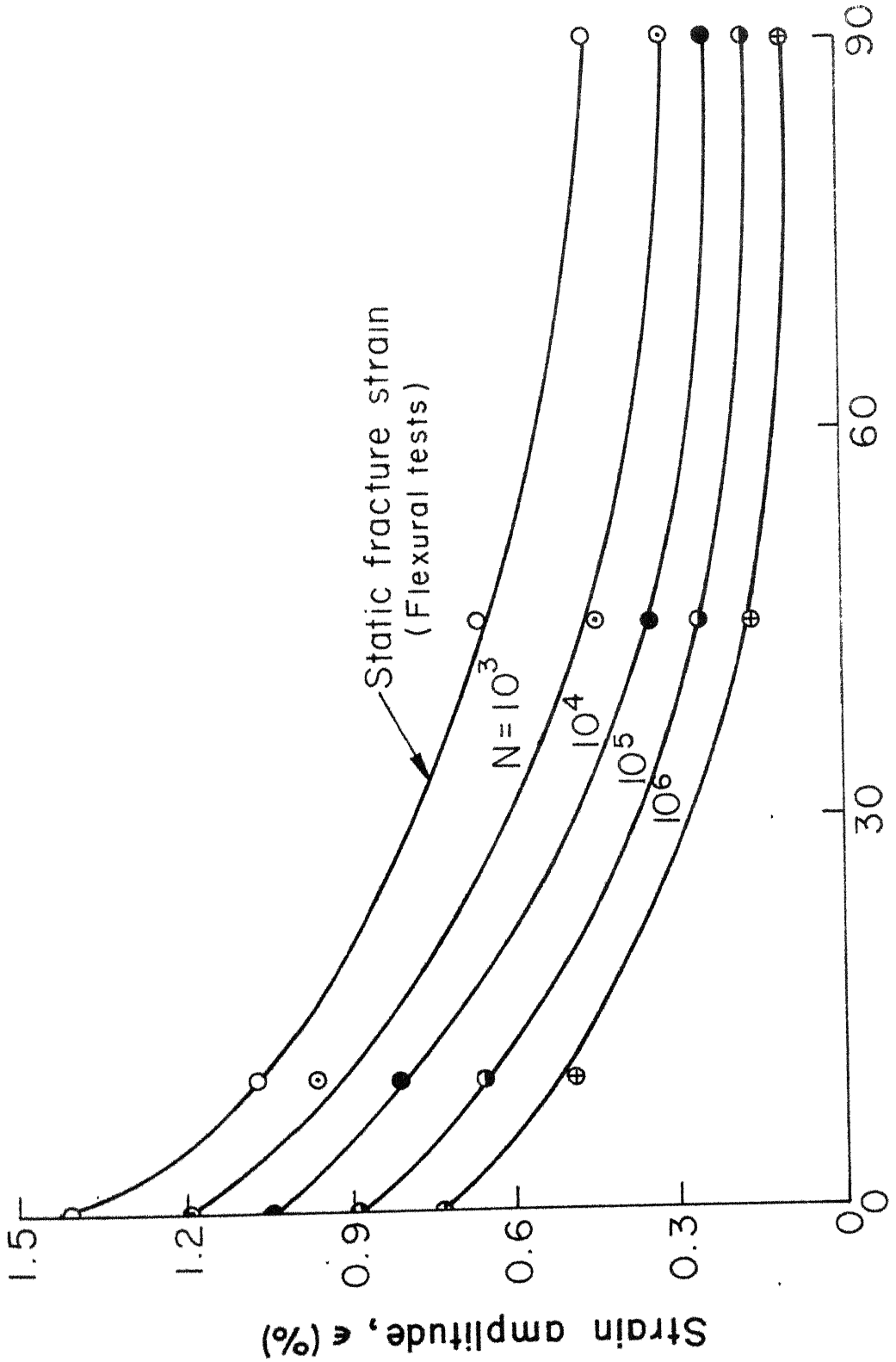

Fig. 4.2 Variations of static and fatigue strengths with fibre orientation

5. Residual static stiffness as obtained from the static tests on precycled specimens has been plotted against loss of dynamic stiffness in Fig. 4.3. The data points correspond to all strain amplitudes at each fibre orientation. Static stiffness has been normalised with respect to the static stiffness of a virgin specimen with corresponding fibre orientation whereas the dynamic stiffness is normalised by the first cycle stiffness. It is observed that all the points are very close to the straight line represented by

$$\frac{E_R}{E_o} = 1 - \frac{\Delta E_d}{E_{do}} \qquad (4.1)$$

It can, therefore, be concluded that normalised static stiffness equals the normalised dynamic stiffness. In view of this conclusion, one can obtain static stiffness from the measurements made during a fatigue test without interruption in fatigue tests.

6. Normalised residual strength is plotted as a function of normalised residual stiffness in Fig. 4.4. The points correspond to all the strain amplitudes at different fibre orientations. Residual strength and stiffness have been normalised with respect to the corresponding values for virgin specimens. The data points are observed to fall below the straight line given by

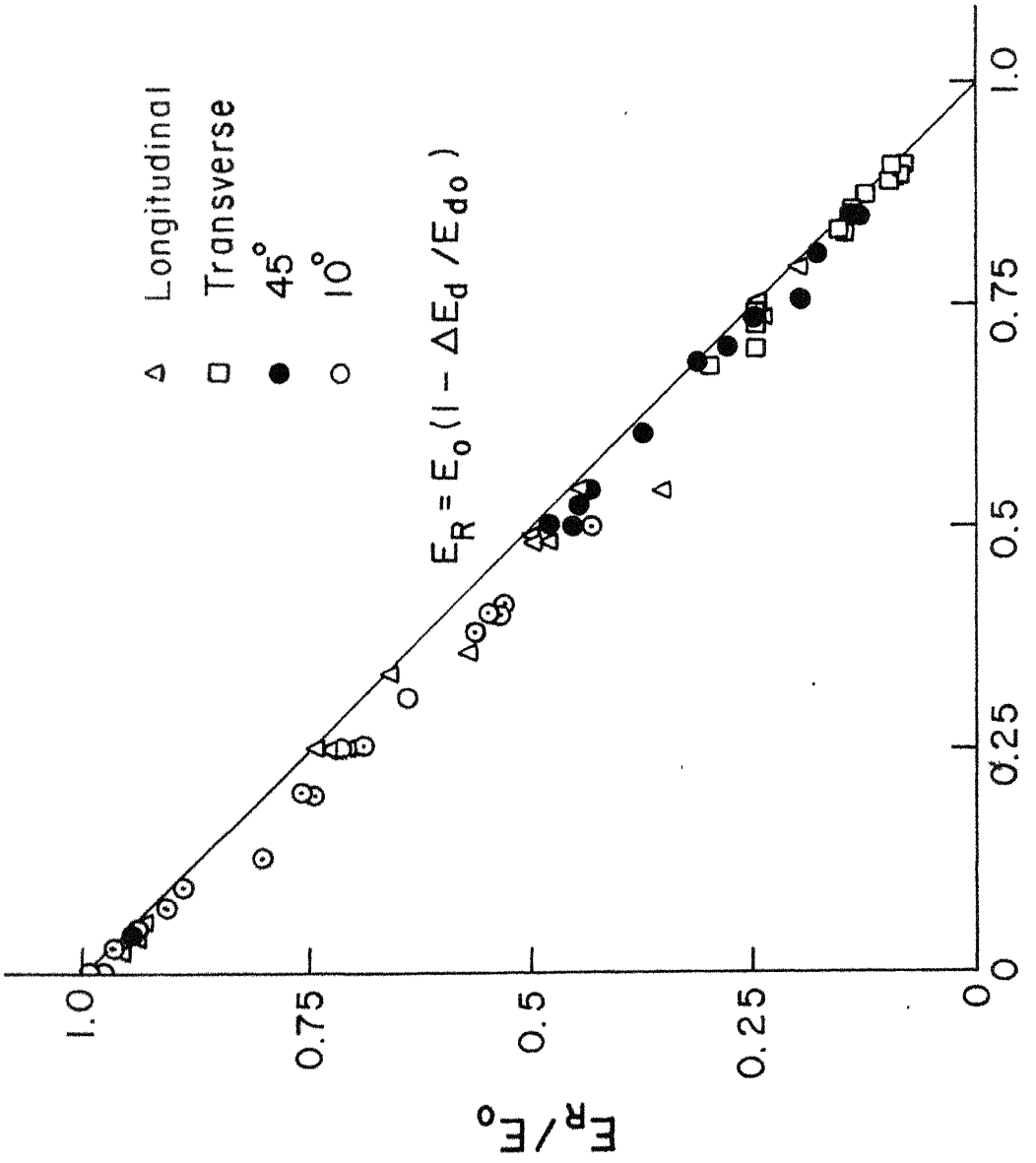

Fig.4.3 Normalised residual stiffness vs normalised loss in dynamic stiffness

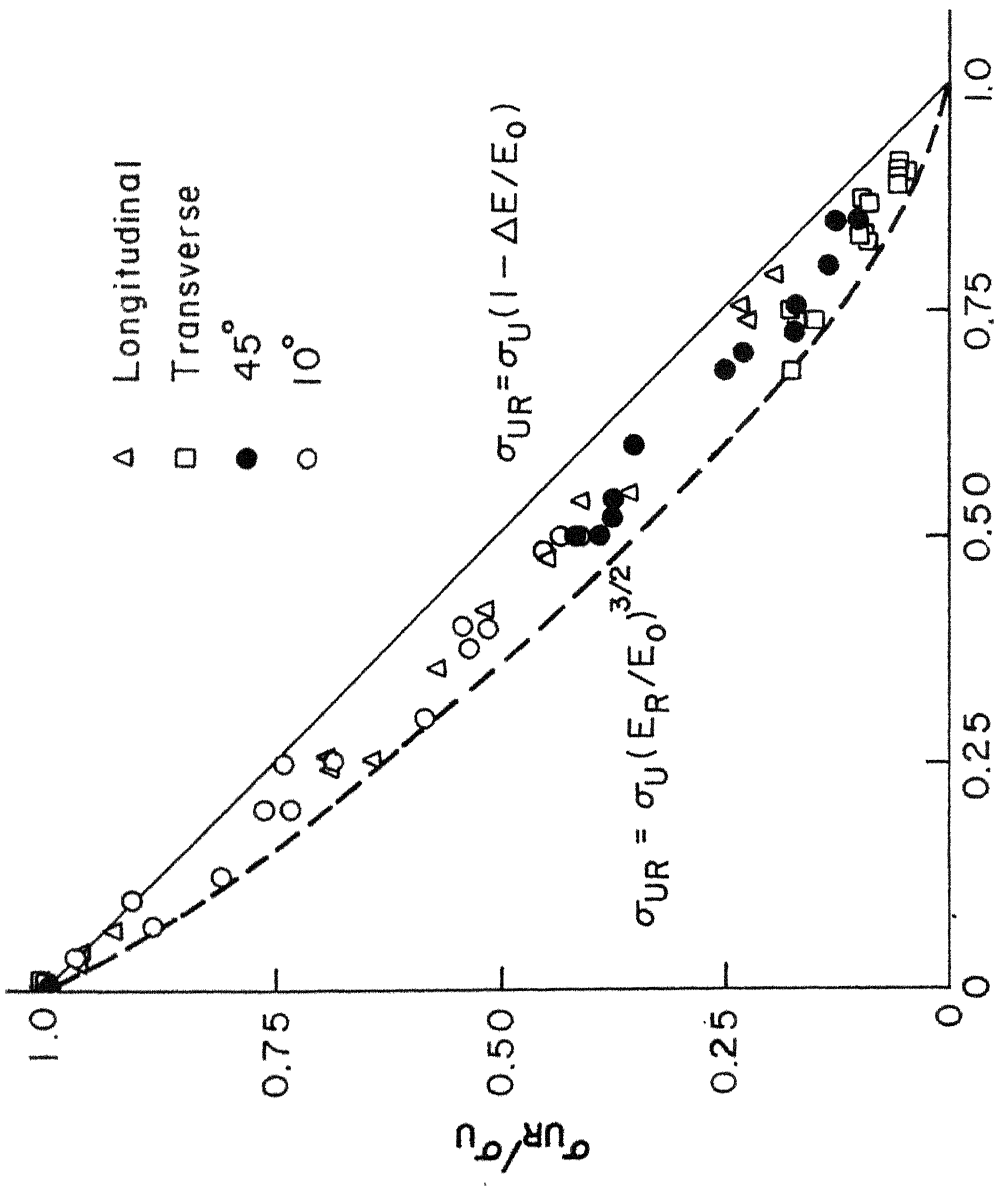

Fig. 4.4 Variation of normalised residual strength with normalised loss in stiffness

$$\frac{\sigma_{UR}}{\sigma_U} = 1 - \frac{\Delta E}{E_o} \qquad (4.2)$$

However the points can be bounded between this straight line and a curve given by the following power law:

$$\frac{\sigma_{UR}}{\sigma_U} = \left(1 - \frac{\Delta E}{E_o} \right)^{3/2} \qquad (4.3)$$

where $\Delta E/E_o$ is the normalised loss in static stiffness. Residual strength can be equivalently written as a function of normalised residual stiffness as

$$\frac{\sigma_{UR}}{\sigma_U} = \left(\frac{E_R}{E_o} \right)^{3/2} \qquad (4.4)$$

These results indicate that the residual strength decreases faster than the residual stiffness. The power law given by Eq. (4.3) or (4.4) will be a good estimate (mostly conservative) for residual strength. In view of this observation and the preceeding observation (observation no. 5), one can easily estimate the residual strength and stiffness from dynamic stiffness measurement alone.

4.2 THEORIES OF FATIGUE FAILURE

An almost infinite variety of laminates can be used for structural applications. Once it has been decided to use a specific laminate, one may obtain its fatigue characteristics through experiments. However, the experimental

methods, if used to obtain guidelines for choice of laminates, become time consuming and cost prohibitive. It is desirable to evolve procedures through which off-axis fatigue strength can be estimated either through the fatigue strengths in the principal material directions or through the knowledge of off-axis static strength.

Hashin and Rotem [24] have suggested the following correlation between the fatigue strength and the static strength of unidirectional composites:

$$\sigma_f = \sigma_U f(A, N, n, \theta) \qquad (4.5)$$

where σ_f and σ_U are fatigue and static strengths respectively and f (A, N, n, θ) is a function of stress ratio A, fatigue life N, frequency of load cycling n and fibre orientation θ. They have suggested that the off-axis fatigue strength at a given cyclic life can be predicted from the fatigue strength in the transverse direction and shear fatigue strength at the same cyclic life and employing the failure theory used to predict off-axis static strength. Thus dependence of 'f' on 'θ' can be obtained through the fatigue tests on specimens with two different fibre orientations (other than zero). Dependence of 'f' on cyclic life could not be expressed through a mathematical relation and has to be evaluated through additional tests. Thus the scope of this theory is limited.

More recently Sims and Brogdon [25] have extended the Tsai - Hill failure theory for static strength to fatigue strength. Their work has shown that the Tsai - Hill failure theory may be extended to predict off-axis fatigue strengths. However, like Hashin and Rotem, Sims and Brogdon have also not attempted to establish a close form dependence of fatigue strength on cyclic life.

Agarwal and Dally [6] noted that the S - N curve of an E glass epoxy cross ply material (Scotchply - 1000) can be represented by the following simple equation:

$$\frac{\Delta\sigma}{\sigma_U} = b + m \log N \qquad (4.6)$$

where $\Delta\sigma$ is the stress range, σ_U is the ultimate tensile strength, m and b are material constants. The experimental data of Hahn and Kim [9] also show a good correlation with this relationship. However, the values of constants m and b could not be related to the static properties of the materials.

Another useful relationship to represent fatigue data is a power law:

$$N^k \Delta\varepsilon = c \qquad (4.7)$$

where $\Delta\varepsilon$ is the strain range and k and c are material constants. This equation has been found to be very useful in predicting fatigue life of metallic materials [35, 36] . For most metals k is known to vary from 0.5

curve intersects the fatigue life of one cycle at a strain amplitude higher than the fracture strain. This obviously means that Eq. (4.8) is not valid for very low cyclic life (less than 10^2). This observation is consistent with the results of Dharan [37, 38] and of Hahn and Kim [9]. Dharan working with unidirectional glass epoxy composites observed that in short fatigue life, applied stress level is only slightly dependent upon cyclic life making S-N curve nearly flat in this region. Results of Hahn and Kim on glass epoxy laminates show the best fit to Eq. (4.6) written in terms of normalised maximum stress with constant 'b' being 1.1156. Predictions of Eq. (4.8) with constants given by Eq. (4.9) are shown in Fig. 4.5 along with experimental results. The figure shows a good correlation between experimental results and predicted values. It is interesting to note that the value of constant m for a different glass epoxy laminate used by Agarwal and Dally as predicted by Eq. (4.9) is - 0.0828 against the reported best fit value of - 0.0806. For the experimental results of Hahn and Kim, predicted and best fit values of 'm' are -0.0783 and - 0.1201. Discrepancy in the two values may be attributed to the fact that their results are with constant stress cycling.

The power law given by Eq. (4.7) can be written in terms of normalised strain:

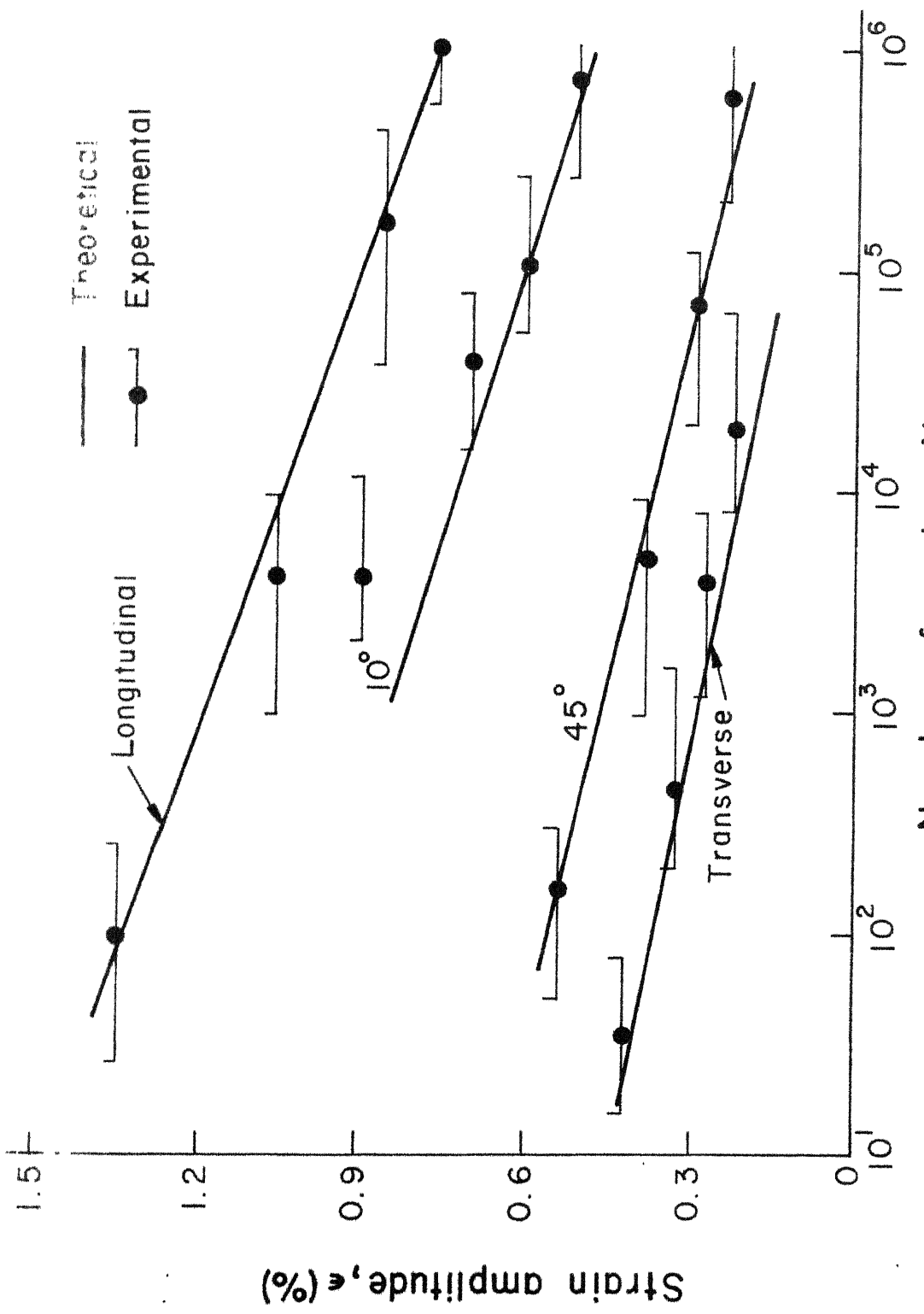

Fig. 4.5 Comparison of experimental results with proposed law ($\epsilon = 1.15\,\epsilon_f - 0.12\sqrt{\epsilon_f}\log N$)

$$N^k \frac{\varepsilon}{\varepsilon_f} = c \qquad (4.10)$$

Through a method of curve fitting it has been established that c is a constant and k is related to the static fracture strain:

$$c = 1.35$$

$$k = \frac{0.08}{\sqrt{\varepsilon_f}} \qquad (4.11)$$

where ε_f is again given in percent strain. The arguments, which were advanced in support of the constant b being different from 1, are once again valid for the constant c being different from 1.

Predictions of Eq. (4.10) with the constant given by Eq. (4.11) are shown in Fig. 4.6 along with the present experimental results. The predictions compare very favourably with the experimental results. Equation (4.11) predicts a value of 0.055 for k for the material used by Agarwal and Dally against the reported best fit value of 0.0475. Their reported value of 0.97 for c is different from the constant 1.35 proposed here. For material of Hahn and Kim, the reported best fit value of c is 1.3597 which is in very good agreement with the proposed constant (1.35). The reported best fit value of k is 0.0858 against the predicted value of 0.055. The discrepancy may be attributed to the fact that their tests were performed under stress controlled conditions.

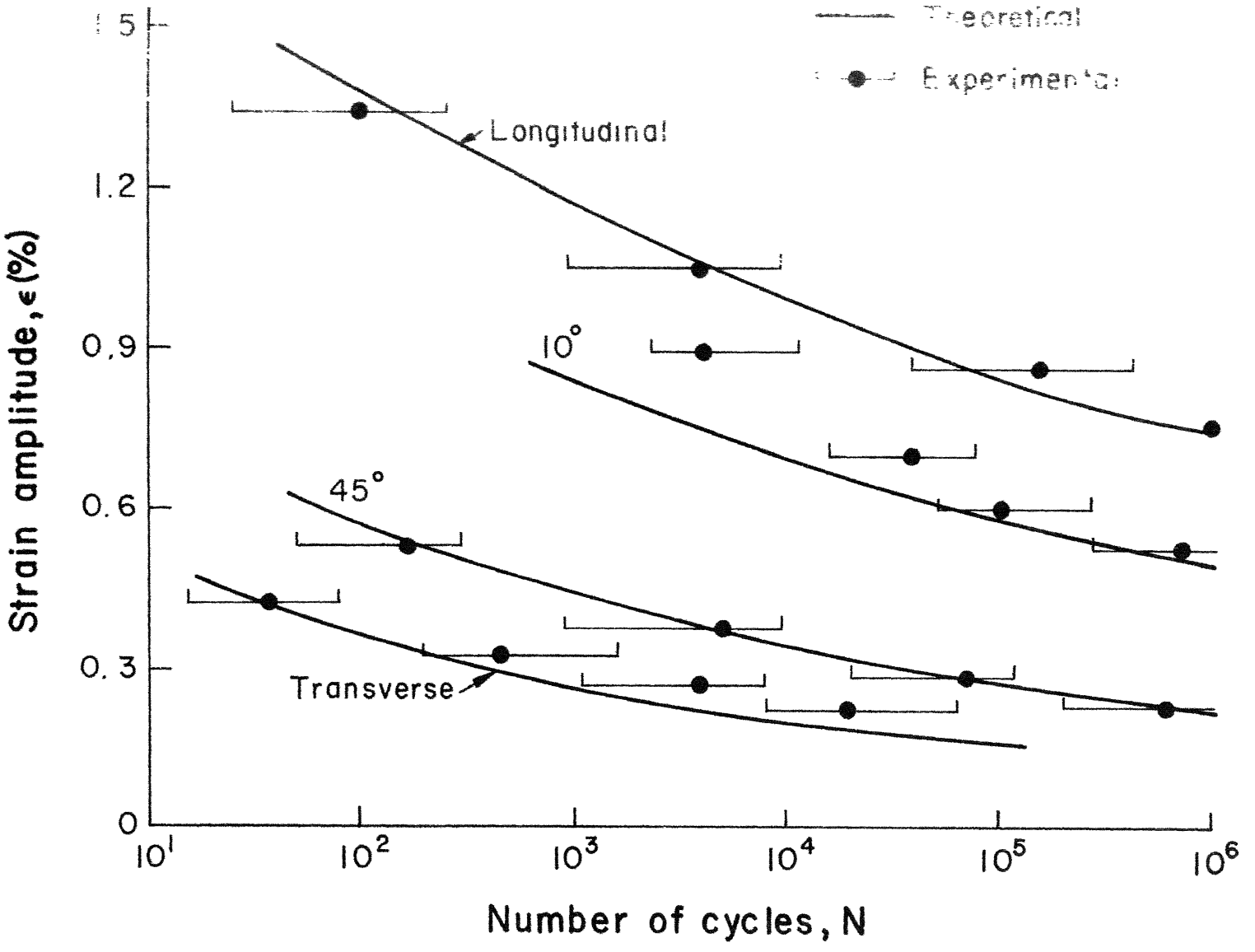

Fig. 4.6 Comparison of experimental results with proposed law ($N^{0.08/\sqrt{\epsilon_f}}\,\epsilon/\epsilon_f = 1.35$)

In view of the above discussions Eqs. (4.8) and (4.10) may be used to predict fatigue strength of composite materials. The constants in these equations can be evaluated from the knowledge of static fracture strain. Predictions of these laws are in good agreement with the present experimental results and also with limited results available in literature. However, applications of these laws to the design procedures should await further experimental results on different types of composite materials so that universality of the constants is established with greater confidence.

CHAPTER V

CONCLUSIONS AND SCOPE FOR FUTURE WORK

5.1 CONCLUSIONS

Fatigue behaviour of unidirectionally reinforced glass fibre epoxy composite in deflection controlled flexural fatigue tests has been studied. The tests on the composite material fabricated in the laboratory by hand winding technique were performed on two fatigue testing machines specially designed, fabricated and instrumented for the purpose. Progressive fatigue damage was investigated through measurements of bending moments during fatigue tests as well as through static tests on precycled specimens. Based on the results discussed earlier the following important observations and conclusions can be made.

1. Conventional strain amplitude versus cyclic life curves have been obtained for four different fibre orientations. The curves, for longitudinal and transverse fatigue strength and that for fatigue strength at 45 degree, have been drawn for fracture as the failure criterion. Whereas the curve for off-axis strength at 10 degree has been drawn with stabilization of stiffness as the failure criterion. For a given cyclic life, strain amplitude decreases as the fibre orientation increases.

2. S-N curves representing different stages of fatigue damage have been obtained from the records of bending moment during fatigue cycling.. Based on the observed variation in stiffness, it has been suggested that different failure criteria should be used for different fibre orientations. For longitudinal specimens, complete seperation may be taken as the failure criterion, for transverse and 45 degree specimens sudden drop in stiffness is a more appropriate failure criterion and for 10 degree specimens stabilization in stiffness is the suggested failure criterion.

3. Behaviour of 10 degree specimens is very peculiar in that the specimens do not fracture under strain controlled fatigue tests. However, complete fracture should be expected to take place in these specimens when subjected to stress controlled fatigue tests.

4. In longitudinal specimens failure occurs by fracture of fibres whereas in transverse specimens failure is predominantly interface failure. At intermediate angles failure occurs due to combined effect of shear failure and interface failure. Fibre fracture is not observed even for small fibre orientation of 10 degree. At small angles (e.g., 10°), shear failure plays a more predominant role than the interface failure whereas at increasing angles (e.g., 45°), interface failure also becomes an important factor.

5. It is observed that in longitudinal and 10 degree specimens, loss in stiffness and strength are gradual whereas those for 45 degree and transverse specimens are sudden. This is because in 45 degree and transverse specimens, interface which plays an important role in transmitting the load, fails suddenly. Moreover, due to predominance of interface in transverse specimens, sudden drop in stiffness and strength occurs very early in fatigue life (0.2 to 5% of expected life) and is more severe (stiffness reduces to nearly 30% and strength reduces to 16% of the virgin specimen) compared to the ones observed in 45 degree specimens where sudden drop in stiffness at 60 to 90% of expected fatigue life reduces stiffness to about 50% and strength to 35% of the corresponding values for a virgin specimen.

6. Variations in the fatigue strengths at different cyclic lives are similar to the variation in static strengths with fibre orientation. Therefore, a theory which predicts off-axis static strength of unidirectional composites, may, with minor modifications, be adopted to predict fatigue strength at a fixed cyclic life.

7. Residual static stiffness normalised with the stiffness of a virgin specimen is equal to the dynamic stiffness normalised with the first cycle stiffness.

8. Residual strength at any stage during fatigue cycling can be bounded as follows:

$$\left(\frac{E_R}{E_o}\right)^{3/2} \leq \frac{\sigma_{UR}}{\sigma_U} \leq \frac{E_R}{E_o} \tag{5.1}$$

9. Fatigue strength (in terms of strain amplitude) can be related to the cyclic life through the following linear relation:

$$\frac{\varepsilon}{\varepsilon_f} = b + m \log N \tag{5.2}$$

where ε and ε_f are fatigue and static fracture strains of the composite respectively and m and b are given by the following relations:

$$b = 1.15$$

$$m = -\frac{0.12}{\sqrt{\varepsilon_f}} \tag{5.3}$$

in which ε_f is given in percent strain.

Fatigue strength can also be related to cyclic life through the following power law:

$$N^k \frac{\varepsilon}{\varepsilon_f} = c \tag{5.4}$$

where

$$c = 1.35$$

$$k = \frac{0.08}{\sqrt{\varepsilon_f}} \tag{5.5}$$

where again ε_f is given in percent strain.

5.2 SUGGESTED FUTURE RESEARCH WORK

In view of the fatigue results discussed in this thesis, it is suggested to carry further research work on the following lines:

1. Study of fatigue behaviour of unidirectional composites at different fibre orientations other than already studied.

2. Verification of fatigue laws (Eqs 4.8 to 4.11) for the same glass epoxy system at different fibre orientations and also for other material systems.

3. Study of fatigue behaviour of laminates and verification of fatigue laws for them.

4. Development of a suitable static strength theory in terms of strains. This would enable to predict off-axis fatigue strength from static tests along the principal material axes only.

5. Study of influence of different parameters on fatigue behaviour such as mean stress, environment conditions, volume fraction etc.

REFERENCES

1. Boller, K.H., "Fatigue Properties of Fibrous Glass Reinforced Plastics Laminates Subjected to Various Conditions," Modern Plastics, Vol. 34, p. 163 (June 1957).

2. Boller, K.H., "Fatigue Characteristics of RP Laminates Subjected to Axial Loading," Modern Plastics, Vol. 41, p. 145 (June 1964).

3. Davis, J.W., McCarthy, J.A. and Schurb, J.N., "The Fatigue Resistance of Reinforced Plastics," Materials in Design Engineering, Vol. 60, p. 87 (December 1964).

4. Broutman, L.J. and Sahu, S., "Progressive Damage of a Glass Reinforced Plastics During Fatigue," SPI, 24th Annual Technical Conference, Section 11-D (February 1969).

5. Dally, J.W. and Agarwal, B.D., "Low Cycle Fatigue Behaviour of Glass Fibre Reinforced Plastics," Proceedings of the Army Symposium on Solid Mechanics, AMMRC MS 70-5 (December 1970).

6. Agarwal, B.D. and Dally, J.W., "Prediction of Low-Cycle Fatigue Behaviour of GFRP: an Experimental Approach," Journal of Materials Science, Vol. 10, p. 193 (January 1975).

7. Tanimoto, T. and Amijima, S., "Fatigue Properties of Laminated Glass Fibre Composite Materials," SPI, 29th Annual Technical Conference, Section 17-B (February 1974).

8. Tanimoto, T. and Amijima, S., "Progressive Nature of Fatigue Damage of Glass Fiber Reinforced Plastics," Journal of Glass Fiber Reinforced Plastics," Journal of Composite Materials, Vol. 9, p. 380 (October 1975).

9. Hahn, H.T. and Kim, R.Y., "Fatigue Behaviour of Composite Laminate," Journal of Composite Materials, Vol. 10, p. 156 (April 1976).

10. Phillips, D.C. and Scott, J.M., "The Shear Fatigue of Unidirectional Fibre Composites," Composites, Vol. 8, p. 233 (October 1977).

11. Phillips, D.C. and Scott, J.M., "Shear Fatigue of CFRP Under Low Frequency Torsion," Fibre Science and Technology, Vol. 11, p.23 (January 1978).

12. Agarwal, B.D. and Joneja, S.K., "Flexural Fatigue Properties of Unidirectional Composites in Transverse Direction," Composites, Vol. 10, p. 28 (January 1979).

13. Agarwal, B.D. and Joneja, S.K., "Progressive Damage in GFRP Under Constant Deflection Flexural Fatigue," To Appear in Fibre Science and Technology.

14. McGarry, F.J., "Crack Propagation in Fiber Reinforced Plastic Composites," in Fundamental Aspects of Fiber Reinforced Plastic Composites, Ed. by Schwartz, H.T. and Schwartz, H.S., Interscience Publisher (1968).

15. Owen, M.J. and Smith, T.R., "Some Fatigue Properties of Chopped-Strand Mat/Polyester-Resin Laminates," Plastics and Polymers, Vol. 36, p. 33 (February 1968).

16. Owen, M.J., Dukes, R. and Smith, T.R., "Fatigue and Failure Mechanisms in GRP with Special Reference to Random Reinforcements," SPI, 23rd Annual Technical Conference, Section 14-A (February 1968).

17. Smith, T.R. and Owen, M.J., "Progressive Nature of Fatigue Damage in RP," Modern Plastics, Vol. 46, p. 128 (May 1969).

18. Nevadunsky, J.J., Lucas, J.J. and Salkind, M.J., "Early Fatigue Damage Detection in Composite Materials," Journal of Composite Materials, Vol. 9, p. 394 (October 1975).

19. Hofer, K.E. (Jr.), Benett, L.C. and Stander, M., "Effect of Various Fiber Surface Treatments on the Fatigue Behavior of Glass Fabric Composites in High Humidity Environments," SPI, 31st Annual Technical Conference, Section 6-A (February 1976).

20. Amijima, S. and Tanimoto, T., "The Effect of Glass Content and Environmental Temperature on the Fatigue Propertics of Laminated Glass Fiber Composite Materials," Proceedings of the 1971 International Conference on Mechanical Behavior of Materials, Volume V, The Society of Materials Science, Japan, p. 269 (1972).

21. Dally, J.W. and Broutman, L.J., "Frequency Effects on the Fatigue of Glass Reinforced Plastics," Journal of Composite Materials, Vol. 1, p.424 (October 1967).

22. Phillips, D.C., Scott, J.M. and Buckley, N., "The Effects of Moisture on the Shear Fatigue of Fibre Composites," United Kingdom Atomic Energy Authority, Harwell AERE - R - 9009 (January 1978).

23. Broutman, L.J. and Sahu, S., "A New Theory to Predict Commutative Fatigue Damage in Fibreglass Reinforced Plastics," Composite Materials : Testing and Design (Second Conference), ASTM STP 497, American Society for Testing and Materials, p. 170 (1972).

24. Hashin, Z. and Rotem, A., "A Fatigue Failure Criterion for Fiber Reinforced Materials," Journal of Composite Materials, Vol. 7, p. 448 (October 1973).

25. Sims, D.F. and Brogdon, V.H., "Fatigue Behavior of Composites Under Different Loading Modes," Fatigue of Filamentary Composite Materials, ASTM STP 636, Reifsnider, K.L. and Lauraitis, K.N., Eds., American Society for Testing and Materials, p. 185 (1977).

26. Tsai, S.W., "Strength Theories of Filamentary Structures," Chapter 1 in Fundamental Aspects of Fiber Reinforced Plastic Composites, Ed. by Schwartz, R.T. and Schwartz, H.S., Interscience Publishers (1968).

27. Salkind, M.J., "Fatigue of Composites," Composite Materials: Testing and Design (Second Conference), ASTM STP 497, American Society for Testing and Materials, p. 143 (1972).

28. Owen, M.J., "Progress Towards a Safe-Life Design Method for Glass Reinforced Plastic Under Fatigue Loading," Paper 17, British Plastics Federation, International Reinforced Plastics Conference, Brighton, p. 167 (1976).

29. Harris, B., "Fatigue and Accumulation of Damage in Reinforced Plastics," Composites, Vol. 8, p. 214 (October 1977).

30. B.D. Agarwal, Lecture Notes on Composite Materials, Department of Mechanical Engineering, Indian Institute of Technology Kanpur, India (To Appear as a Book with Broutman, L.J.)

31. Halpin, J.C., Pagano, N.J., Whitney, J.M. and Wu, E.M., "Characterization of Anisotropic Composite Materials," Composite Materials : Testing and Design, ASTM STP 460, American Society for Testing and Materials, p. 37 (1969).

32. Whitney, J.M. and Dauksys, R.J., "Flexure Experiments on Off-Axis Composites," Journal of Composite Materials, Vol. 4, p. 135 (January 1970).

33. Chamis, C.C. and Sinclair, J.H., "10° Off-Axis Tensile Test for Intralaminar Shear Characterization of Fiber Composites," NASA Technical Note D - 8215 (April 1976).

34. Chiao, C.C., Moore, R.L. and Chiao, T.T., "Measurement of Shear Properties of Fibre Composites Part 1. Evaluation of Test Methods," Composites, Vol. 8, p. 161 (July 1977).

35. Manson, S.S., "Fatigue: A Complex Subject-Some Simple Approximations," Experimental Mechanics, Vol. 5, p. 193 (June 1965).

36. Coffin, L.F., Jr., "A Study of The Effects of Cyclic Thermal Stresses in Ductile Metals," Trans. ASME, Vol. 76, p. 931 (August 1954).

37. Dharan, C.K.H., "Fatigue Failure Mechanisms in a Unidirectionally Reinforced Composite Material," Fatigue of Composite Materials, ASTM STP 569, American Society for Testing and Materials, p. 171 (1975).

38. Dharan, C.K.H., "The Fatigue Behavior of Fiber-Reinforced Polymers and Advanced Composites," Contributed by Design Engineering Division of The American Society of Mechanical Engineers, Design Engineering Conference and Show, Chicago, Ill. (May 1977).